α-synuclein in *Saccharomyces cerevisiae*: model for aggregate clearance, cell survival and influence of autophagy

PhD Thesis

in partial fulfilment of the requirements
for the degree “Doctor rerum naturalium”
in the Molecular Biology Program
at the Georg-August University Göttingen,
Faculty of Biology

submitted by

Doris Petroi

born in

Galati, Romania

2012

I hereby declare that the PhD thesis entitled "**α-synuclein in *Saccharomyces cerevisiae*: model for aggregate clearance, cell survival and influence of autophagy**" has been written independently and with no other sources and aids than quoted.

Doris Petroi

Acknowledgements

This work was carried out in the department of Molecular Microbiology and Genetics in the Institute of Microbiology and Genetics under the supervision of Prof. Gerhard H. Braus.

I would like to express my deep gratitude to Prof. Braus for providing me with the great opportunity and challenge to work on Parkinson's disease in a Microbiology laboratory. The success of this work would not have been possible without his excellent mentoring, encouragement and support.

I am very thankful to Dr. Blaga Popova and Dr. Stefan Irniger for their precious involvement in my work as well as for their friendship and support.

I appreciate the time and helpful suggestions of Prof. Stefanie Pöggler and Prof. Michael Thumm as members of my doctoral thesis committee.

During my doctoral years I enjoyed a good working atmosphere and a sense of team work for which I thank all members of the department. I would particularly like to thank Mrs. Maria Meyer for technical assistance, Dr. Naimeh Taheri-Talesh for help with α-synuclein constructs, Dr. Oliver Valerius for mass spectrometry analysis, Dr. Özgur Bayram and Mrs. Özlem Sarikaya Bayram for inspiring discussions and laboratory protocols, Dr. Martin Christmann and Dr. Henriette Irmer for advice on new molecular biology techniques, as well as Mrs. Heidi Northemann and Mrs. Nicole Scheiter for assistance with official matters and ordering reagents. Moreover, I thank the bachelor and master students whom I guided and who offered me very rewarding moments.

I consider myself privileged to have been a PhD student of the Molecular Biology Program of the International Max Plank Research School in Göttingen. The program provided me with wonderful opportunities for scientific learning and for personal development, and I especially thank Dr. Steffen Burkhardt, the program co-ordinator.

Last but not least, I would like to convey my gratitude to my family and friends for their patience, love and faith in me. My dearest appreciation goes to my mother, Mrs. Aurora Petroi, who has given me everything I need.

Table of contents

Publication

Aggregate clearance of α-synuclein in *S. cerevisiae* depends more on autophagosome and vacuole function than on the proteasome

Doris Petroi, Blagovesta Popova, Naimeh Taheri-Talesh, Stefan Irniger, Hedieh Shahpasandzadeh, Markus Zweckstetter, Tiago Outeiro and Gerhard H. Braus

Submitted

Abstract

α-synuclein is a neuronal protein involved in several neurodegenerative disorders, including Parkinson's Disease (PD). Misfolding and accumulation of α-synuclein into cytoplasmic inclusions correlate with the pathogenesis of PD and are reproducible upon overexpression in yeast. *GAL1* promoter-driven wild type (WT) and mutant α-synucleins were studied in parallel with their fluorescently tagged counterparts. Overexpression of WT and of A53T mutant α-synuclein impaired yeast growth and resulted in cytoplasmic accumulations. Fluorescently-tagged versions preserved these effects when the tag was fused C-terminally via a linker. Three WT copies or two A53T copies integrated into one genomic locus resulted in significant growth impairment and accumulation in yeast and represent thresholds for toxicity. A30P mutant α-synuclein had only a mild inhibitory effect to yeast growth and formed aggregates transiently when overexpressed. The triple proline designer mutant A30P/A56P/A76P did not affect growth or formed inclusions. Promoter shut-off experiments revealed that yeast cells can recover from transient α-synuclein expression by clearing aggregates. Proteasomal inhibition by the drug MG132 or by a *cim3-1* genetic mutation did not significantly impair aggregate clearance. This suggests only a minor contribution of the 26S proteasome to α-synuclein degradation. In contrast, a major impairment in clearance in yeast cells treated with vacuolar protease inhibitor phenylmethylsulfonyl fluoride suggested a prominent function of vacuolar proteases. Consistently, a *Δpep4* yeast mutant characterized by vacuolar defects presented impaired clearance ability. A *Δatg1* yeast mutant deficient in autophagy showed a delay in the aggregate clearance response, suggestive of autophagy involvement in the process. α-synuclein aggregates were also cleared when cells were treated with the autophagy-inducing drug rapamycin. Aggregate formation was impaired when cells were pre-treated with the drug, validating the involvement of autophagy in α-synuclein pathobiology. In turn α-synuclein was able to influence autophagy. While A30P α-synuclein transiently up-regulated autophagy, A53T had an inhibitory effect. WT and A53T α-synucleins additionally delayed the induction of autophagy. A *cim3-1Δatg1* double mutant cleared α-synuclein aggregates after promoter shut-off, suggesting that additional cellular mechanisms contribute to clearance. These data provide insight into the pathways yeast cells use for clearing α-synuclein and offer novel perspectives for therapeutic intervention.

Zusammenfassung

α-Synuclein ist ein neuronal exprimiertes Protein, das an neurodegenerativen Krankheiten wie Morbus Parkinson beteiligt ist. Fehlenhafte Faltung und Akkumulation in zytoplasmatische Einschlusskörper charakterisieren die Pathogenese dieser Krankheit. Diese sind auch durch Überexpression von α-synuclein in Hefezellen nachvollziehbar. In dieser Arbeit wurden das *GAL1*-Promotor gesteuerte Wildtyp (WT) α-Synuclein mit mehreren Varianten mit und ohne Fluoreszenzmarkierung im Modellsystem *Saccharomyces cerevisiae* untersucht. Die Überexpression des WT- und A53T-mutierten α-synucleins hemmte das Hefewachstum und resultierte in zytoplasmatischen Aggregaten. C-terminal fluoreszenzmarkierte Varianten zeigten die gleichen Effekte. Die Integration von drei WT- oder zwei A53T-Kopien in einen einzigen genomischen Lokus resultierten in einer signifikanten Wachstumshemmung sowie Akkumulation und wurden somit als Toxizitätsschwelle definiert. Die A30P Variante hatte nur einen gering hemmenden Effekt auf das Hefewachstum und bildete nur transiente Aggregate bei Überexpression. Im Gegensatz dazu zeigte die triple-Prolin-Variante A30P/A56P/A76P weder eine Wachstumshemmung noch nachweisbare Aggregate. Promoterabschaltungsexperimente zeigten, dass Hefezellen Aggregate auflösen können. Das 26S Proteasom spielt bei diesem α-Synuclein Abbau keine wichtige Rolle, da eine Proteasomhemmung durch das Medikament MG132 oder durch eine genetische *cim3-1* die Auflösung der Aggregate wenig beeinflußt. Im Gegensatz dazu fuhrt die Hemmung durch den vakuolaren Proteaseninhibitor Phenylmethylsulfonylfluorid zu einer deutlichen Inhibition bei der Auflösung von α-Synuclein Aggregaten. Ebenso zeigte die *Δpep4* Hefemutante eine verminderte Fähigkeit der Aggregatklärung. Die Autophagie-defiziente Hefemutante *Δatg1* zeigte eine verzögerte Klärung, was auf eine Beteiligung von Autophagie an dem Prozess schließen lässt. Dies wurde dadurch bestätigt, dass α-synuclein-Aggregate auch reduziert wurden, wenn die Zellen mit dem Autophagie-induzierenden Medikament Rapamycin behandelt wurden. Rapamycin vorbehandelte

Zellen zeigten zusätzlich eine verminderte Aggregatbildung, was die Bedeutung von Autophagie in der α-synuclein Pathobiologie weiter validiert. Im Gegenzug hatte α-Synuclein auch einen Einfluss auf Autophagie. Während A30P α-Synuclein Autophagie transient hoch-regulieren konnte, hatte A53T einen hemmenden Effekt. WT und A53T α-synuclein zusätzlich verzögerten die Induktion von Autophagie. Eine *cim3-1Δatg1* Doppelmutante klärte Aggregate nach Promotorabschaltung, was andeutet dass zusätzliche zellulare Mechanismen zur Klärung beitragen müssen. Diese Daten bieten neue Einsichten in die Prozesse, die Hefezellen benutzen um α-synuclein Aggregate zu entfernen und eröffnen neue Perspektiven für therapeutische Eingriffe.

List of Figures

List of tables

Abbreviations

%	percent
µg	microgram
2 µm (2µ)	2 micrometer high-copy yeast expression vector
µl	microliter
AAA+	ATPases associated with various cellular activities
A30P	exchange from Alanine to Proline at position 30
A53T	exchange from Alanine to Threonine at position 30
Amp^r	ampicillin resistance
ATG	autophagy-related gene
A30P/A56P/A76P	exchange from Alanine to Proline at positions 30, 56 and 76
°C	degree Celsius
CMA	chaperone-mediated autophagy
C-terminal	carboxy-terminal
Cvt	cytoplasm-to-vacuole targeting
DMSO	dimethyl sulfoxide
EtOH	ethanol
GABA	gamma-aminobutyric acid
GFP	green fluorescent protein
h	hour
HPLC	high-performance liquid chromatography
kb	kilobasepair
kDa	kilodaltons
LB	Luria-Bertani
LBs	Lewy bodies
LiOAc	lithium acetate
log	decadic logarithm

MAT	mating type
M	molar
min	minutes
MG132	N-(benzyloxycarbonyl)leucinylleucinylleucinal
ml	milliliter
MS	mass spectrometry
myeGFP	monomeric enhanced GFP
N-terminal	amino-terminal
OD_{600}	optical density at 600 nanometer
PCR	polymerase chain reaction
PE	phosphatidyl-ethanolamine
PMSF	phenylmethanesulfonyl fluoride
PD	Parkinson’s disease
rpm	rotation per minute
SC	synthetic complete
SDS	sodium-dodecylsulfate
SLAD	synthetic low ammonia dextrose
SOB	super optimal broth
TAP	tandem affinity purification
TOR	target of rapamycin
ura	uracil
UPS	ubiquitin-proteasome system
WT	wild type
YPD	yeast extract, peptone, dextrose

"It is the theory that decides what we can observe."

Albert Einstein

1. INTRODUCTION

1.1 Parkinson's Disease

Parkinson's disease (PD) is the second most common neurodegenerative disease, belonging to the group of motor system disorders (Lang and Lozano, 1998). The disease progresses as the dopaminergic neurons of the ventral midbrain region called *substantia nigra pars compacta* begin to die (Fearnley and Lees, 1991; Meissner *et al*., 2011). Neuronal cell death affects the central nervous system and leads to a series of symptoms, such as postural instability, tremor, akinesia (muscle rigidity), bradykinesia (slowness of movement) and overall poor balance and coordination (Galvin *et* al., 2001; Meissner *et al*., 2011). Very often, these symptoms are accompanied by psychological syndromes like depression and emotional instability (Giupponi *et al*., 2008). This is due to the depletion of dopamine, which leads to an imbalance of other neurotransmitters such as acetylcholine, glutamate or GABA (Wichmann and DeLong, 2003). Typically, sporadic PD symptoms are more subtle at the onset of the disease, before the age of 60, and worsen progressively (Lang and Lozano, 1998).

While the causes of PD are still unclear, several factors, including environmental (e.g. trauma, drugs, toxins), epigenetic and genetic, have been proposed to contribute to the disease. Toxins suspected to promote PD are pesticides and heavy metals, such as manganese, copper and iron, which are able to generate reactive oxygen species characteristic of PD (Chiueh *et al*., 2000; Jenner, 1998). Genetic causes of PD can be divided in two categories: sporadic/idiopathic (95% of the cases) and familial (5% of the cases). Mutations in genes like *SNCA*, *PRKN*, *PINK1*, *DJ-1*, *MAPT*, *UCH-L1*, *ATP13A2*,

LRRK2 and *HtrA2/Omi* involved in oxidative stress, mitochontrial disfunction and protein quality control are often associated with the disease (Biskup *et al*., 2008; Kawamoto *et al*., 2008).

Since there is currently no cure for PD, common therapies aim at delaying or ameliorating the symptoms while research focuses on understanding toxicity mechanisms and providing protective solutions. Due to the ageing of the world population, the importance of Parkinson's disease as a public health issue has tremendously increased over the past decades.

1.2. α-synuclein in Parkinson's disease

The molecular basis of PD is the accumulation of intracellular proteinaceous inclusions known as Lewy bodies (LBs) (Figure 1), which contain proteins like α-synuclein, ubiquitin, synphilin-1 and several cytoskeletal proteins (Forno *et al*., 1996). The major constituent of LBs is the aggregated protein α-synuclein (Spillantini *et al*., 1997).

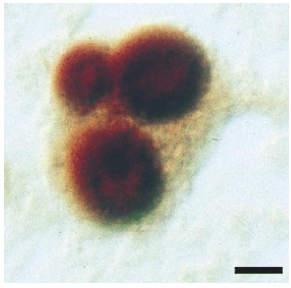

Figure 1. **Morphology of Lewy bodies in Parkinson patients**. Nerve cell with three Lewy bodies double-stained for α-synuclein and ubiquitin. The halo of each Lewy body is strongly immunoreactive for ubiquitin, whereas both the core and the halo of each Lewy body are immunoreactive for α-synuclein. Scale bar = 10 µm. (Spillantini *et al*., 1998a).

α-synuclein inclusions have also been reported in other neurodegenerative diseases besides PD, such as Multiple System Atrophy, neurodegeneration with brain iron accumulation type-1, dementia with Lewy Bodies and Alzheimer's disease, collectively referred to as α-synucleinopathies (Duda *et al*., 2000; Spillantini *et al*., 1998a; Spillantini *et al*., 1997; Tofaris and Spillantini, 2007).

α-synuclein is a small neuronal protein encoded by the *SNCA* gene in the *PARK1* gene locus (Cookson, 2005). The protein belongs to the synuclein family along with β and γ isoforms encoded by the *SNCB* and *SNCG* alleles respectively (Maroteaux and Scheller, 1991). Concerning molecular features, α-synuclein is a 140 amino acid protein with a molecular weight of 17 kDa. It contains a series of N-terminal imperfect repeats based on the amino acid motif KTKEGV which occurs seven times starting from the N-terminus until the core region of the protein (Figure 2). The central region of α-synuclein is strongly hydrophobic and promotes dimerization (Giasson and Lee, 2001, Tong *et al*., 2010).

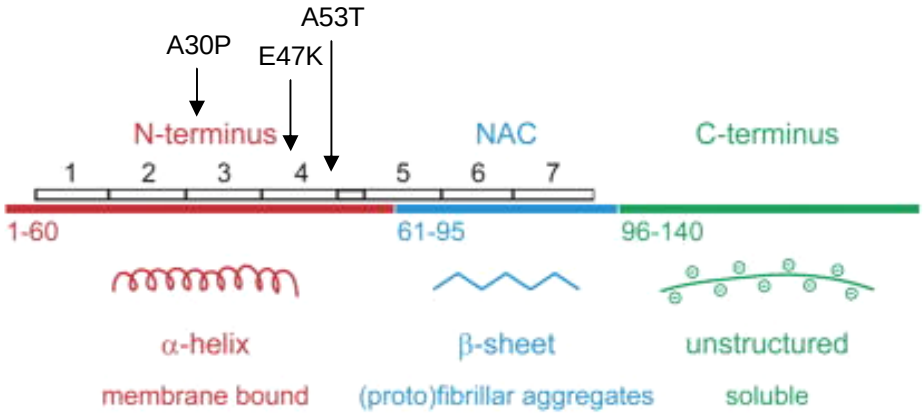

Figure 2. α-synuclein and secondary structure propensity. The N-terminus of α-synuclein (red) adopts an α-helical structure upon binding to lipid membranes. Seven 11-mer repeats of the motif KTKEGV spread from the N-terminus towards the core of the protein (gray). The non-amyloid component or NAC (blue) is hydrophobic and prone to forming β-sheet aggregates. The C-terminus (green) is largely negatively charged and promotes protein solubility. Amino acid positions 30, where an alanine is exchanged to a proline, 53, where an alanine is exchanged to a threonine and 47, where a glutamic acid residue is exchanged to a lysine are PD-related mutations associated with early onset of the disease. Adapted from Vamvaca *et al*., 2009.

The N-terminal region of α-synuclein is essential for oligomerization (Karube *et al*., 2008), whereas the highly acidic C-terminal region is involved in protein-protein interactions (Cookson, 2005) and may inhibit aggregation (Murray *et al*., 2003). Interestingly, alterations in the C-terminus accelerate aggregation (Mishizen-Eberz *et al*., 2005; Vamvaca *et al*., 2009). α-synuclein misses a stable tertiary structure in solution. Hence, starting from its monomeric structure, the protein can form coiled-coils, β sheets and

complex multimeric structures like fibrils, fibers and aggregates (Giasson *et al*., 1999) (Figure 2).

Several observations have been made with respect to the function of α-synuclein. The protein was primarily found in neural tissue at presynaptic terminals where it may serve as molecular chaperone in vesicular fusion (Bonini and Giasson, 2005; Chandra *et al*., 2005). α-synuclein has been shown to function in maintaining neurotransmitter vesicular pools (Jensen *et al*., 1998), synaptic plasticity (Abeliovich *et al*., 2000; Clayton and George, 1998) and phospholipid metabolism (Golovko *et al*., 2009; Sharon *et al*., 2001). Furthermore, it was reported to interact with tubulin (Alim *et al*., 2002) and to act as a microtubule-associated protein, similarly to tau protein involved in Alzheimer's disease (Alim *et al*., 2004).

The involvement of α-synuclein in PD is sustained by the fact that allele multiplication of the wild type *SNCA* locus such as duplication or triplication was linked to a familial form of the disease (Hardy *et al*., 2006; Singleton *et al*., 2003). Additionally, three missense mutations, A30P, A53T and E46K, correlated with autosomal dominant early-onset PD (Krüger *et al*., 1998; Polymeropoulos *et al*., 1997). These mutations rendered α-synuclein more prone to forming amyloid fibrils (Cookson *et al.*, 2005; Greenbaum *et al*., 2005). To understand the relationship between α-synuclein's structural features and its toxicity, research has further focused on artificially designing new α-synuclein mutants (Karpinar *et al*., 2009). For example, A30P/A56P/A76P or triple proline (TP) α-synuclein is a structure-based designer mutant which besides the A30P mutation bears two additional Alanine to Proline substitutions in the β sheet-forming region of α-synuclein. These changes interfere drastically with aggregation. However, despite reducing α-synuclein's fibril formation rate, they do not prevent the protein from being toxic (Karpinar *et al*., 2009).

1.2.1. α-synuclein aggregation and toxicity

The aggregation pathway of α-synuclein begins with the formation of soluble unstable oligomeric species and is promoted by an initial binding of the protein to the plasma membrane. Due to its hydrophobic core defined by amino acids 71-82 (Chandra *et al*., 2003), α-synuclein has a high affinity for binding to lipid membranes. Upon binding, the protein changes conformation and forms two helical domains connected by a small non-helical linker. The interaction of the hydrophobic residues between the α-helices leads to β-sheet formation and oligomerization (Zhu and Fink, 2003). Later on, α-synuclein self-assembles into protofibrils which mature into fibrils and amyloids (Figure 3). These accumulate in inclusion bodies (Auluck *et al.*, 2010), often denominated aggregates. Interestingly, it is assumed that the fibrilar forms not the aggregates are toxic α-synuclein species in PD (Goldberg and Lansbury, 2000; Karpinar *et al*., 2009). Aggregates might thus have a cytoprotective role, isolating toxic α-synuclein species (Tanaka *et al*., 2004).

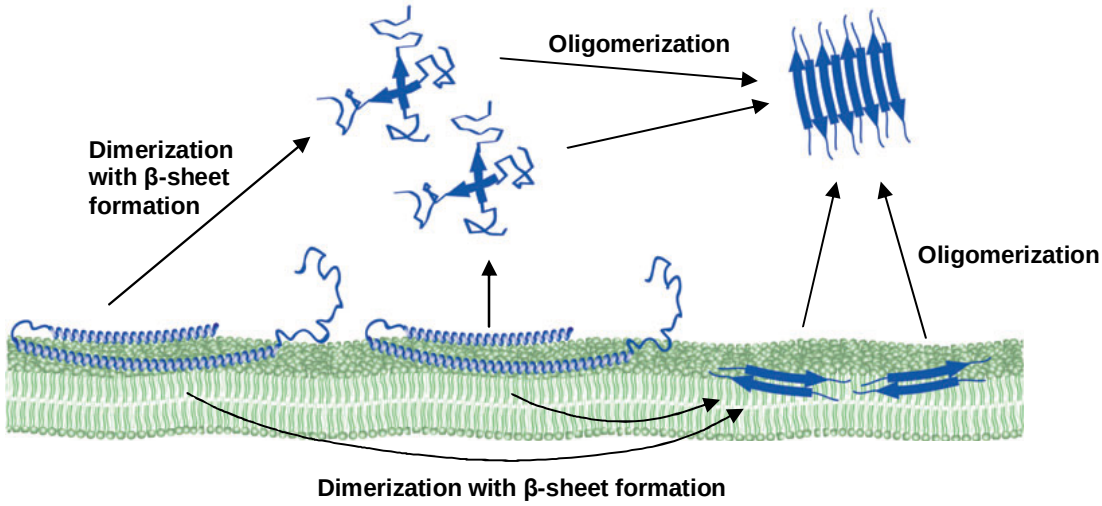

Figure 3. α-synuclein requires lipid interactions to form dimers, oligomers and mature fibrils. In the presence of a lipid membrane, the N terminus of α-synuclein forms two α-helices which allow the protein to associate with the surface of the membrane. An increase in α-synuclein concentration stabilizes membrane interactions and facilitates the formation of α-synuclein dimers on the membrane surface. Through dimerization, α-synuclein adopts a β-sheet secondary structure which, by association with α-synuclein monomers or other dimers, leads to oligomer formation. Oligomers promote the development of fibrils which deposit as amyloids within Lewy bodies. (Auluck *et al.*, 2010).

It has been proposed that α-synuclein may first be nitrated (Giasson *et al*., 2000; Paxinou *et al*., 2001), phosphorylated (Ellis *et al*., 2001; Fujiwara *et al*., 2002; Recchia *et al*., 2004), glycosylated (Shimura *et al*., 2001) or truncated (Liu *et al*., 2005), rather than engage in aggregation as the full-length unmodified protein. Moreover, LBs containing α-synuclein are ubiquitinated (Cookson *et al*., 2005).

Accumulation of misfolded α-synuclein elicits toxic effects on common cellular processes. Consequences include mitochondrial dysfunction, accumulation of reactive oxygen species, impaired protein clearance, defective ER-Golgi trafficking and inhibition of histone acetylation (Cole *et al*., 2002; Cooper *et al*., 2006; Greenamyre *et al*., 2003; Kontopoulos *et al*., 2006; Martin *et al*., 2006; Tanaka *et al*., 2001).

1.2.2 Yeast as model for Parkinson's disease

While humans, mice and rats have well-conserved α-synuclein, no homologues have been reported in lower organisms like *E. coli*, *S. cerevisiae*, *C. elegans* or *D. melanogaster* (Lavedan *et al*., 1998). Nevertheless, mice, rats, flies, worms and yeasts altogether have been implemented as model systems to understand the molecular basis of PD (Chen and Feany, 2005; Giasson *et al*., 2002; Kahle *et al*., 2000; Lakso *et al*., 2003; Maroteaux and Scheller, 1991; Matsuoka *et al*., 2001; Outeiro and Lindquist, 2003; van der Putten *et al*., 2000).

In particular, the budding yeast *Saccharomyces cereisiae* is a powerful model system due to extensive genetic tools available and rapid growth. Belonging to the group of fungi, *S. cerevisiae* is a single-cell organism with the typical cellular compartmentalization of an eukaryote. The haploid genome of yeast contains 16 chromosomes with more than 6000 open reading frames (Goffeau *et al*., 1996) and yeast genes bear 60% homology to human genes (Mager and Winderickx, 2005). Due to the fact that basic molecular pathways involved in cellular homeostasis are highly conserved from yeast to human, *S. cerevisiae* is a very convenient model to study human diseases.

Although yeast does not endogenously produce α-synuclein or homologues (Lavedan *et al*., 1998), heterologous expression of the protein results in cytoplasmic inclusions and yeast growth impairment (Outeiro and Lindquist, 2003), reminiscent of PD pathogenesis. Many other aspects of α-synuclein pathobiology present in higher eukaryotes can be mimicked in yeast, for example, lipid droplet accumulation or defects in vesicle trafficking (Outeiro and Lindquist, 2003).

1.3. Cellular degradation systems

Protein homeostasis plays an important role in maintaining a balance between the synthesis of new proteins and the degradation of proteins which are damaged or which are no longer needed in a specific environment. Protein degradation is essential for normal cell growth and development in processes like cell cycle progression, transcription and cell signaling (DeMartino and Slaughter, 1999). Similarly to mammalian cells, two major cellular systems are responsible for protein degradation in yeast: the ubiquitin-proteasome system (UPS) and autophagy/vacuolar pathways. The importance of these systems in cellular homeostasis has been demonstrated by inhibition with drugs like MG132, acting on the proteasome, and phenylmethanesulfonyl fluoride (PMSF), blocking vacuolar pathways (Lee and Goldberg, 1998) (Figure 4).

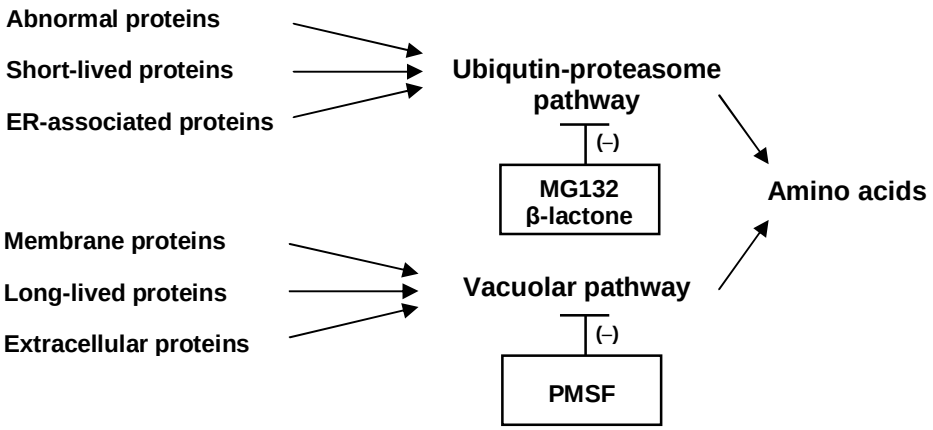

Figure 4. Protein degradation routes in yeast. Abnormal, short-lived and ER-associated proteins are targeted for proteasomal degradation while membrane-associated, long-lived and extracellular proteins are degraded by vacuolar pathways. Drugs used to inhibit these systems are MG132 and β-lactone for the proteasome and PMSF for vacuolar pathways. (Lee and Goldberg, 1998).

1.3.1 The Ubiquitin-Proteasome System (UPS)

In eukaryotic cells, proteasomes are found in the cytoplasm, in perinuclear regions and inside the nuclei (Wojcik and DeMartino, 2003). The 26S proteasome is a multienzyme complex which degrades cellular polyubiquitinated proteins to short peptides in an ATP-dependent manner. It consists of two major subcomplexes, the 19S regulatory particle and the 20S core particle involved in catalysis.

The 19S complex determines substrate specificity and contains two subcomplexes, the base and the lid. The 19S base is composed of six distinct AAA+ family ATPases (Rpt1 to 6) and three non-ATPase subunits (Rnp1, 2 and 10). The 19S lid complex is made up of eight non-ATPase subunits which can be released from the proteasome (Ciechanover, 2006). Two such 19S particles are positioned at both ends of the 20S subunit, where the ATP-dependent interaction promotes opening of pores and provides an access channel for substrates entering the catalytic maw (Glickman and Ciechanover, 2002).

The 20S complex is composed of two copies of fourteen different gene products (α1 to 7 and β1 to 7) arranged in four axially stacked heptameric rings. The two central β rings which contain multiple proteolytic sites and are involved in degradation (Glickman and Ciechanover, 2002).

Protein degradation by the UPS follows a well-defined pathway which begins with labeling of the protein to be degraded. Labeling corresponds to the covalent attachment of the small protein ubiquitin which is first activated by the ubiquitin-activating enzyme E1 in an ATP-dependent reaction. An ubiquitin carrier protein, E2, undertakes the ubiquitin molecule and binds ubiquitin-protein ligase E3 which is already bound to the target protein. E3 finally transfers the ubiquitin molecule to a lysine side chain of the target protein. Once this ubiquitination round on the target protein is completed, additional rounds follow on the ubiquitin lysine residues, resulting in a polyubiquitin chain on the protein to be degraded. Apart from degradation purposes, polyubiquitin labelling at different lysine residues of ubiquitin regulates protein stability, activity and localization

(Glickman and Ciechanover, 2002; Haas and Siepmann, 1997). The ubiquitinated protein is recognized by the 19S regulatory particle of the proteasome, which unfolds it and passes it to the 20S core particle for degradation. The peptide products are hydrolyzed to amino acids and recycled (Figure 5) (Lee and Goldberg, 1998).

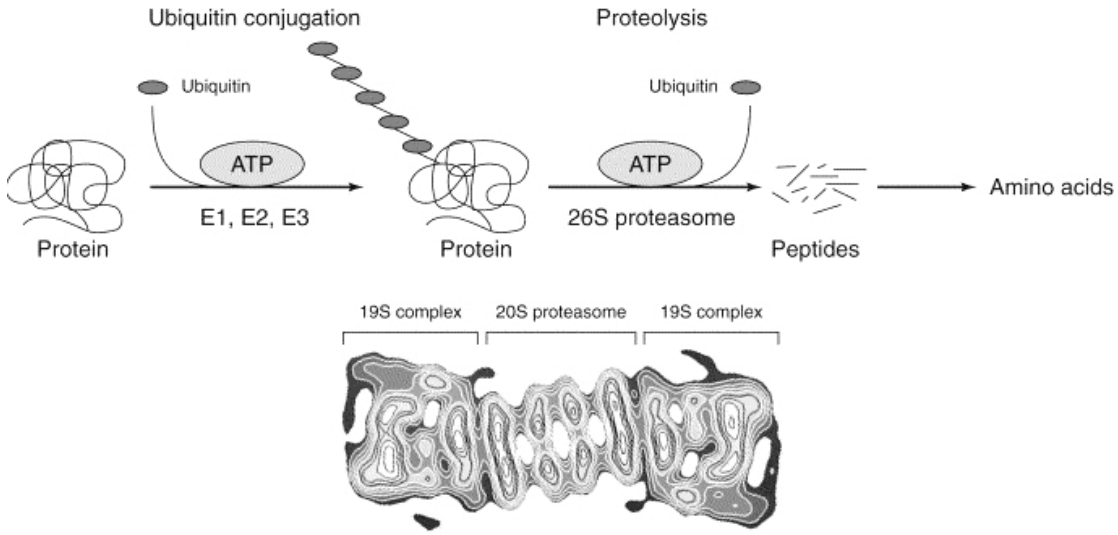

Figure 5. Protein degradation via the ubiquitin-proteasome pathway. The target protein is first conjugated to ubiquitin in a reaction involving an ubiquitin-activating enzyme (E1), an ubiquitin-carrier enzyme (E2) and an ubiquitin-protein ligase (E3). Upon several rounds of ubiquitination, the substrate is recognized by the 19S complex of the 26S proteasome and degraded in the 20S core to small peptides which are further hydrolysed into amino acids. (Lee and Goldberg, 1998).

Control of cellular protein levels by the UPS is essential for many cellular functions, including cell proliferation, differentiation, stress response and apoptosis (Naujokat and Hoffmann, 2002). UPS inhibition leads to an accumulation of undegraded proteins which can aggregate and lead to pathological conditions, such as neurodegeneration (Bedford *et al*., 2008; Betarbet *et al.*, 2005; Olanow and McNaught, 2006).

1.3.2 Autophagy and the vacuole

The yeast vacuole is the correspondent of the mammalian cell lysosome. In yeast, this is the largest organelle, taking up 60% of the cell volume. Similarly to the UPS, the vacuole is also involved in protein degradation. Contrary to the UPS, which is responsible for the hydrolysis of short-lived proteins, the vacuole degrades long-lived proteins (Lee and

Goldberg, 1998). There are several pathways used by proteins to reach the vacuole: sorting of vacuolar proteins in the late Golgi, endocytosis of proteins from the cell surface, cytoplasm to vacuole targeting, autophagy and vacuolar inheritance from mother to daughter cells using homotypic fusion to fuse vacuolar vesicles (Bryant and Stevens, 1998).

Autophagy or “self-eating” is the highly conserved degradation of long-lived cytosolic proteins or organelles and it can be divided into three processes: microautophagy, macroautophagy and chaperone-mediated autophagy (CMA). Micro- and macroautophagy are present in yeast while CMA is not (Klionsky, 2005). Microautophagy defines the transfer of cytosolic components into the lysosome by direct invagination of the lysosomal membrane, followed by the budding of vesicles into the lysosomal lumen (Marzella *et al*., 1981). Macroautophagy is based on the formation of a double-membrane vesicle, the autophagosome, which sequesters cytosolic material and delivers it to the lysosome for degradation (Marzella *et al*., 1981). Chaperone-mediated autophagy is the only selective form of autophagy, where the substrates to be degraded are specifically recognized and transported inside the lysosome (Cuervo and Dice, 1998) (Figure 6).

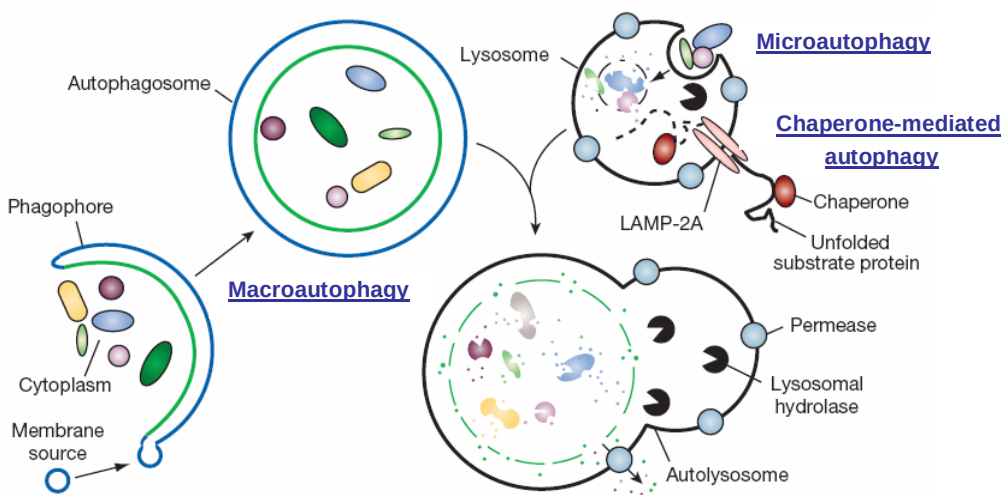

Figure 6. Types of autophagy. Microautophagy refers to the direct sequestration of cytosolic components through lysosomal membrane invaginations. In macroautophagy, cargoes are sequestered within a unique double membrane cytosolic vesicle, the autophagosome. Chaperone-mediated autophagy involves direct translocation of unfolded substrate proteins across the lysosome membrane through the action of a cytosolic and lysosomal chaperone hsc70 and the integral membrane receptor LAMP-2A. (Mizushima *et al*., 2008).

Characterization of molecular mechanisms involved in autophagy has been possible based on the identification of ~27 autophagy-related genes (ATGs) by yeast genetic screens (Klionsky *et al.*, 2003). ATGs are involved in fundamental steps in autophagy, like signaling, autophagosome formation, transport and fusion with the vacuole, and bear a high similarity with the mammalian counterparts (Yorimitsu and Klionsky, 2005). ATGs are also involved in cytoplasm-to-vacuole targeting (Cvt), which transports inactive precursors of hydrolases from the cytoplasm to the vacuole where they are activated by the acidic pH (Khalfan and Klionsky, 2002).

Several ATGs are essential for autophagy induction. Under nutrient availability conditions, TOR, a negative regulator of autophagy, inhibits formation of the Atg1 kinase complex by inducing the hypherphosphorylation of Atg13. As the binding affinity of Atg13 to Atg1 decreases, the first step in autophagy induction is inhibited (Kamada *et al*., 2000). Under starvation conditions, Atg1 binds Atg13 and Atg17, forming a complex. Together with the sub-complex formed by Atg17, Atg31 and Atg29, the induction of autophagy is complete (Suzuki and Ohsumi, 2007).

ATGs have an important role in the two conjugation systems involved in autophagosome formation, Atg12-Atg5 and Atg8-phosphatidylethanolamine. The Atg12-Atg5 conjugation system is required for the expansion of the autophagosomal membrane. Similarly to ubiquitination, Atg12 is conjugated to Atg5 by Atg7, an E1-like protein, and by Atg10, an E2-like protein (Mizushima *et al*., 1998). As part of the newly formed complex, Atg5 binds Atg16 for a complete activation (Kuma *et al*., 2002). In the Atg8 conjugation system, Atg8 is processed by Atg4 (Kirisako *et al*., 2000) and activated by Atg7, an E1-like protein. Atg3 functions next as an E2 conjugation enzyme, rendering Atg8 able to interact with phosphatidyl-ethanolamine (PE). Upon this interaction, Atg8 changes conformation and acts on the dynamic of the autophagosomal membrane, necessary for autophagosome formation (Ichimura *et al*., 2000).

Autophagy is involved in cellular processes like development, adaptation to starvation, removal of damaged organelles and programmed cell death (Marino and Lopez-Otin, 2008). Due to ist important role in cellular homeostasis, autophagy confers protection against progression of several human diseases like cancer, muscular disorders and neurodegeneration (Cuervo, 2004; Mizushima *et al*., 2004).

1.4. α-synuclein degradation

A central question for Parkinson's disease remains α-synuclein degradation which has been investigatigated in cell culture PD models (Opazo *et al*., 2008; Riedel *et al*., 2010). Although the degradation route of α-synuclein in PD has not been fully elucidated, studies suggest that the protein can be cleared by both autophagic pathways and the UPS (Vogiatzi *et al*., 2008; Webb *et al*., 2003).

1.4.1 The UPS in Parkinson's disease

There are several indications that defective proteasomal degradation is associated with α-synuclein. One of them is the fact that the misfolded protein accumulates in LBs which were found ubiquitinated (Cookson *et al*., 2005).

Apart from the ubiquitinated Lewy bodies, mutations in the E3 ubiquitin ligase Parkin and in the ubiquitin carboxy-terminal hydrolase L1(UCH-L1) cause some forms of inherited PD (Polymeropoulos *et al*., 1997), suggesting that a dysfunctional UPS contributes to the disease.

According to several reports, α-synuclein may be degraded by the 26S proteasome (Bennett *et al*., 1999; Tofaris *et al*., 2001). On the other hand, α-synuclein does not appear to be targeted to the proteasome (Ancolio *et al*., 2000), but rather to inhibit it (Chen *et al*., 2005; Lindersson *et al*., 2004). While it was already shown that proteasomal activity is decreased in PD (McNaught and Jenner, 2001), several groups observed that impairing the proteasome further enhances α-synuclein accumulation (Sharma *et al*., 2006;

Zabrocki *et al*., 2005). It is still under debate whether proteasomal inhibition in PD is due to α-synuclein accumulation or whether α-synuclein accumulation is caused by proteasomal malfunction.

1.4.2 Autophagy and Parkinson's disease

Autophagic pathways may clear α-synuclein oligomeric species and aggregates which cannot be processed by the proteasome (Pan *et al*., 2008). It has also been proposed that once the proteasome becomes impaired, autophagy takes over α-synuclein degradation (Pandey *et al*., 2007; Rubinsztein, 2007).

The involvement of autophagy in α-synuclein clearance is often investigated upon its up-regulation or inhibition, commonly achieved by the drugs rapamycin and 3-Methyladenine respectively (Berger *et al*., 2006; Cuervo, 2008; Ravikumar *et al*., 2002). In cell culture models of PD, chemical inhibition of autophagy was shown to promote α-synuclein accumulation (Rott *et al.*, 2008). Since autophagy inhibition was additionally shown to be more effective in preventing α-synuclein clearance than proteasomal inhibition, autophagy might be the predominant pathway of α-synuclein degradation (Rott *et al.*, 2008). Supporting this conclusion, the autophagy-activating drug rapamycin was shown to stimulate α-synuclein clearance (Webb *et al*., 2003).

In neuronal cells, α-synuclein was shown to be degraded via two autophagic routes, chaperone mediated autophagy and macroautophagy (Cuervo *et al*., 2004; Vogiatzi *et al*., 2008). Additionally, an increased number of autophagic markers found in Parkinson patients (Anglade *et al.*, 1997) suggests that autophagy might be up-regulated in response to α-synuclein accumulation. Autophagy up-regulation means an enhanced protein degradation which could protect neurons from α-synuclein toxicity. However, α-synuclein can impair macroautophagy (Winslow *et al*., 2010) and trigger autophagic cell death (Stefanis *et al.*, 2001), suggesting an interplay between α-synuclein and autophagy.

1.5. Aims of this study

Based on the model introduced by Outeiro and Lindquist in 2003, many studies employ *S. cerevisiae* to investigate α-synuclein mechanisms of toxicity (Dixon *et al*., 2005; Fiske *et al*., 2011; Soper *et al*., 2011). Nevertheless, studies have been reporting inhibition of yeast growth despite lack of α-synuclein aggregation (Dixon *et al*., 2005), α-synuclein aggregation despite normal yeast growth (Zabrocki *et al*., 2005) or lack of both cytotoxicity and of aggregation (Fiske *et al*., 2011). Since different α-synuclein constructs are used and the amount of α-synuclein in the cell is usually not quantified, it is difficult to compare results. The first question addressed by this study concerned the potential and the limits of yeast as a Parkinson's disease model. In a systematic analysis, a variety of α-synuclein constructs with and without a fluorescent tag, containing various fluorescent markers at either termini and containing or lacking linker sequences were examined for their ability to aggregate and impair yeast growth.

α-synuclein was previously shown to impair yeast growth and to form aggregates when integrated in two yeast genomic loci (Outeiro and Lindquist, 2003). On the other hand, normal yeast growth and only minimal intracellular aggregates were reported with high-copy expression (Sharma *et al*., 2006). Considering the inconsistency in literature, the next question concerned the relevance of α-synuclein concentration for aggregation and growth impairment. A gene dosage analysis was performed to determine the threshold for α-synuclein aggregation and toxicity. The PD model characterized in the first part of the study was further employed to examine α-synuclein degradation pathways.

A hallmark of PD is the progressive death of dopaminergic neurons in the cortical region of the brain while surviving neurons contain proteinaceous inclusions (Spillantini *et al*., 1997). Another aim of this work was to investigate the ability of cells to cope with α-synuclein inclusions. In this respect, promoter shut-off experiments addressed the potential of yeast cells to recover from α-synuclein toxicity and their ability to clear α-synuclein accumulation.

Since α-synuclein has been proposed to be degraded by both the proteasome and autophagic pathways (Webb *et al*., 2003), a major objective of this study was to investigate which of the two systems is predominant in α-synuclein aggregate clearance. The involvement of the 26S proteasome as well as of autophagy and the vacuole in this process was analyzed through a chemical and a genetic approach. Chemical treatments with the proteasome-inhibitor MG132 and with the vacuolar protease inhibitor phenylmethanesulfonyl fluoride (PMSF) confirmed the data obtained with degradation-related mutants covering proteasomal, vacuolar and autophagic defects. Autophagy involvement in α-synuclein aggregate clearance was further addressed by testing the effect of the autophagy-inducing drug rapamycin on α-synuclein aggregation.

It has recently been suggested that α-synuclein can inhibit macroautophagy (Winslow *et al*., 2010). A final goal of this study was to analyze the regulation of yeast macroautophagy (further referred to as autophagy) in response to α-synuclein overexpression. Together with α-synuclein clearance data, this offered a new insight into the interplay between α-synuclein and autophagy in yeast.

"We think in generalities, but we live in detail."

Alfred North Whitehead

2. MATERIALS AND METHODS

2.1 Materials

2.1.1. Yeast strains

All *S. cerevisiae* strains used in this study are listed in Table 1. The yeast background generally employed for α-synuclein experiments was wild type W303-1A (EUROSCARF, Frankfurt, Germany). Several strains were constructed in this background by integrating the cDNA of the α-synuclein-encoding gene (*SNCA*) fused to GFP via linker in the triple-mutated *ura3-52* genomic locus. Strains with one, two and three tandemic integrations of wild type (WT) α-synuclein or α-synuclein mutants A30P and A53T were selected for analysis. The W303 background was also used for constructing TAP strains with two genomic integration of TAP-tagged WT α-synuclein at the C- and at the N-terminus. W303 further served as parent strain for the temperature-sensitive proteasome mutant *cim3-1*, for the autophagy mutant *Δatg1* and for the double mutant *cim3-1Δatg1*. The *Δerg6* (*Δise1*) mutant in the BY4741 genetic background (EUROSCARF, Frankfurt, Germany) was employed for drug-treatment experiments. BY4741 also served as background for *Δpep4* and *Δypt7* mutants. The diploid strain Sigma1278B was employed for experiments involving pseudohyphal growth.

Table 1. Yeast strains used in this study.

Strain	Genotype	Source
W303-1A	*MATa; ura3-52; trp1D2; leu2-3_112; his3-11; ade2-1; can1-100*	EUROSCARF
RH3465	W303 containing *GAL1::GFP* in *ura3* locus	AG Braus
RH3466	W303 containing 1 genomic copy of *GAL1::SNCA^{WT}::GFP* in *ura3* locus (KLID linker)	AG Braus
RH3467	W303 containing 2 genomic copies of *GAL1::SNCA^{WT}::GFP* in *ura3* locus (KLID linker)	AG Braus
RH3468	W303 containing 3 genomic copies of *GAL1::SNCA^{WT}::GFP* in *ura3* locus (KLID linker)	AG Braus
RH3469	W303 containing 1 genomic copy of *GAL1::SNCA^{A30P}::GFP* in *ura3* locus (KLID linker)	This study
RH3470	W303 containing 2 genomic copies of *GAL1::SNCA^{A30P}::GFP* in *ura3* locus (KLID linker)	This study
RH3471	W303 containing 3 genomic copies of *GAL1::SNCA^{A30P}::GFP* in *ura3* locus (KLID linker)	This study
RH3472	W303 containing 1 genomic copy of *GAL1::SNCA^{A53T}::GFP in ura3* locus (KLID linker)	This study
RH3473	W303 containing 2 genomic copies of *GAL1::SNCA^{A53T}::GFP* in *ura3* locus (KLID linker)	This study
RH3474	W303 containing 3 genomic copies of *GAL1::SNCA^{A53T}::GFP* in *ura3* locus (KLID linker)	This study
RH3443	W303 containing 2 genomic copies of *GAL1::SNCA^{WT}::myeGFP* in *ura3* locus (AAAG linker)	AG Braus
RH3483	W303 containing 2 genomic copies of *GAL1::SNCA^{WT}::TAP tag* in *ura3* locus (KLID linker)	This study
RH3484	W303, containing 2 genomic copies of *GAL1::TAP tag::SNCA^{WT}* in *ura3* locus (KLID linker)	This study
RH3475	W303 with *YGL180w::kanMX4 (Δatg1), GAL1::SNCA^{WT}::GFP* in *his* and *trp* genomic loci	AG Braus
RH3477	W303 with *YGL180w::kanMX4*, *cim3-1*, temperature sensitive (*cim3-1Δatg1* double mutant), *GAL1::SNCA^{WT}::GFP* in *his* and *trp* genomic loci	AG Braus
RH3486	W303 with *cim3-1*, temperature sensitive, *GAL1::SNCA^{WT}::GFP* in *his* and *trp* genomic loci	AG Braus
HiTox	W303 containing *GAL1::SNCA^{WT}::GFP* in *ura3* and *trp1* genomic loci	Outeiro and Lindquist, 2003

BY4741	*MATa; his3Δ 1; leu2Δ0; met15Δ0; ura3Δ0*	EUROSCARF
Δerg6	BY4741; *MATa; his3D1; leu2D0; met15D0; ura3D0; YML008c::kanMX4*	EUROSCARF
Δpep4	BY4741; *MATa; his3D1; leu2D0; met15D0; ura3D0; YPL154c::kanMX4*	EUROSCARF
Δypt7	BY4741; *MATa; his3D1; leu2D0; met15D0; ura3D0; YML001w::kanMX4*	EUROSCARF
RH2447	Sigma1278B; *MATa/α, ura3-52/ura3-52, leu2::hisG/LEU2, TRP1/trp1::hisG*	EUROSCARF

2.1.2. Yeast plasmids

All plasmids used in this study are listed in Table 2. WT, A30P or A53T α-synuclein cDNA sequences preceded by the *GAL1* promoter and followed by the *CYC1* terminator were cloned into the pRS426 high-copy expression plasmid and into the pRS306 integrative plasmid (Sikorski and Hieter, 1989). pRS426 additionally served as a vector for cloning the TP α-synuclein sequence (Karpinar *et al.*, 2009). All plasmids contained an intact *URA3* gene for selection. For microscopic studies α-synuclein and variants were tagged with GFP via linker (Outeiro and Lindquist, 2003), with monomeric enhanced GFP (myeGFP, Maeder *et al*., 2007) with and without linker, with mCherry via linker or with eGFP via linker. The cDNA of the human wild type *SNCA* gene fused via the KLID linker to GFP was amplified by PCR from the genomic DNA of the yeast strain HiTox (Outeiro and Lindquist, 2003). α-synuclein variants were tagged either at the N- or at the C-terminus. N-terminal fusions were connected by SAAAG linker and C-terminal fusions by either AAAG or KLID linkers. For TAP experiments integrative pRS306 plasmids were used containing a TAP tag (EUROSCARF) either at the N- or at the C-terminus of α-synuclein, attached through the KLID linker. Autophagy-monitoring assays were performed with a pRS416 plasmid containing the chimeric fusion GFP-Atg8 under the copper-inducible promoter *CUP1* (Cheong *et al*., 2005). A *TRP1* gene on this plasmid served as selection marker. For experiments involving pseudohyphae induction α-synuclein was placed under the *CUP1* promoter in a pRS426 vector.

Table 2. Yeast plasmids used in this study.

Plasmid	Description	Source
pME2795	*pRS426-GAL1-promoter, CYC1-terminator, URA3, 2µm, pUC origin, Amp^R*	AG Braus
pME3760	pME2795 with *GAL1::SNCA^{WT}*	This study
pME3761	pME2795 with *GAL1::SNCA^{A30P}*	This study
pME3762	pME2795 with *GAL1::SNCA^{A53T}*	This study
pME3941	pME2795 with *GAL1::SNCA$^{A30P/A56P/A76P}$*	AG Braus
pME3526	pME2795 with *GAL1::eGFP-SNCA^{WT}* (SAAAG linker)	AG Braus
pME3527	pME2795 with *GAL1::eGFP-SNCA^{A30P}* (SAAAG linker)	AG Braus
pME3528	pME2795 with *GAL1::eGFP-SNCA^{A53T}* (SAAAG linker)	AG Braus
pME3759	pME2795 with *GAL1::GFP*	AG Braus
pME3763	pME2795 with *GAL1::SNCA^{WT}::GFP* (KLID linker)	AG Braus
pME3764	pME2795 with *GAL1::SNCA^{A30P}::GFP* (KLID linker)	AG Braus
pME3765	pME2795 with *GAL1::SNCA^{A53T}::GFP* (KLID linker)	AG Braus
pME3942	pME2795 with *GAL1::SNCA$^{A30P/A56P/A76P}$::GFP* (KLID linker)	AG Braus
pME3766	pME2795 with *GAL1::SNCA^{WT}::myeGFP* (AAAG linker)	AG Braus
pME3943	pME2795 with *GAL1::SNCA^{WT}::GFP* (AAAG linker)	AG Braus
pME3769	pME2795 with *GAL1::SNCA^{WT}::myeGFP* (no linker)	AG Braus
pME3770	pME2795 with *GAL1::SNCA^{A30P}::myeGFP* (no linker)	AG Braus
pME3771	pME2795 with *GAL1::SNCA^{A53T}::myeGFP* (no linker)	AG Braus
pME3772	pME2795 with *GAL1::SNCA^{WT}::mCherry* (KLID linker)	AG Braus
pME3773	pME2795 with *GAL1::SNCA^{WT}::myeGFP* (KLID linker)	AG Braus
pME3774	pRS306-*GAL1-promoter, CYC1-terminator, URA3, integrative, pUC origin, Amp^R*	AG Braus
pME3945	pME3774 with *GAL1::SNCA^{WT}::GFP* (KLID linker)	AG Braus
pME3946	pME3774 with *GAL1::SNCA^{A30P}::GFP* (KLID linker)	AG Braus
pME3947	pME3774 with *GAL1::SNCA^{A53T}::GFP* (KLID linker)	AG Braus
pME3948	*pRS416-CUP1-promoter, CYC1-terminator, TRP1, pUC origin, Amp^R* with *GFP::Atg8*	Cheong *et al.*, 2005
pME3780	pBS1479, plasmid for TAP-tagging of proteins at the C-terminus	EUROSCARF

pME3781	pBS1761, plasmid for TAP-tagging of proteins at the N-terminus	EUROSCARF
pME3952	pME3774 with *GAL1::SNCA^{WT}::TAP* tag(KLID linker)	This study
pME3953	pME3774 with *GAL1::TAP* tag::*SNCA^{WT}* (KLID linker)	This study
pME3954	*pRS426-CUP1-promoter, CYC1-terminator, URA3, 2µm, pUC origin, Amp^{R}*	AG Braus
pME3955	pME3954 with *CUP1::SNCA^{WT}*	This study
pME3956	pME3954 with *CUP1::SNCA^{A30P}*	This study
pME3957	pME3954 with *CUP1::SNCA^{A53T}*	This study

2.1.3 Oligonucleotides

The oligonucleotides with which the plasmids listed in Table 2 were prepared are given in Table 3.

Table 3. Oligonucleotides used in preparing the plasmids in this study.

Name	Sequence (5'- 3')	Use
NTTP68	ATG TCT AAA GGT GAA GAA TTA TTC (24-mer)	myeGFP forward primer
NTTP69	TTA ACC CGG GGA TCC TTT GTA C (22-mer)	myeGFP reverse primer
NTTP70	CCC AAG CTT ATG GAT GTA TTC ATG AAA G (28-mer)	*SNCA* forward primer containing *Hin*dIII site before start codon
NTTP71	CCG CTC GAG TTA GGC TTC AGG TTC GTA G (28-mer)	*SNCA* reverse primer containing *Xho*I restriction site after the stop codon
NTTP77	CCC AAG CTT ATG TCT AAA GGT G (22-mer)	Forward nested primer for the amplification of myeGFP-*SNCA* PCR fragment
NTTP78	CCG CTC GAG TTA GGC TTC AGG (21-mer)	Reverse nested primer for the amplification of myeGFP-*SNCA* PCR fragment
NTTP79	GCT GCA TAA CCA CTT TAA CTA (21-mer)	*GAL1* forward primer used for sequencing

NTTP95	GCC ATA CCG TTA AAG AAG CAA GC (23-mer)	Forward primer for amplifying the knock out cassette of *atg1*
NTTP96	ATC TAA GTT AAT TGT CAT GTC GGA TC (26-mer)	Reverse primer for amplifying the knock out cassette of *atg1*
NTTP127	CCG CTC GAG TCA TCA GTC GAG CTT GTA CAG CTC G (34-mer)	Reverse primer for mCherry with *Xho*I restriction site and stop codon
NTTP126	CCG CTC GAG TTA TTA AGA TCC TTT GTA CAA TTC ATC C (37-mer)	Reverse primer for myeGFP with *Xho*I restriction site and stop codon
NTTP128	CGG ACT AGT ATG GAT GTA TTC ATG AAA GG (29-mer)	*SNCA* forward primer containing *Spe*I site before start codon
DP1	AAA CTC GAG TCA GGT TGA CTT CCC C (25-mer)	Reverse primer for TAP tag with *Xho*I restriction site for C terminal TAP
DP2	AAG CTT ATC GAT ATG GAA AAG AGA AGA TGG AAA AAG (36-mer)	Forward primer for C-terminal TAP starting with KLID linker sequence
DP3	ATC GAT AAG CTT GGC TTC AGG TTC GTA GTC TTG (33-mer)	Reverse primer for *SNCA* with KLID linker sequence at the end
DP4	GGG ACT AGT ATG ATA ACT TCG TAT AGC ATA CAT TAT AC (38-mer)	Forward primer for N-terminal TAP tag with *Spe*I restriction site at the beginning
DP5	TTT CCC GGG TTA GGC TTC AGG TTC GTA (27-mer)	Reverse primer for *SNCA* with *Xma*I restriction site at the end
DP6	AAG CTT ATC GAT ATG GAT GTA TTC ATG AAA GGA C (34-mer)	Forward primer for *SNCA* with KLID linker sequence at the beginning
DP7	ATC GAT AAG CTT TAG GGC GAA TTG GGT ACC G (31-mer)	Reverse primer for N-terminal TAP tag with KLID linker sequence at the end

2.2 Methods

2.2.1 Molecular Biology methods

2.2.1.1 DNA sequences

All constructs used in this study were verified by DNA sequencing. Sequences were analyzed with the 4Peaks software (www.mekentosj.com) and the LASERGENE application of the DNASTAR software package.

Yeast chromosomal sequences employed as templates for DNA amplification were analyzed using the tools available on the SGD (*Saccharomyces* genome database) website (www.yeastgenome.org).

2.2.1.2 Polymerase Chain Reaction (PCR)

DNA amplification was performed by PCR according to pre-established protocols (Saiki *et al.*, 1988). Phusion polymerase (New England Biolabs, Frankfurt, Germany) was employed for cloning purposes and Taq polymerase (Fermentas, St.Leon-Rot, Germany) was employed for checking the correctness of the amplified sequences. PCRs performed with Phusion polymerase followed manufacturer's instructions. For PCRs performed with Taq, the amplification program started with an initial denaturation step at 95°C for 2 min, followed by 31 cycles of denaturation at 95°C for 1 minute, annealing at different temperatures for 45 seconds and extension at 72°C for 1 min/kb. Annealing temperatures varied from 55°C to 65°C. The program ended with a final extension step at 72°C for 10 min. All reactions were performed in Primus 96plus PCR cyclers (MWG-Biotech, Ebersberg, Germany). PCR products were purified using the QIAspin Gel Extraction Kit (Qiagen, Hilden, Germany).

2.2.1.3 Restriction digestions

Digestions of PCR-amplified DNA sequences were performed with the appropriate restriction enzymes (Fermentas, St.Leon-Rot, Germany). Cloning vectors were digested with the same enzymes as the inserts. The reactions were incubated at 37°C for 2-3 hours then subjected to agarose gel electrophoresis. The restricted fragments were purified using the QIAspin Gel Extraction Kit (Qiagen, Hilden, Germany).

2.2.1.4 Ligations

Vectors were incubated with inserts in a molar ratio of 1:3. Ligations were carried out by T4 DNA ligase (Fermentas, St.Leon-Rot, Germany) in 1xT4 DNA ligase buffer (Fermentas, St.Leon-Rot, Germany). The reactions were incubated at 16°C overnight and heat-inactivated at 65°C for 10 min.

2.2.1.5 Transformation into chemically competent *E. coli* cells

Escherichia coli (*E. coli*) DH5α competent cells (DSMZ, Braunschweig, Germany) were thawed on ice and 5 µl of the inactivated ligation reaction were added to 250 µl cells. After 30 min incubation on ice, the cells were subjected to heat shock at 42°C for 60 seconds and placed back on ice for 5 min. 800 µl of SOC medium (SOB + 20 mM glucose) was added to the mixture, followed by incubation at 37°C for 1h with constant shaking. The cells were finally centrifuged at 2500 rpm for 3 min (Biofuge pico, Heraeus, Hanau, Germany) and plated on LB agar. Since the transformed plasmids carried an ampicillin resistance gene for selection, the agar plates contained ampicillin at a final concentration of 100 µg/ml. After 1 day incubation at 37°C, clones were picked and analyzed by PCR. The reaction was performed as previously described, with the exception that instead of a DNA template a bacterial clone was dissolved in the PCR mixture. Apart from colony PCR, clones were sequenced to ensure the presence and the right orientation of the insert.

2.2.1.6 Plasmid isolation from *E. coli*

E. coli colonies harboring plasmids of interest were inoculated in 5 ml LB medium supplemented with 100 µg/ml ampicillin and cultured at 37°C overnight. Cells were harvested by centrifugation at 13 000 rpm in a tabletop centrifuge (Biofuge pico, Heraeus, Hanau, Germany). Plasmid isolation was further carried out following the QIAprep Spin Miniprep kit and protocol (Qiagen, Hilden, Germany). Plasmid DNA was eluted in 50 µl water out of which 2 µl checked by agarose gel electrophoresis. In parallel, DNA concentrations were measured using the NanoDrop spectrophotometer (Thermo Fisher Scientific Inc., Waltham, MA, USA).

2.2.1.7 Immunoblotting

10 µg yeast protein were incubated with SDS loading buffer, denatured at 95°C and run on a 12% SDS polyacrylamide gel. Proteins were transferred on a nitrocellulose membrane by blotting for one hour at 100V. The membrane was blocked for one hour at room temperature in 5% non-fat milk solution then probed with a primary antibody at 4°C overnight. Primary antibodies used in this study are listed in Table 4. After several washes, the membrane was probed with a secondary antibody for two hours at room temperature. Peroxidase-coupled goat anti-mouse or goat anti-rabbit immunoglobulins G served as secondary antibodies (1:5000, Invitrogen, Karlsruhe, Germany). The membrane was washed several times and incubated with reagents from the Immobilon Western Chemiliminiscent HRP Substrate detection kit (Millipore, Schwalbach, Germany) then exposed to ECL film (GE Healthcare Limited, Buckinghamshire, UK) in the dark. The film was developed in the PROTEC Processor Compact film-developing machine (Siemens, Erlangen, Germany). In parallel, the signal was analyzed using the QUANTUM ST4-3000 gel documentation system equipped with the BIO-1D advanced analysis software (Vilber Lourmat, Eberhardzell, Germany).

Table 4. Primary antibodies used in this study.

Antibody	Animal	Type	Dilution	Source
anti-α-synuclein	mouse	monoclonal	1:3000	AnaSpec, Fremont, CA, USA
anti-α-synuclein	rabbit	ploYclonal	1:500	Santa Cruz Biotechnology, CA, USA
anti-GFP	mouse	monoclonal	1:500	Santa Cruz Biotechnology, Santa Cruz, CA, USA
anti-ubiquitin	mouse	monoclonal	1:1000	Millipore, Billerica, MA, USA
anti-Smt3	rabbit	polyclonal	1:1000	LifeSpan Biosciences, Seattle, WA, USA
anti-3-nitrotyrosine	mouse	monoclonal	1:1400	abcam, Cambridge, UK

2.2.1.8 Southern hybridization

To verify the integration of α-synuclein constructs into the *ura3-52* mutated genomic locus of W303 yeast, several transformants were analyzed by Southern hybridization (Southern, 1975). 10 µg of isolated genomic DNA were subjected to overnight restriction digestion with *Hin*dIII (Fermentas, St.Leon-Rot, Germany), and the restriction fragments were resolved on a 1% agarose gel. The gel was washed in 0.25 M HCl for 10 min, in 0.5 M NaOH/1.5 M NaCl for 25 min and finally in 1.5 M NaCl/0.5 M Tris for 30 min. The DNA was transferred on a nitrocellulose membrane (Pall, Dreieich, Germany) during three-hour blotting. After washing and drying the membrane, the DNA was crosslinked by UV irradiation for 5 min. Hybridization with the DNA probe was done overnight at 55°C. To prepare the hybridization probe, 100 ng of DNA corresponding to a *URA3* gene fragment were denatured at 95°C and labeled with horseradish peroxidase using the ECL Direct Labeling and Detection System (GE Healthcare Limited, Buckinghamshire, UK). After several washing steps, the membrane was incubated with detection solution (GE Healthcare Limited, Buckinghamshire, UK) and exposed to ECL film (GE Healthcare Limited, Buckinghamshire, UK) in the dark. The film was developed in the PROTEC Processor Compact film-developing machine (Siemens, Erlangen, Germany).

Multiple genomic integrations of α-synuclein constructs were estimated with the ImageJ software (Abramoff *et al*., 2004). One copy of the construct corresponded to the 2.7kb + 4.7kb fragments, two copies corresponded to the 2.7kb + 4.7kb + 6.2kb fragments and three copies corresponded to the 2.7kb + 4.7kb + 6.2kb fragments, where the 6.2kb band had a higher intensity.

2.2.2. Yeast methods

2.2.2.1 Growth conditions

Yeast cells harboring α-synuclein constructs were typically cultured at 30°C in selective synthetic complete (SC) medium (Guthrie and Fink, 1991) lacking uracil (-ura). For growth without α-synuclein induction, the SC medium contained 2% raffinose. To induce the *GAL1* promoter of α-synuclein, the SC medium contained 2% galactose. Typically, cells growing overnight in rafinose medium were shifted to galactose medium at an OD_{600} of 0.1. For promoter shut-off experiments, cells growing in raffinose medium overnight were transfered to galactose for 2 or 4h then shifted to SC medium supplemented with 2% glucose. For experiments involving pseudohyphae induction in diploid yeast, solid SLAD medium containing 0.17% Yeast Nitrogen Base without amino acids and ammonium sulfate, 50 µM ammonium sulfate, 2% glucose and 2% Bacto-agar (Gimeno *et al*., 1992) was employed. Additionally, to induce the *CUP1* promoter of α-synuclein, the SLAD medium was supplemented with 10 µM $CuSO_4$. For autophagy-monitoring assays, cells harboring both α-synuclein and GFP-Atg8 plasmids were grown in SC medium lacking uracil and tryptophan. The *CUP1* promoter of GFP-Atg8 was induced with 50 µM $CuSO_4$. All strains were cultured at 30°C, except for temperature-sensitive mutants *cim3-1* and *cim3-1Δatg1*, which were grown and induced to express α-synuclein at 25°C. The *cim3-1* mutation was induced by shifting the cells from 25°C to 37°C. For experiments with these mutants, control strains were cultivated under the same conditions for consistency. In

autophagy-monitoring assays with *cim3-1*, cells were grown overnight at 25°C and transferred to 37°C concomitantly with α-synuclein induction.

2.2.2.2 Yeast transformation

Yeast transformations were performed according to standard protocols (Gietz *et al*., 1992). Yeast cells were grown in 10 ml nutrient-rich YPD medium (Guthrie and Fink, 1991) overnight. Cultures were centrifuged for 3 min at 3000 rpm (Sigma 4K15C, Sigma Laboratory Centrifuges, Osterode am Harz, Germany) and cells were resuspended in 10 ml 100mM LiOAc/TE (5 ml 1M Tris-Cl pH 8.0, 1 ml 0.5 M Na-EDTA pH 8.0, 100 mM LiOAc in a total volume of 50 ml H_2O). After two washes in LiOAc/TE, cells were competent for transformation. 20 µl carrier (salmon sperm) DNA and 5 µl of a concentrated 2µ plasmid suspension were added to 200 µl competent yeast cells together with 800 µl of 50% polyethylene glycol (PEG) in LiOAc. For transformations targeting the *ura3* genomic locus, the plasmids were integrative thereby requiring linearization prior to transformation. 10 ng plasmid DNA was thus digested for 2h at 37°C with *Stu*I (Fermentas, St.Leon-Rot, Germany) for *SNCA-GFP* integration, with *EcoR*V (Fermentas, St.Leon-Rot, Germany) for *SNCA*-TAP tag integration and with *Bsp*119I (Fermentas, St.Leon-Rot, Germany) for TAP tag-S*NCA* integration. Cells were incubated with the particular plasmids on a shaking platform at 30°C for 30 min. Subsequently, cells were subjected to heat shock at 42°C for 20 min. After a short centrifugation at 4000 rpm, the cell pellet was resuspended in 1 ml YPD medium and incubated at 30°C for 1h. Cells were finally centrifuged at 4000 rpm for 1 min and plated on SC-ura solid medium, as the transformed plasmids carried a *URA3* auxotrophic marker. For the co-transformation of α-synuclein and GFP-Atg8 plasmids, cells were plated on solid medium lacking both uracil and tryptophan as selection markers. After 2-4 days incubation at 30°C or at 25°C in the case of temperature-sensitive mutants, colonies were selected and restreaked.

2.2.2.3 Spotting tests

To assess yeast growth on solid medium, cells were grown to mid-log phase in SC medium containing raffinose and lacking uracil. Cells were 10-fold serially diluted starting with an OD_{600} of 0.1 and spotted on SC-ura agar plates containing either 2% glucose or 2% galactose. The plates were incubated at 30°C for 2 days then photographed.

2.2.2.4 Prepraration of yeast crude extracts

Yeast cultures were grown overnight in synthetic complete medium containing 2% raffinose and lacking uracil. For induction of the *GAL1* promoter, cells were inoculated in 50 ml SC-ura with galactose to an OD_{600} of 0.1 and further incubated for 6h. Cells were collected by centrifugation at 4000 rpm for 3 min, washed with TE buffer (10 mM Tris-Cl pH 7.5/8.0, 1 mM EDTA, pH 8.0), and resuspended in 200 µl of R-buffer (150 µl 1M Tris pH 7.5, 6 µl 0.5 M EDTA, 150 µl 1M DTT, 120 µl PIM complete (Roche, Mannheim, Germany). Cells mixed with 0.45 mm glass beads were mechanically broken by vigorous vortexing for 10 min at 4°C. Crude cell extracts were obtained by centrifugation at 13 000 rpm for 10 min at 4°C (Biofuge fresco, Heraeus, Hanau, Germany). The supernatants were collected and protein concentrations were determined in a Bradford assay (Bradford, 1976).

2.2.2.5 Isolation of yeast DNA

Isolation of genomic DNA from *S. cerevisiae* was performed according to standard procedures (Hoffman and Winston, 1987). Cells growing overnight in 10 ml YPD medium at 30°C were collected by centrifugation and shortly washed. 200 µl breaking buffer (2% V/V TritonX 100, 1% V/V SDS, 100 mM NaCl, 10 mM Tris-Cl, pH 8.0, 1 mM EDTA, pH 8.0), 200 µl Phenol:Chloroform:Isomyl (25:24:1) and 0.45 mm glass beads were added to the cell pellet. Cells were mechanically broken by rigorous vortexing for 10 min at 4°C then centrifuged at 13 000 rpm for 5 min. The supernatant was collected and mixed with 1

ml cold ethanol for DNA precipitation. After a short centrifugation step the pellet was incubated with 400 µl TE buffer (10 mM Tris-Cl pH 7.5/8.0, 1 mM EDTA, pH 8.0) and 3 µl RNase at 37°C for one hour. 1 ml cold etanol was added and the samples were centrifuged at 13 000 rpm for 5 min. The DNA pellet was dried at room temperature and dissolved in 50 µl TE buffer. 2 µl of the DNA suspension were verified by agarose gel electrophoresis.

2.2.2.6 Promoter shut-off

W303 cells harboring three genomic integrations of WT α-synuclein were grown overnight in raffinose then incubated in galactose for either two or four hours. To shut off the *GAL1* promoter, cells were transfered to glucose. In combined promoter shut-off and drug-treatment experiments, W303 cells expressing α-synuclein from a high-copy vector were pre-incubated in galactose for 4h then shifted to glucose supplemented with the corresponding drugs at pre-established concentrations (Lee and Goldberg, 1996). For promoter shut-off analysis of degradation-related mutants, W303 and BY4741 wild type strains and *Δatg1*, *cim3-1*, *cim3-1Δatg1* and *Δpep4* mutants were employed. α-synuclein was overexpressed from a 2µ plasmid to achieve higher aggregation levels. Temperature-sensitive mutants *cim3-1* and *cim3-1Δatg1* were grown overnight at 25°C and induced to express α-synuclein for 3h at 25°C and for 1h at 37°C. The temperature shift was necessary to induce the *cim3-1* mutation. Promoter shut-off and subsequent growth was carried out at 37°C. For consistency, the parent strain W303 and the *Δatg1* mutant were grown under the same conditions. Experiments with BY4741 and *Δpep4* cells were performed at 30°C. Cells were observed by fluorescence microscopy before and after promoter shut-off and percentages of cells with aggregates were calculated.

2.2.2.7 Autophagy monitoring assays

W303 yeast cells were co-transformed with pCu416GFP-Atg8 (Cheong *et al*., 2005) and with pRS426 plasmids carrying α-synuclein. Cells grown overnight at 30°C in SC medium containing raffinose and lacking uracil and tryptophan were induced for 2h with 50 µM $CuSO_4$ to produce GFP-Atg8. Cells were washed twice, diluted to an OD_{600} of 0.5 and incubated in 50 ml SC medium containing galactose and lacking uracil and tryptophan. From 10 ml culture collected at 2, 4 and 8h of induction cell extracts were prepared and subjected to immunoblotting as described. To induce autophagy, at the 4h time point of α-synuclein induction, cells were washed twice and transferred to nitrogen starvation medium, SD(-N) (Takeshige *et al*., 1992), prepared with galactose. Probes were taken at 2 and 4h after the shift and analyzed by western hybridization.

2.2.3 Imaging methods

2.2.3.1 Fluorescence microscopy and quantifications

Yeast cultures were grown in synthetic complete medium containing raffinose and lacking uracil until mid-log phase then transferred to galactose medium for α-synuclein induction. Cells were visualized at different time points of induction using a Zeiss Axiovert S100 microscope (Zeiss, Göttingen, Germany). Images were aquired with either a CoolSnap camera or with a QuantEM camera (Photometrics, Tucson, AZ, USA) and the spinning-disc function at a 100x magnification. Depending on the fluorescent marker employed, a GFP or a dsRed filter was used. The images were analyzed with the SlideBook3I software (Intelligent Imaging Innovations, Göttingen, Germany).

To quantify α-synuclein aggregation a minimum of 100 cells were counted per sample. The percent of cells with aggregates was determined by reporting the number of cells displaying cytoplasmic foci to the total number of cells counted. These included cells exhibiting only bright peripheral halos (plasma membrane localization), perivacuolar fluorescence and cytoplasmic distribution of the fluorescent signal.

2.2.3.2 Immunofluorescence

Cultures of W303 cells transformed with high-copy plasmids containing WT, A30P or A53T α-synuclein were grown overnight in synthetic complete medium containing 2% raffinose and lacking uracil. For α-synuclein induction, cells were inoculated in SC medium containing 2% galactose and lacking uracil to an OD_{600} = 0.1. After 6h incubation, cells were collected, washed and fixed with 37% formaldehyde for 30 min. Cell walls were digested with 20 mg/ml zymolase, and the resulting protoplasts were permeabilized in 0.5% Triton X-100 phosphate buffer. After 1h preblocking with 5% fetal bovine serum, protoplasts were incubated overnight with a mouse anti-α-synuclein antibody (1:3000, AnaSpec, Fremont, CA, USA). The protoplasts were washed and a donkey anti-mouse Alexa Fluor 594(red)-conjugated secondary antibody (1:200, Invitrogen, Karlsruhe, Germany) was applied. The samples were fixed and microscopically observed with a dsRed fluorescence filter as described.

2.2.3.3 FM4-64 stainings

Cells were grown in raffinose and induced in galactose medium to express GFP-tagged α-synuclein. To demonstrate co-localization of the protein with endosomal vesicles and with the vacuolar membrane, cells were stained with the FM4-64 red-fluorescence dye (Vida and Emr, 1995). After two hours of α-synuclein induction, cells were treated with FM4-64 at a final concentration of 1 nM. After 20 min incubation in the dark, cells were washed, resuspended in galactose medium and microscopically observed with a dsRed filter for the dye and a GFP filter for the tagged α-synuclein. Merged images were acquired.

2.2.3.4 Light microscopy and colony formation quantification

W303 cells harbouring two genomically-integrated copies of A53T α-synuclein were pre-grown in raffinose then diluted to an OD_{600} of 0.1 in galactose. After 8h of α-synuclein induction, cells were 10-fold serially diluted starting with an OD_{600} of 0.1 and plated on

solid YPD medium containing glucose. Cells were observed at several time points after plating with an Olympus SZX12 light microscope (Olympus, Essesx, UK). Colony formation was quantified by reporting the number of cells forming colonies to the total number of cells. A colony was defined as a group of five or more cells.

2.2.4 Drug treatments

2.2.4.1 Inhibition of cellular degradation systems

Drug treatments were applied to W303 cells concomitantly with transfer to glucose in promoter shut-off experiments. Carbobenzoxyl-leucinyl-leucinyl-leucinal (MG132) (SIGMA-ALDRICH, Steinheim, Germany) dissolved in dimethylsulfoxide (DMSO) was supplemented to the cell suspension to a final concentration of 50 µM. W303 cultures treated with 0.1% DMSO served as control. Phenylmethanesulfonyl fluoride (PMSF) (ROTH, Karlsruhe, Germany) dissolved in ethanol (EtOH) was added to the cell suspension at a final concentration of 1 mM. W303 cultures treated with 1% EtOH served as control. The concentrations of drugs and solvents followed pre-established protocols (Lee and Goldberg, 1996).

MG132 and PMSF treatments were also applied to W303 cells growing in galactose. For control, cells were treated with the respective solvent. Besides single-drug treatments, cells were also treated with both drugs simultaneously. For control, cells were treated with both solvents. Drugs and solvents were applied as described (Lee and Goldberg, 1996).

2.2.4.2 Rapamycin treatments

Several concentrations of rapamycin (Merck KGaA, Darmstadt, Germany), including 20, 50 and 100 nM, were initialy tested on W303 cells expressing α-synuclein from two genomic loci (HiTox strain, Outeiro and Lindquist, 2003). Next, cells expressing α-synuclein from two genomic copies or overexpressing the protein were subjected to three scenarios of rapamycin treatment: pre-treatment, treatment at the same time with α-

synuclein induction and treatment after α-synuclein induction. For pre-treatment, cultures were incubated in raffinose medium overnight and 1h before α-synuclein induction rapamycin was added to the medium. Cells were then washed and transferred to galactose medium. For treatment and induction, cells grown in raffinose were shifted to galactose medium supplemented with 100 nM rapamycin. For treatment after induction, cells were induced for 3h in galactose then the medium was supplemented with 100 nM rapamycin. Cells were visualized at different time points of α-synuclein induction. Aggregation percentages were recorded and compared.

2.2.5 Protein purification methods

2.2.5.1 Tandem Affinity Purification (TAP)

A TAP tag (EUROSCARF, Frankfurt, Germany) was fused to the C- or N- terminus of α-synuclein and cloned into the pRS306 integrative plasmid. Upon transformation, W303 strains harboring two genomic integrations of the TAP-tagged α-synuclein constructs were selected. TAP followed a pre-established protocol (Puig *et al.*, 2002). 100 ml pre-culture of each strain was inoculated into an overnight 2 liter culture in galactose medium. Cells were harvested in a 10 minute centrifugation at 4000 rpm at 4°C. All further steps were performed at 4°C. Cells were resuspended in 20 ml NP-40 buffer (15 mM Na_2HPO_4, 10 mM NaH_2PO_4-H_2O, 1.0% NP-40, 150 mM NaCl, 2 mM EDTA, 50 mM NaF, 0.1 mM Na_3VO_4) and mechanically broken by vortexing with glass beads for 10 min. After 5 min centrifugation at 2500 rpm, the supernatants were subjected to ultracentrifugation at 40 000 rpm in a TH-641 swinging bucket rotor (Thermo Fisher Scientific Inc., Waltham, MA, USA) for 1,5 hours. Protein extracts were incubated for three hours on IgG Sepharose 6 Fast Flow beads (Invitrogen, Karlsruhe, Germany) on a rotating platform. Lysates were incubated with tobacco etch virus (TEV) protease overnight then eluted. The eluates were further incubated with calmodulin beads (Invitrogen, Karlsruhe, Germany) for one hour and eluted in EGTA-containing buffer. Protein samples were precipitated with 25%

trichloroacetic acid (TCA) on ice for 30 min. After centrifugation at 13 000 rpm for 30 min and two washing steps with acetone, the pellets were vacuum dried at 60°C using the Savant SPD11V SpeedVac Concentrator (Thermo Fisher Scientific Inc., Waltham, MA, USA). The pellets were resuspended in SDS loading buffer, denatured at 95°C and resolved on a 12% SDS polyacrylamide gel. Coomassie staining was next performed (Neuhoff *et al*., 1988) and the stained protein bands were tryptically digested (Shevchenko *et al*. 1996). Tryptic peptides extracted from each gel piece were separated using the *ultimate* HPLC system (Dionex, Amsterdam, Netherlands) and subjected to electrospray ionization mass spectrometry using the LCQ DecaXP machine (Thermo Electron Corp., San Jose, CA, USA).

2.2.5.2 Co-immunoprecipitation

W303 cells expressing α-synuclein overnight were harvested and broken by vortexing with glass beads in NP-40 buffer (also used in TAP). Lysates were clarified in a 10 minute centrifugation step at 13 000 rpm. Supernatants were incubated with a rabbit anti-α-synuclein antibody (1:500, Santa Cruz Biotechnology, CA, USA) for one hour at 4°C then with Protein G Sepharose beads (Invitrogen, Karlsruhe, Germany) for two additional hours. After three washing steps, samples were incubated with SDS loading buffer at 95°C and analyzed on a 12% SDS polyacrylamide gel. The gel was Coomassie stained and the stained protein bands were subjected to tryptic digestion and mass spectrometry.

2.2.5.3 Purification of GFP-tagged α-synuclein by GFP-Trap_A

W303 cells expressing GFP-tagged α-synuclein overnight were harvested and mechanically broken by vortexing with glass beads in NP-40 buffer (also used in TAP). Lysates were clarified in a 10 minute centrifugation at 13 000 rpm. Subsequent steps were performed according to the GFP-Trap protocol (chromotek, Martinsried, Germany). GFP-Trap_A beads coated with anti-GFP antibodies were incubated with the clear cell lysates

for two hours at 4°C on a rotating platform. The beads were washed twice, resuspended in SDS loading buffer, boiled at 95°C for 10 min and sedimented at 300 rpm. The supernatants were resolved on a 12% SDS polyacrylamide gel. Protein bands were Coomassie stained and subjected to mass spectrometry as descriebed.

"Each problem that I solved became a rule, which served afterwards to solve other problems."

Rene Descartes

3. RESULTS

3.1. The yeast model for α-synuclein aggregation and toxicity

3.1.1 α-synuclein overexpression impairs yeast growth

α-synuclein has been expressed in many model systems to reconstruct a Parkinson-like scenario that facilitates the investigation of PD cytotoxic mechanisms. The pathobiology of α-synuclein is also reproducible in the yeast *Saccharomyces cerevisiae*. Toxicity of heterologously expressed α-synuclein was questioned here according to the ability of the protein to impair yeast growth. The cDNA of the α-synuclein-encoding gene sequence, further denoted *SNCA*, was cloned into a high-copy yeast vector (2μ) under the control of galactose-inducible promoter *GAL1.* Growth of wild type W303 haploid yeast cells was compared in the presence and absence of α-synuclein at the ambient yeast growth temperature of 30°C both on solid medium and liquid culture.

Overexpression of α-synuclein caused severe growth reduction for cells producing wild type (WT) and A53T versions, had a mild inhibitory effect on cells producing the A30P variant and led to uninhibited growth for cells expressing the triple proline (TP) mutant. In comparison, control cells expressing the empty vector grew uninhibited (Figure 7A).

When modelling α-synuclein toxicity in yeast, different yeast strains could respond differently to α-synuclein overproduction. To check for possible background effects, the haploid strain BY4741 was employed for comparison. WT and A53T α-synuclein overexpressed here impaired growth, while the effect of A30P α-synuclein on BY4741 was only partial (Figure 7B). These results were similar to those obtained in the W303

background and suggested that yeast genetic background does not affect α-synuclein toxicity. W303 cells were employed for further experiments.

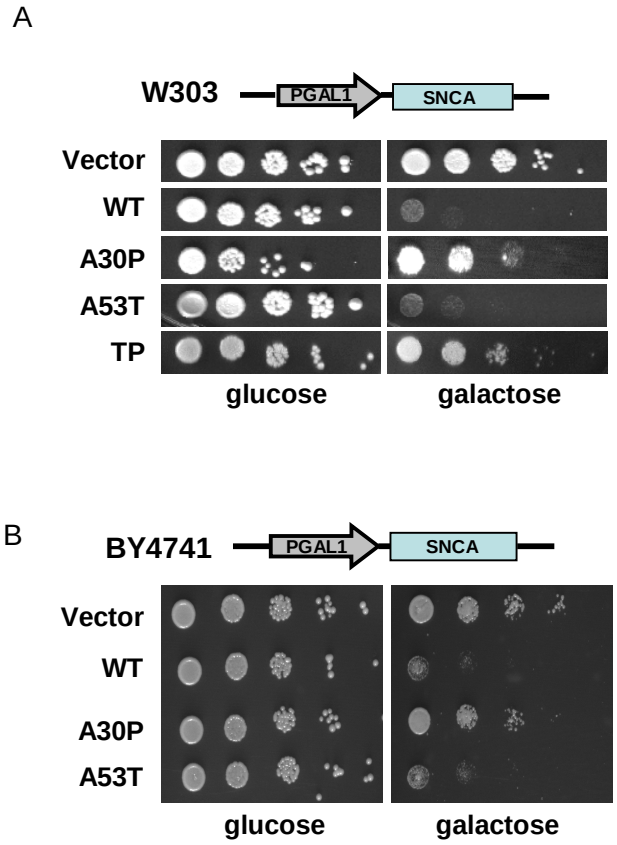

Figure 7. α-synuclein inhibits yeast growth. Spotting analyses. (A) W303 and (B) BY4741 yeast cells were transformed with a high-copy plasmid carrying wild type (WT), A30P, A53T or triple proline (TP) α-synuclein under the control of *GAL1* promoter. Tenfold serially-diluted cells were spotted on inducing (galactose) and non-inducing (glucose) solid medium. Cells expressing the empty high-copy vector served as control. The plates were incubated at 30°C for 2 days then photographed.

3.1.2 α-synuclein overexpression inhibits pseudohyphae formation in diploid yeast

To further study the toxicity of α-synuclein on yeast growth, the effect of α-synuclein overexpression on pseodohyphal development was questioned. The diploid yeast strain Sigma1278B is able to form pseudohyphae under nitrogen starvation conditions. This can be achieved by providing the cells with a prefered fermentable carbon source (glucose)

and a decreased nitrogen supply, e.g. by plating them on SLAD medium with 50 µM ammonium sulfate (Gimeno *et al*., 1992).

Previously used *GAL1*-controlled α-synuclein constructs could not be used for this experiment because the *GAL1* promoter is repressed in the presence of glucose (Traven *et al*., 2006) necessary for growth during nitrogen starvation. α-synuclein was therefore placed under a copper-inducible promoter, *CUP1,* and overexpressed in nitrogen-starved Sigma cells (Figure 8). To induce the promoter, several $CuSO_4$ concentrations were preliminary tested. The optimal $CuSO_4$concentration which did not affect pseudohyphal development of control cells and at the same time allowed for sufficient α-synuclein expression was 10 µM.

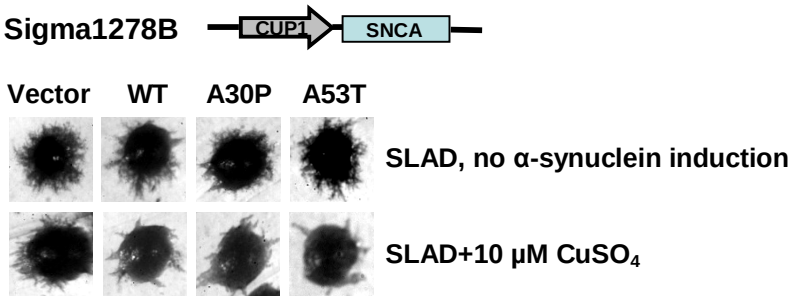

Figure 8. α-synuclein inhibits pseudohyphae development. Sigma1278B yeast cells were transformed with high-copy plasmids harboring WT, A30P or A53T α-synuclein under *CUP1* promoter. Cells were plated on SLAD medium supplemented with 10 µM $CuSO_4$ to induce the promoter and photographed after two days. Cells expressing the empty vector served as control.

Under these conditions, cells expressing WT α-synuclein or variants presented few and abnormal pseudohyphae. Control cells which did not express α-synuclein developed pseudohyphae normally. This suggested that an additional consequence of α-synuclein overexpression in yeast is impairment of pseudohyphal development.

3.1.3 C-terminally tagged α-synuclein is cytotoxic and aggregates

In order to visualize α-synuclein in living cells and to follow its localization throughout time, fluorescent tags are necessary. α-synuclein-GFP fusions had already been applied in previous PD studies, yet with contradictory results. Since the attachment of a fluorescent

tag poses the risk of interference with the protein's natural behavior, derermining the requirements for functional α-synuclein-GFP constructs was mandatory.

In the past, it has been observed that C-terminally GFP-tagged α-synuclein affected yeast growth in the same manner as untagged α-synuclein versions (Outeiro and Lindquist, 2003). These results were also tested here with high-copy vectors carrying α-synuclein-GFP sequences connected via a linker (KLID). Cells expressing GFP-tagged WT and A53T α-synuclein presented growth inhibition (Figure 9). In comparison, the growth deficit of cells producing GFP-tagged A30P α-synuclein was milder. TP α-synuclein-GFP remained untoxic, similarly to the untagged version. The data suggested that attachment of a C-terminal tag does not interfere with the natural ability of α-synuclein to compromise cell growth.

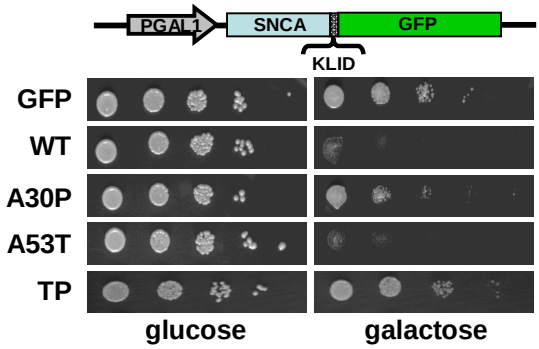

Figure 9. C-terminally tagged α-synuclein inhibits yeast growth. Spotting analysis. W303 yeast cells were transformed with a high-copy plasmid carrying WT, A30P, A53T or TP α-synuclein followed by linker (KLID) and GFP under the control of *GAL1* promoter. Tenfold serially-diluted cells were spotted on inducing and non-inducing solid medium. Cells transformed with a plasmid carrying GFP downstream the *GAL1* promoter served as control. Plates were incubated at 30°C for 2 days then photographed.

To inspect α-synuclein aggregation, the localization of the protein was monitored by live-cell fluorescence microscopy in a time-course experiment. After an initial localization at the plasma membrane, GFP-tagged WT, A30P and A53T α-synuclein formed cytoplasmic inclusions further referred to as aggregates. In contrast, GFP-tagged TP remained distributed throughout the cytoplasm and did not aggregate (Figure 10A).

Aggregates were well defined already after 2h of induction and appeared to increase in size throughout time. Proportional with larger inclusions, cells displayed less fluorescence intensity at the plasma membrane, suggesting that as it starts aggregating, α-synuclein dissociates from the plasma membrane to accumulate in the cytoplasm.

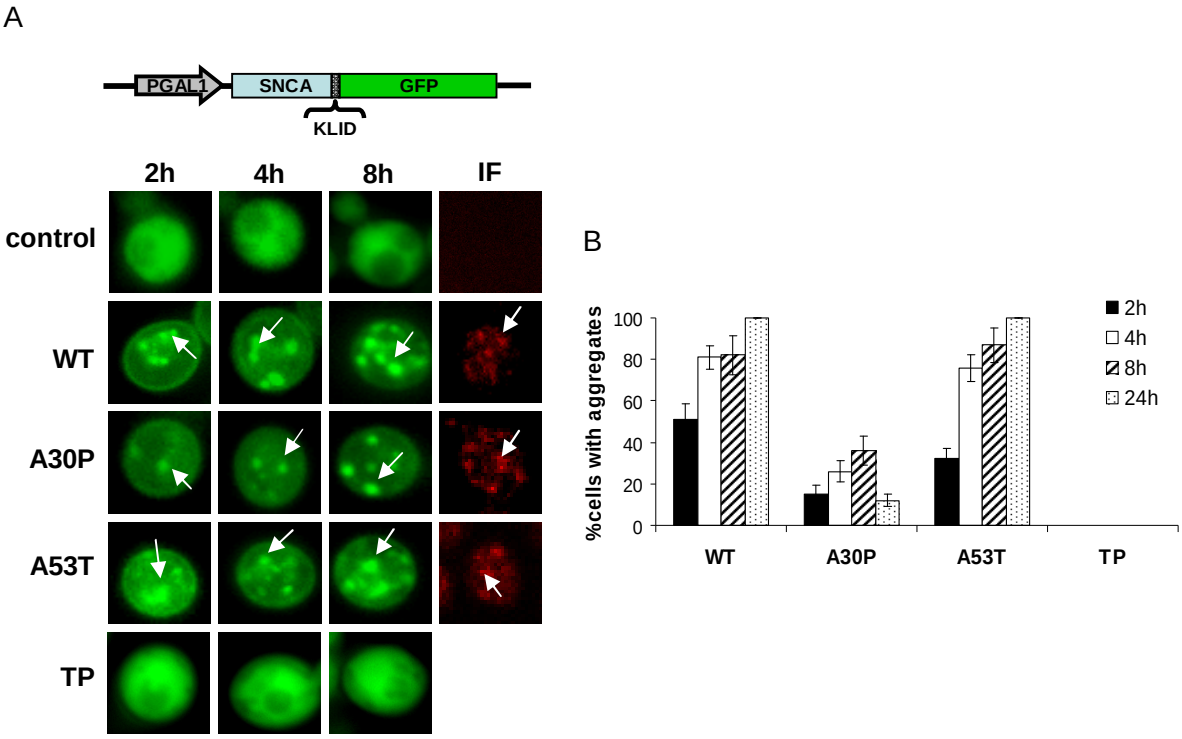

Figure 10. C-terminally tagged α-synuclein forms aggregates. (A) Live-cell fluorescence microscopy of W303 yeast cells expressing α-synuclein-GFP connected via KLID linker from a high-copy plasmid. Cells expressing GFP were used as a control. Cells were pre-grown in non-inducing medium to mid-log phase, transferred to inducing medium and visualized at 2, 4 and 8 hours of induction. The aggregates of untagged WT, A30P and A53T α-synuclein were visualized by immunofluorescence (IF). Uninduced W303 cells were used for IF control. The white arrows indicate cytoplasmic inclusions. (B) Aggregation quantification. Columns represent the average aggregate percentage values of three independent experiments.

Aggregation kinetics revealed that the percentage of cells containing aggregates increased over time (Figure 10B). At 8h of induction the population of cells displaying WT or A53T α-synuclein aggregates reached 80% whereas the aggregation percentage of A30P α-synuclein-expressing cells was only 35%. At 24h of induction the aggregation percentage of WT and A53T α-synuclein-expressing cells was 100%. At the same time point, the aggregation percentage of cells expressing A30P was reduced to 12%, suggesting that this mutant forms aggregates only transiently.

To ensure that the aggregate-formation ability of the three α-synuclein versions is not a GFP artifact, imunofluorescence (IF) was performed. W303 cells expressing untagged WT, A30P and A53T α-synuclein were permeabilized and incubated with an anti-α-synuclein antibody subsequently bound by an Alexa Fluor-conjugated secondary antibody. Since the Alexa fluorophore is able to emit red fluorescence, a red signal is visible by fluorescence microscopy at the sites where the antibody has bound. All three untagged α-synucleins displayed red foci (Figure 10A), confirming the same aggregation patterns as the GFP-tagged counterparts.

The fact that the α-synucleins which inhibited growth were also able to aggregate suggested a link between α-synuclein cytotoxicity and aggregation.

3.1.4 Nature of fluorescent tag and of linker does not alter α-synuclein toxicity or aggregation

The possibility that a specific tag might be responsible for influencing α-synuclein aggregation or the protein's ability to impair yeast growth was excluded by proving that the combination linker-tag tolerates exchanges. To this aim, several constructs were made by keeping the WT α-synuclein-KLID sequence and replacing the GFP with myeGFP or with mCherry. To show that the linker sequence does not interfere with α-synuclein's behavior, an additional construct was tested, keeping the WT α-synuclein and the GFP sequence and exchanging the KLID linker by an AAAG linker (Figure 11).

These constructs were compared based on α-synuclein toxicity and aggregation ability. As demonstrated by a spotting analysis, cells overexpressing any of the differently tagged α-synucleins were unable to grow (Figure 11A), which suggested that all tags and linkers had the same effect in preserving α-synuclein ability to inhibit growth.

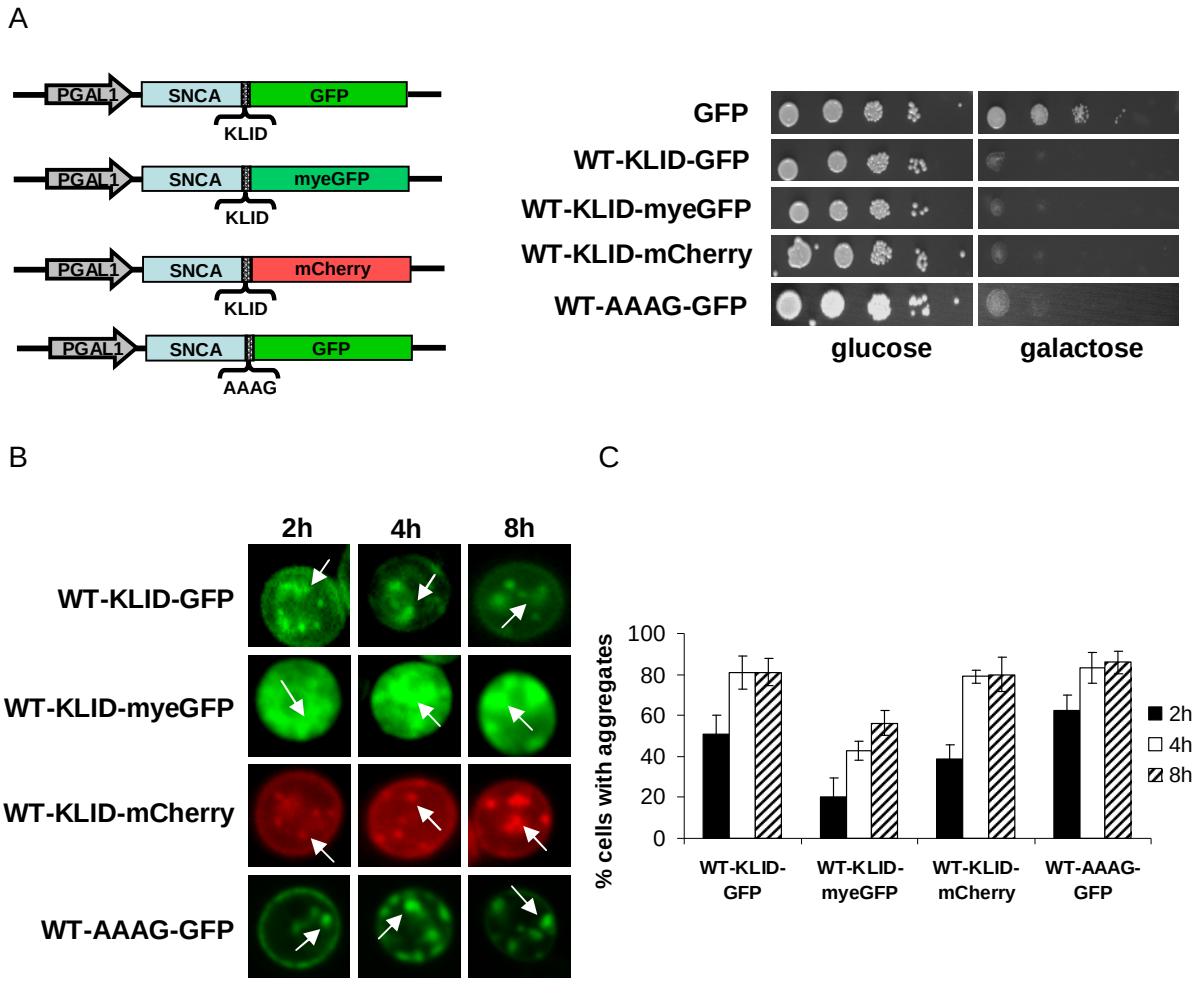

Figure 11. Different C-terminal tags connected to α-synuclein via linker result in similar toxicity and aggregation. (A) Construct schemes and spotting analysis. Cells were transformed with a high-copy plasmid carrying *GAL1*-controlled WT α-synuclein C-terminally fused to GFP, myeGFP or mCherry via the KLID linker and fused to GFP via the AAAG linker. Cultures were pre-grown in non-inducing medium to mid-log phase, serially-diluted tenfold and spotted on inducing and non-inducing medium. After incubation at 30°C for 2 days the plates were photographed. Cells overexpressing GFP served as control. (B) Live-cell microscopy of yeast cells expressing WT α-synuclein tagged with GFP, myeGFP and mCherry. Cells were pre-grown in non-inducing medium to mid-log phase, transferred to inducing medium and visualized at 2, 4 and 8h of induction. Cytoplasmic inclusions are indicated by white arrows. (C) Aggregation quantification. The column bars represent the percentages of cells with cytoplasmic inclusions as average values of three independent experiments.

In addition, all constructs gave rise to aggregates (Figure 11B). Nevertheless, aggregates differed in morphology and accumulation kinetics. While GFP and mCherry α-synuclein aggregates were prominent and formed with a fast kinetic reaching 80-90% of cells in the first 8h of induction, myeGFP aggregates were rather diffuse and reached less than 60% of cells in 8h of induction (Figure 11C).

Since different α-synuclein-tag and linker combinations exhibited the same growth reduction phenotype and were able to aggregate, it can be concluded that once coupled to a tag at the C terminus via a linker sequence, irregardless of the choice of fluorescent tag, α-synuclein maintains its cellular toxicity and ability to aggregate.

3.1.5 Tag position and presence of linker are important in preserving α-synuclein toxicity and aggregation

In many reports the importance of the tag position in α-synuclein constructs is often neglected. Additionally, there is often no description regarding the presence or absence of a linker between α-synuclein and the tag. To address the relevance of tag position and linker in designing α-synuclein constructs, an eGFP tag was connected N-terminally to α-synuclein via linker and a myeGFP tag was fused C-terminally without a linker. The nature of the tag was previously shown not to interfere with α-synuclein aggregation and ability to inhibit yeast growth (Figure 11). Spotting analysis of W303 cells overexpressing WT, A30P and A53T α-synucleins coupled N-terminally to the tag or fussed to it without a linker revealed no growth inhibition (Figure 12A and B). Furthermore, none of the constructs gave rise to aggregates. Either N-terminally tagged via linker or C-terminally fused to the tag, WT and A53T α-synucleins remained at the plasma membrane, while A30P α-synuclein was distributed throughout the cytoplasm.

Since α-synuclein was previously able to inhibit growth and to aggregate when C-terminally tagged via linker (Figure 11), the new lack of growth inhibition and aggregation implied that tag position and presence of a linker are mandatory in maintaining α-synuclein cytotoxicity and aggregation. Additionally, these data offered a direct correlation between lack of growth toxicity and lack of α-synuclein aggregation. In further experiments, only constructs with C-terminal GFP tags connected to α-synuclein via linker were studied.

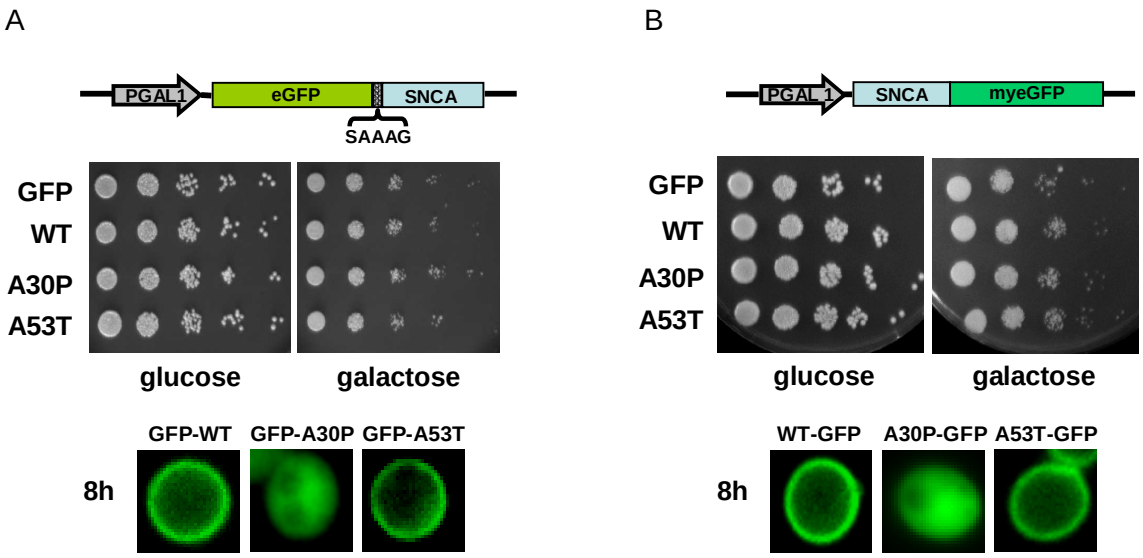

Figure 12. N-terminal linked tags and C-terminal tags fused without a linker prevent α-synuclein cytotoxicity and aggregation. Spotting analysis and fluorescence microscopy. Cells were transformed with a high-copy plasmid carrying WT α-synuclein or mutants (A) N-terminally connected to eGFP via SAAAG linker or (B) C-terminally coupled to myeGFP without a linker under the control of *GAL1* promoter. Cells were pre-grown in non-inducing medium to mid-log phase. Tenfold serially-diluted cells were spotted on inducing and non inducing solid medium and incubated at 30°C for two days. Cells expressing GFP served as control. Corresponding live-cell fluorescent microscopy pictures are shown bellow the spotting assays. Cells were visualized at 8h of induction.

3.1.6 Three tandemic copies of WT and two of A53T are thresholds for α-synuclein toxicity and aggregation

It was previously reported that in yeast α-synuclein aggregation and toxicity can be achieved by expressing the protein from two genomic loci (Outeiro and Lindquist, 2003). A main goal in extending the current yeast PD model was to determine the threshold for α-synuclein cytotoxicity in yeast. Since transformation targeting one genomic locus often results in tandemic copy integrations, a quantitative assay was performed to determine whether tandem repeats of α-synuclein-KLID-GFP integrated into the *ura3* genomic locus are sufficient to render α-synuclein toxic and aggregation-prone. This had the additional advantage of avoiding genetic interference effects which might arise through second-locus integrations. Upon copy-number determination by Southern analysis, strains with one, two and three copy integrations of GFP-tagged WT, A30P or A53T α-synuclein were selected for analysis.

Spotting assays revealed that in the presence of galactose cells expressing one or two copies of WT α-synuclein grew uninhibited, while cells expressing three copies were unable to grow (Figure 13A). Cells expressing one copy of A53T α-synuclein grew uninhibited. Cells expressing two copies of A53T already presented significant growth inhibition and cells expressing three copies were unable to grow. The amounts of α-synuclein in these strains correlated with growth patterns and with gene copy numbers, as determined in a western analysis. The protein band corresponding to one copy was lower in intensity than the band corresponding to two copies, which was lower in intensity than the band corresponding to three copies of the integrated construct. A similar correlation was observed at gene level in Southern analysis (Figure 13A). This applied to all α-synucleins.

Moreover, α-synuclein copy numbers also correlated with aggregation patterns (Figure 13B). WT α-synuclein expressed from one genomic copy remained at the plasma membrane and at 8h of induction started to develop aggregates in a small percentage of cells. Two copies resulted in a low and stable aggregation, while three copies aggregated with fast kinetics (Figure 13C). One copy A53T α-synuclein did not present aggregates until the 8th hour of induction, similarly to the WT version. Two A53T α-synuclein copies aggregated faster than two WT copies and slower than three A53T copies.

Regarding the A30P variant, neither toxicity nor aggregation had previously been described in yeast (Dixon *et al*., 2005; Outeiro and Lindquist, 2003). Indeed, when expressed from one, two or three copies, A30P α-synuclein was not toxic to yeast growth (Figure 13A) and localized throughout the cytoplasm without forming aggregates (Figure 13B). In comparison, when overexpressed from a high-copy vector, A30P was able to aggregate (Figure 10A) and to mildly affect yeast growth (Figures 9 and 13A). In the western analysis (Figure 13A), the intensity of the band corresponding to the high-copy expressed A30P α-synuclein was considerably higher than the intensities of any of the bands corresponding to the integrated α-synuclein copies. This suggested that A30P

requires a much higher expression level in comparison to the other α-synuclein variants in order to have an effect on yeast growth and to form aggregates.

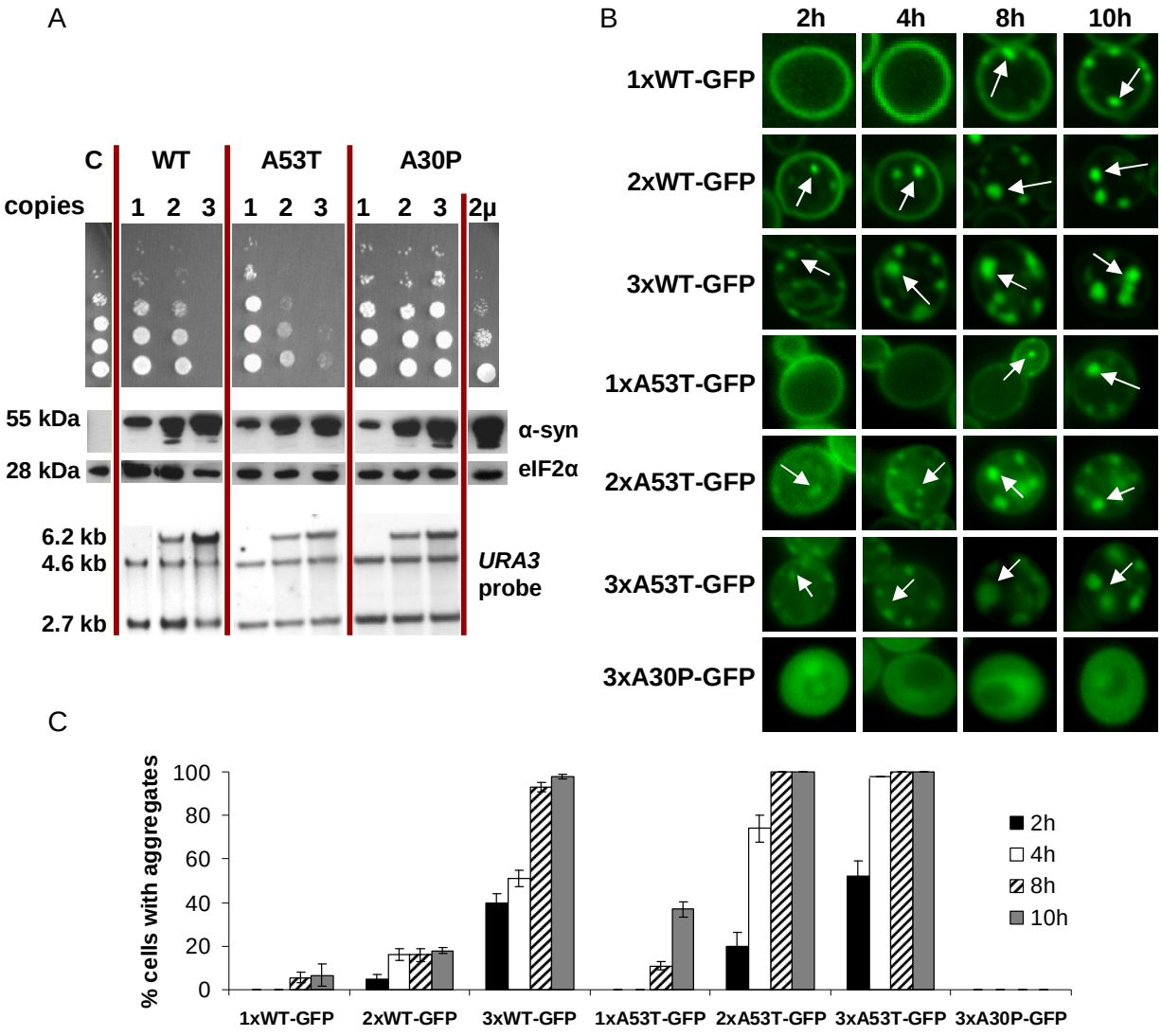

Figure 13. Three copies WT α-synuclein and two copies A53T α-synuclein in one genomic locus represent thresholds for toxicity and aggregation. Phenotypic analysis of W303 yeast strains carrying increasing numbers of WT, A30P or A53T α-synuclein-KLID-GFP integrated into the triple-mutated *ura3-52* locus. A30P α-synuclein was additionally expressed from a 2µ plasmid for comparison. W303 cells carrying integrated GFP in the *ura3* locus were used for control (denoted C). (A) Spotting analysis (top) reflecting yeast growth impairment with increasing copy numbers for WT and A53T and not for A30P α-synuclein. Protein levels (middle) were visualized 6h after induction by western analysis using an anti-α-synuclein antibody and, as loading control, an anti-eiF2α antibody. Equal amounts of total protein (10 µg/sample) were loaded. α-synuclein gene copies were determined by Southern hybridization (bottom) using labeled *URA3* as probe. Integrated α-synuclein copies correspond to 2.7kb + 4.7kb (1x), 2.7kb + 4.7kb + 6.2kb (2x), 2.7kb + 4.7kb + higher intensity 6.2kb (3x). Copy numbers were determined with the ImageJ software. (B) Copy number-dependent α-synuclein aggregate formation visualized by live-cell fluorescence microscopy at indicated time points. White arrows point at the intracellular inclusions. (C) Quantification of α-synuclein aggregate percentages at different time points. The column bars represent the average values of three independent experiments.

Taken together, these results show that integration of multiple copies of tagged WT or A53T α-synuclein into a single yeast genomic locus is sufficient to elicit cytotoxicity and to result in aggregates. Three tandemic gene copies of WT α-synuclein were set as threshold for cytotoxicity and aggregation, while the threshold for the A53T version was lower and closer to two gene copies. In the case of A30P α-synuclein, aggregation and a mild yeast growth reduction can be achieved only by strong overexpression.

3.1.7 TAP, co-immunoprecipitation and GFP-Trap reveal no interaction partners for α-synuclein in yeast

To obtain more insight into the toxicity mechanisms of PD, next experiments focused on finding interaction partners and post-translational modifications of α-synuclein. To this aim, α-synuclein was subjected to purification by three alternative methods and analyzed by Mass Spectrometry (MS).

Tandem affinity purification (TAP) was first performed. A TAP tag consisting of a calmodulin binding peptide, a tobacco etch virus protease cleavage site and Protein A was connected to α-synuclein. As protein A has the property to tightly bind to immunoglobulin G (IgG), the entire complex was retrieved using an IgG matrix (Puig *et al*., 2001). Two integrative constructs were prepared, one containing C-terminally TAP-tagged WT α-synuclein and one carrying N-terminally TAP-tagged WT α-synuclein, both under the control of *GAL1* promoter. Transformation of the TAP construct targeting the *ura3* locus of W303 yeast resulted in multiple-copy integrations. Strains with two genomic copies of TAP-tagged α-synuclein were selected for the experiment. While purification of N-terminally TAP-tagged α-synuclein was not successful, purification of the C-terminally TAP-tagged α-synuclein resulted in α-synuclein (17 kDa), as shown in a Coomassie staining (Figure 14A). MS analysis identified only α-synuclein and no interaction partners. An additional query was performed to identify post-translational modifications on the protein, yet none was found. The fact that TAP resulted in no α-synuclein interaction

partners or post-translational modifications suggested that either there are no α-synuclein interaction partners identifiable in yeast or the method was not sensitive enough.

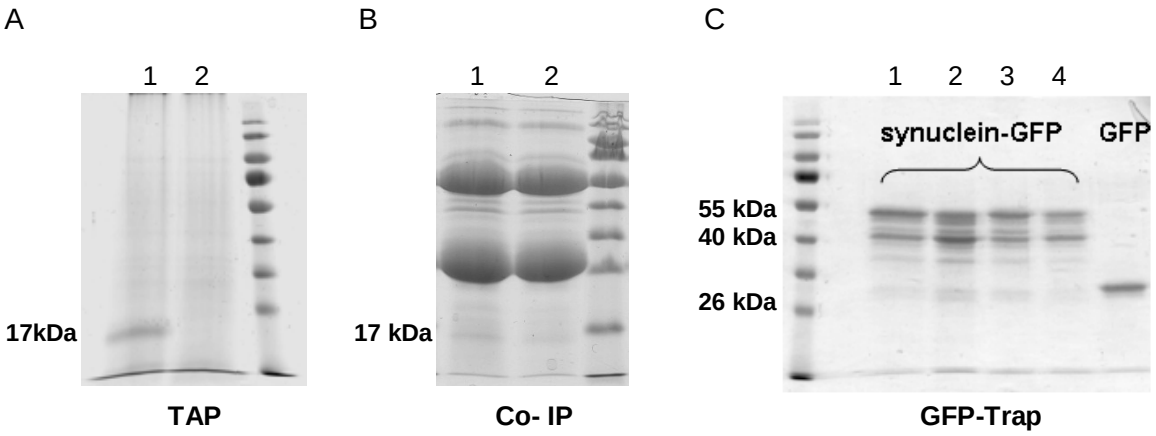

Figure 14. Three protein purification methods reveal no interaction partners for α-synuclein in yeast. (A) Coomasie staining of protein extracts from W303 cells expressing (1) C-terminally TAP-tagged and (2) N-terminally TAP-tagged WT α-synuclein from two genomic copies. Cells were induced for 24h and subjected to TAP purification. (B) Coomasie staining on co-immunoprecipitated (co-IP) α-synuclein. Overnight-grown cells were induced for 24h to express WT α-synuclein (1) from a high-copy vector and (2) from two genomic copies then subjected to Co-IP. (C) Coomassie staining of GFP-Trap-ed α-synuclein. W303 cells expressed (1) WT, (2) A30P and (3) A53T GFP-tagged α-synuclein from a 2μ plasmid and (4) GFP-tagged WT α-synuclein from two genomic copies for 24h. Cells expressing GFP alone served as control.

An alternative method employed to purify α-synuclein while pulling it down together with interaction partners was co-immunoprecipitation (Co-IP). Co-IP is based on precipitating the protein of interest as part of an interaction complex using an antibody that specifically binds to the protein. Co-IP was performed both with low-copy expressed and with overexpressed WT α-synuclein. For purification, the complex was pulled out on an IgG matrix (Phizicky and Fields, 1995). The proteins were pulled down successfully (Figure 14B). MS data identified only α-synuclein and contaminating proteins such as ribosomal factors. Additionally, no post-translational modifications were detected on α-synuclein.

A last attempt to find interaction partners or post-translational modifications of α-synuclein was GFP-Trap. The principle of GFP-Trap relies on trapping the GFP-tagged protein of interest on IgG beads coated with anti-GFP antibodies (chromotek, Martinsried, Germany). The experiment was performed with overexpressed WT, A30P and A53T α-synuclein as well as with low copy-expressed WT α-synuclein. A Coomassie staining of

the purified GFP-tagged α-synucleins showed that the purification was successful (Figure 14C). The protein bands were subjected to MS, which identified ony α-synuclein and GFP. No interaction partners and no post-translational modifications were found.

Aiming to identify post-translational modifications besides interaction partners of α-synuclein and assuming that the sensitivity of MS might not suffice to detect them, a western hybridization was performed on the purified tagged and untagged α-synucleins. The membrane was probed with antibodies against ubiquitin, Smt3 and 3-nitro-tyrosine, yet no signals were detected.

Several purification methods tested and optimized to find α-synuclein interaction partners resulted in the identification of either α-synuclein or α-synuclein-GFP alone. This suggested that in yeast α-synuclein and α-synuclein-GFP do not interact stoichiometrically with other proteins except themselves.

3.2 Degradation pathways involved in α-synuclein aggregate clearance

3.2.1 Yeast cells can recover from transient α-synuclein expression

Having established the criteria for a functional yeast PD model, the next aim was to investigate whether and how yeast cells cope with α-synuclein aggregation. Subsequent experiments questioned whether yeast can recover from α-synuclein-induced toxicity by clearing α-synuclein aggregates. This idea was supported by the observation that yeast cells overexpressing A30P α-synuclein were only mildly affected in growth and were able to reduce aggregation from 35% at 8h of induction to 12% at 24h (Figure 10B), suggesting an intrinsic cellular clearing mechanism to counteract aggregation.

Recovery from α-synuclein toxicity was investigated by promoter shut-off experiments. W303 yeast cells were induced for 8h in galactose to express WT α-synuclein or the A30P and A53T variants in both low and high copies. The *GAL1* promoter was switched off by spotting cells on solid medium supplemented with glucose, as glucose promptly represses *GAL1* (Lamphier and Ptashne, 1992). In parallel, for control, cells were spotted on galactose solid medium (Figure 15A). Cells plated on glucose grew uninhibited (Figure 15B), suggesting that they were able to recover from transient α-synuclein exposure. This was observed for all α-synuclein versions. Cells plated on galactose for control presented a growth deficit, as established in previous spotting analyses (Figures 9 and 13).

To gain more insight into the rapidity of recovery, the ability of cells to form colonies after promoter shut-off was quantified. The yeast strain employed for this experiment was W303 harboring three genomic copies of A53T α-synuclein (3xA53T), as this strain had the most toxic phenotype in the gene dosage analysis (Figure 13).

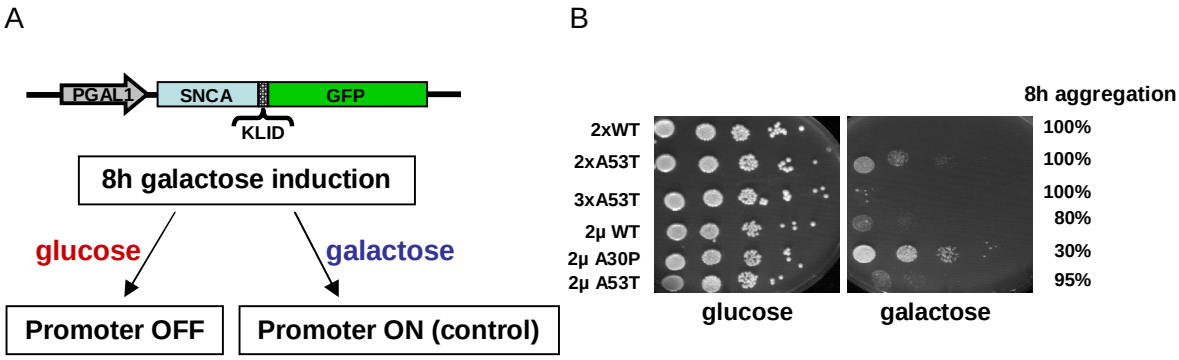

Figure 15. Yeast cells can recover from transient α-synuclein expression. (A) Experimental scheme for promoter shut-off. Cells were induced for 8h in galactose to express α-synuclein either from genomic copies or from high-copy plasmids. The *GAL1* promoter was shut off by plating the cells on glucose. In parallel, as control, the promoter was kept on by plating the cells on galactose. (B) Spotting analysis. Yeast cells were induced in galactose medium for 8h to express GFP-tagged WT, A30P or A53T α-synuclein from genomically-integrated copies or from high-copy plasmids then spotted on glucose and galactose. Aggregation percentages at 8h of induction are shown on the right.

Yeast cells were induced in galactose for 8h to express either 3xA53T α-synuclein or GFP as control. In parallel, the cells were cultured in non-inducing media (raffinose). After being plated on glucose, cells grew normally despite having been subjected to α-synuclein stress for 8h, which validated the recovery ability (Figure 16A). Cells plated on galactose continued to express A53T α-synuclein and presented inhibited growth. Cells pre-incubated in galactose had a more pronounced growth inhibition than cells pre-incubated in raffinose, which corroborated the increased toxicity of α-synuclein with longer expression time. Control cells expressing GFP were able to grow normally both on glucose and galactose, underlining the non-toxic effect of GFP on yeast growth in comparison to α-synuclein.

The same cells harboring three genomic copies of A53T α-synuclein used in the spotting analysis (Figure 16A) were investigated for their ability to form colonies once the 8h-expression of α-synuclein was interrupted. Uninduced cells served as control. After 8h pre-incubation, cells were plated on solid YPD medium containing glucose and observed by light microscopy. Colony formation was quantified by counting developing colonies and reporting them to the total number of cell groups. In the first ten hours after promoter shut-

off, cells which had expressed A53T α-synuclein were distinctly delayed with cell division and had a significantly slower colony formation kinetic compared to uninduced cells (Figure 16B). 24h after promoter shut-off, α-synuclein-exposed cells were forming colonies at a rate comparable to the control. The data suggested that yeast cells need 24h for recovery from 8h-induced α-synuclein toxicity.

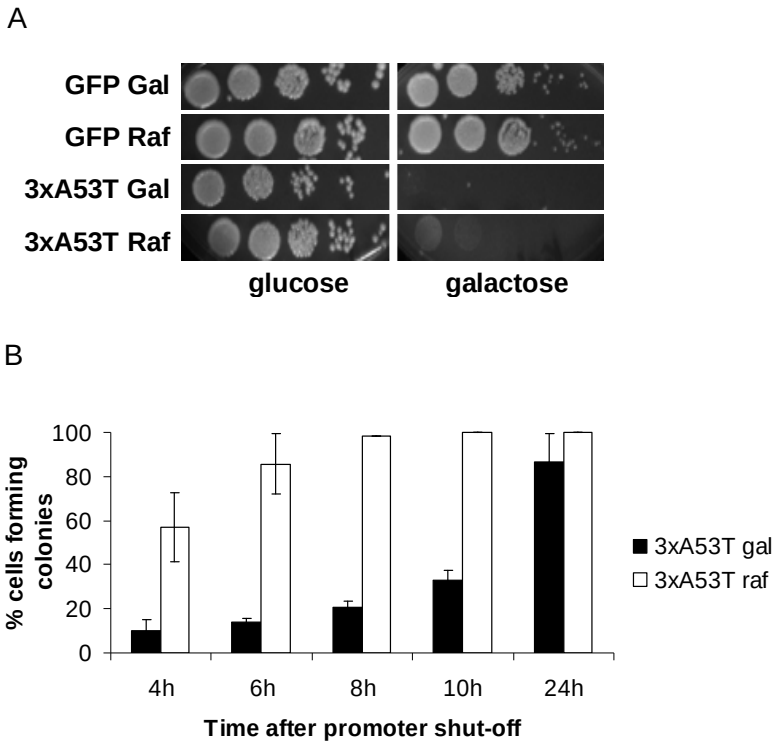

Figure 16. Yeast cells need 24h to grow normally after transient α-synuclein expression. (A) Spotting analysis. W303 cells were induced for 8h in galactose to express GFP-tagged A53T α-synuclein from three genomic copies (3xA53T) then spotted on glucose and galactose. Cells expressing GFP served as control. For comparison, the same strains were grown in raffinose and spotted. (B) Quantification of colony formation. The graph shows the percentages of cells forming colonies after promoter shut-off. The column bars represent the mean values of 3 independent experiments.

3.2.2 Yeast cells can clear cytoplasmic α-synuclein inclusions

Assuming that recovery from growth toxicity may be related to α-synuclein aggregate clearance, the effect of promoter shut-off on α-synuclein aggregates was next investigated. To this aim, W303 yeast cells harboring three genomically-integrated copies of WT α-synuclein-KLID-GFP were induced in galactose medium for 2h then shifted to glucose for promoter shut-off. Fluorescence microscopy and aggregation quantification at

several time points after promoter shut-off revealed a drastic reduction of α-synuclein aggregates in time (Figure 17A and B), suggesting that yeast is able to clear α-synuclein aggregates once the induction of α-synuclein is stopped. An increase in the galactose pre-incubation time to 4h resulted in a slower aggregate clearance kinetic than the one corresponding to 2h pre-incubation (Figure 17B). Thus, the longer the induction of α-synuclein, the more difficult it is for cells to clear aggregates. The data showed that yeast not only recovers from α-synuclein exposure but also clears α-synuclein aggregates in a dosage-dependent manner, as soon as the further α-synuclein supply is interrupted.

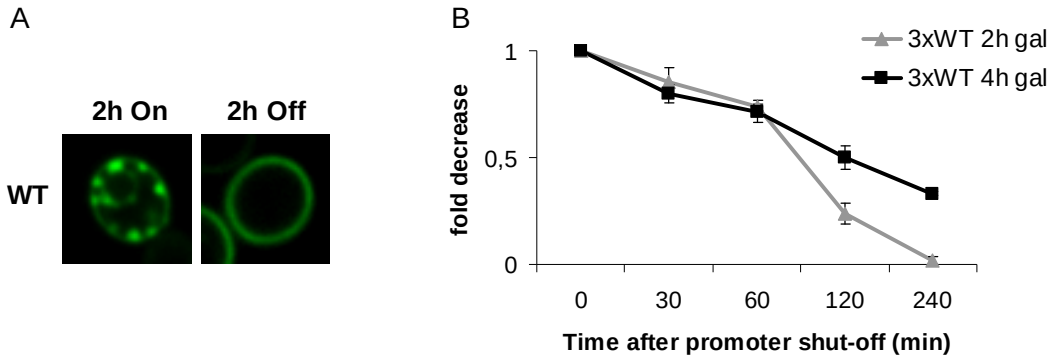

Figure 17. Yeast cells can clear α-synuclein aggregates upon promoter shut-off. (A) Live-cell fluorescence microscopy of W303 cells harboring three copies of genomically-integrated wild type α-synuclein-KLID-GFP (3xWT) at 2h of galactose (left) and after 2h of glucose (right). (B) Fold decrease of α-synuclein aggregation after promoter shut-off at the indicated time points. Pre-incubation in galactose was done for two or four hours. Aggregation percentages were calculated from three independent experiments.

3.2.3 Vacuolar proteases are required for α-synuclein aggregate clearance

Promoter shut-off after transient α-synuclein induction resulted in aggregate clearance, which raised the question of α-synuclein degradation. In the past, α-synuclein was proposed to be degraded by both autophagy and the proteasome (Webb *et al.*, 2003). The importance of these two degradation systems was investigated here by inhibiting the systems and analyzing subsequent impact on α-synuclein aggregate clearance. Inhibition was achieved through a chemical and a genetic approach.

Drug treatments in yeast have always posed the challenge of cell wall penetration (Lee and Goldberg, 1996). While drugs can easily penetrate mammalian membranes, in yeast they would encounter the resistance of a chitin cell wall. A practical solution for drug treatments in yeast is offered by the *Δerg6* (*Δise1*) mutant defective in the biosynthesis of ergosterol, the main membrane sterol of yeast. This modification leads to biochemical and structural alterations in the cell wall, increasing its permeability (Graham *et al*., 1993).

In this study, drug inhibition experiments were performed with the *Δerg6* mutant. The drug MG132 was used to inhibit proteasomal activity and phenylmethylsulfonyl fluoride (PMSF) was used to inhibit the activity of vacuolar proteases (Lee and Goldberg, 1998). Promoter shut-off experiments were performed simultaneously with drug treatments. *Δerg6* cells were induced for 4h to overexpress WT α-synuclein from high-copy plasmids before being shifted to glucose media supplemented with drugs or their corresponding vehicles.

Treatment of yeast cells with MG132 was previously reported to block cell cycle progression, increase accumulation of polyubiquitinated proteins, inhibit the proteasome and decrease transcription of several genes (Collins *et al*., 2010). As proof that MG132 actually affected cells, a western hybridization revealed a three-fold increase in the amount of ubiquitinated proteins in treated cells compared to untreated cells (Figure 18).

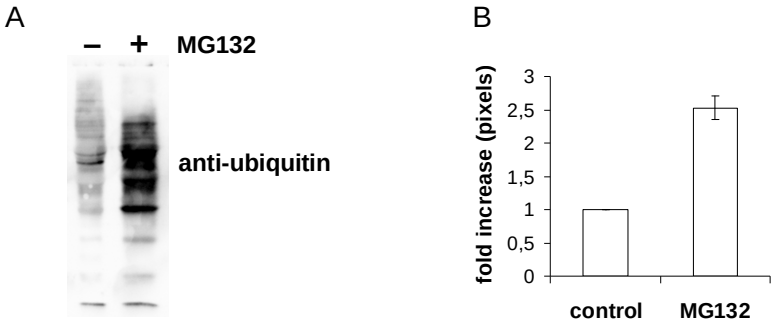

Figure 18. MG132 increases the amount of ubiquitinated proteins three-fold. (A) Western blot. *Δerg6* cells were induced for 4h in galactose to express GFP-tagged WT α-synuclein from a 2µ plasmid then shifted to glucose with 50 µM MG132. For control, cells were transferred to glucose without the drug. 4h after the transfer, cells were broken and the protein extracts were subjected to western analysis. A mouse anti-ubiquitin antibody was used to assess the total levels of ubiquitinated proteins. (B) Quantification of ubiquitin signals. Pixel volumes corresponding to total ubiquitinated protein were compared in MG132-treated and control samples. The factor difference of 2,53 was estimated at 3-fold increase in the amount of ubiquitinated proteins in the MG132 sample.

Quantification of aggregate percentages after α-synuclein promoter shut-off showed that MG132-treated cells were able to clear aggregates in a similar manner as cells treated with the vehicle (DMSO) and as untreated cells (Figure 19). Since the effect of MG132 on aggregate clearance was not significant, it could be concluded that proteasome inhibition does not prevent cells from clearing α-synuclein aggregates, therefore, this degradation system has a minor contribution to α-synuclein aggregate clearance.

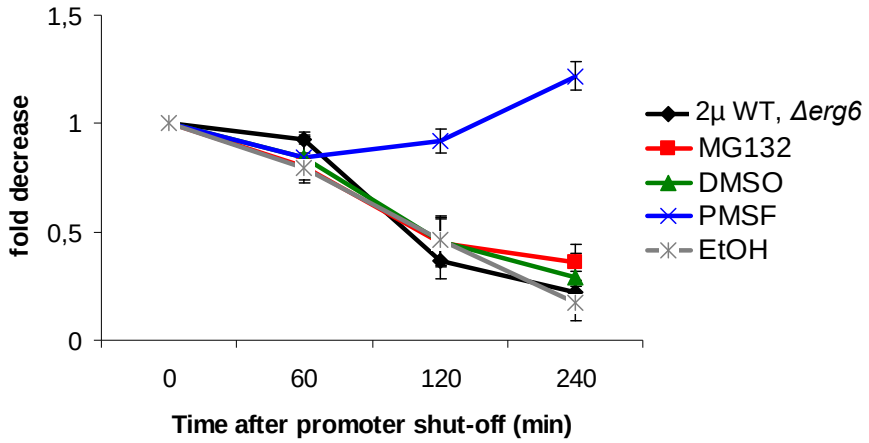

Figure 19. Cells treated with the vacuolar serine protease inhibitor PMSF but not with the proteasome inhibitor MG132 have lost the potential to clear α-synuclein aggregates upon promoter shut-off. *Δerg6* cells were induced for 4h in galactose to overexpress GFP-tagged WT α-synuclein then transferred to glucose. The glucose media were supplemented with 50 µM MG132 or the respective vehicle (DMSO) and with 1 mM PMSF or the respective vehicle (EtOH). Additionaly, cells were transferred to glucose but not treated. Fold decrease in aggregation percentages was calculated as a result of three independent experiments.

Phenylmethylsulfonyl fluoride (PMSF) inhibits the activity of many vacuolar serine proteases (Jones, 1991) without affecting proteasome function (Dubiel *et al*., 1992). PMSF treatment was done under similar conditions as MG132 treatment. Quantification of α-synuclein aggregation after promoter shut-off and PMSF treatment revealed that cells were no longer able to clear the aggregates (Figure 19). Control cells treated with the PMSF vehicle (EtOH) and untreated cells cleared aggregates, suggesting that the observed inhibitory effect on aggregate clearance is due to PMSF. The data indicated that PMSF had blocked pathways which play an important role in α-synuclein aggregate

clearance. Since PMSF is a serine protease inhibitor, it is likely that serine proteases are required for aggregate clearance.

To further verify the effects of MG132 and PMSF on α-synuclein aggregate clearance drug treatments were also applied to *Δerg6* cells induced in galactose to express WT α-synuclein. The medium was supplemented with MG132, PMSF or both drugs. For control, the galactose medium was either left drug-free or was supplemented with the vehicles of the drugs. Aggregation quantification in the early hours of induction showed that α-synuclein aggregated in a similar manner in MG132-treated cells, in DMSO-treated cells and in untreated cells (Figure 20), meaning that MG132 had an insignificant effect on α-synuclein aggregation. α-synuclein aggregation percentages of cells treated with PMSF were higher than those of untreated cells and than those of cells incubated with the EtOH vehicle (Figure 20). This suggested that PMSF treatment not only prevents yeast cells from clearing α-synuclein aggregates, but also enhances α-synuclein aggregation.

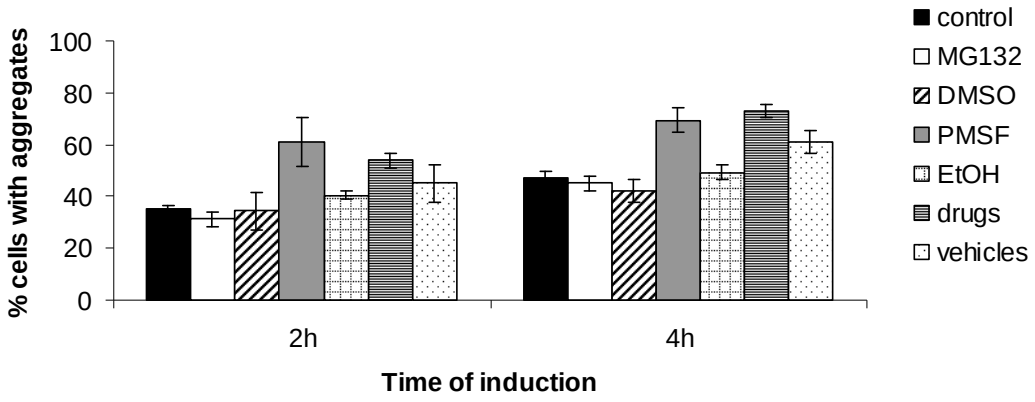

Figure 20. Enhanced α-synuclein aggregation upon PMSF-mediated inhibition of vacuolar proteases. Aggregation quantification in *Δerg6* cells expressing GFP-tagged WT α-synuclein from a high-copy plasmid at indicated time points. Galactose media were supplemented with 50 μM MG132 or the respective vehicle (DMSO), with 1 mM PMSF or the respective vehicle (EtOH) and with 50 μM MG132 and 1 mM PMSF (drugs) or the corresponding solving agents, DMSO and EtOH (vehicles). Additionaly, cells were induced in galactose without being exposed to drugs. Quantifications were done as a result of three independent experiments.

Since no significant differences were recorded between the aggregation percentages of cells treated with PMSF and of cells treated with both drugs and since the effect of MG132 treatment was not substantial on its own, the effect observed with both drugs was due to

PMSF. This additionally implied that combined inhibition of the proteasome and of vacuolar pathways does not enhance aggregation more than inhibition of vacuolar pathways does. Therefore, vacuolar degradation plays a significantly more important function in α-synuclein aggregate clearance than the ubiquitin-proteasome system.

3.2.4 Higher contribution of autophagy and the vacuole than of the proteasome in α-synuclein aggregate clearance

To validate the lack of proteasome involvement in α-synuclein aggregate clearance, a genetical approach was employed. The temperature-sensitive *cim3-1* mutant was considered. This mutant is defective in one of the AAA+ ATPases of the 19*S* proteasome regulatory subunit which unfolds target proteins (Ghislain *et al*., 1993). Proteasomal degradation is thereby abolished in this mutant. Wild type W303 and *cim3-1* cells were transformed with high copy plasmids carrying WT α-synuclein under the control of *GAL1* promoter. Compared to the parental strain, 4h incubation of *cim3-1* cells in galactose resulted in lower α-synuclein aggregation percentages. Upon promoter shut-off, the mutant was able to clear α-synuclein aggregates even with a faster kinetic than the wild type W303 parental strain (Figure 21), confirming a minor contribution of the proteasome to α-synuclein aggregate clearance.

Since PMSF was reported to affect autophagic body formation (Takeshige *et al*., 1992) and PMSF-treated cells were unable to clear α-synuclein aggregates (Figure 19), the next question addressed was whether aggregate clearance could occur via autophagic pathways. Promoter shut-off studies were performed with a *Δatg1* mutant unable to perform autophagy. *ATG1* stands for autophagy-specific gene 1 and the Atg1 protein is a serine/threonine kinase essential for autophagy induction (Matsuura *et al*., 1997). WT α-synuclein was expressed in the *Δatg1* mutant from a high-copy plasmid. Promoter shut-off analysis indicated that *Δatg1* cells did not clear aggregates for the first 120 min, in

contrast to the parental strain which did (Figure 21). This suggested that autophagy contributes to aggregate clearance.

Previous cell culture studies reported that once the proteasome is impaired and cannot clear aggregates efficiently, autophagy becomes the main degradation pathway (Rideout *et al*., 2004). To test whether the specific inhibtion of both these systems would prevent clearance, the double mutant *cim3-1Δatg1* was considered. Promoter shut-off analysis showed that *cim3-1Δatg1* cells cleared aggregates in a similar manner as *Δatg1* cells (Figure 21). This validated the minor contribution of the proteasome to α-synuclein aggregate clearance and favored the previous conclusion that vacuolar pathways have a higher contribution to the process. The fact that the double inhibition did not completely prevent cells from clearing α-synuclein aggregates suggested that there could be additional pathways involved in clearance.

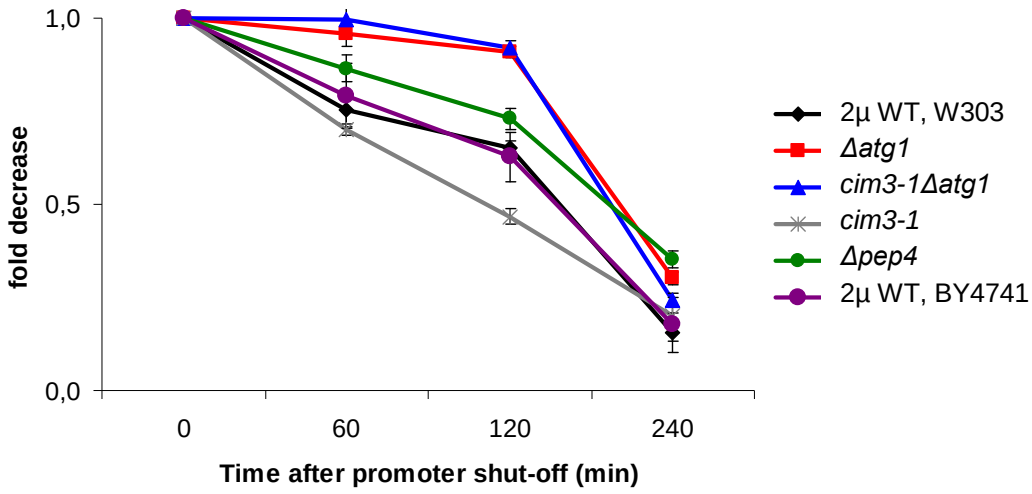

Figure 21. Involvement of autophagy and vacuolar pathways in α-synuclein aggregate clearance upon promoter shut-off. Degradation-related mutants *cim3-1*, *Δatg1, cim3-1Δatg1* and *Δpep4* together with W303 and BY4741 wiltd-type strains were preincubated in galactose to express GFP-tagged α-synuclein from a high-copy vector. After four hours, the cells were shifted to glucose. Aggregation percentages after promoter shut-off were used to calculate the fold decrease in aggregation. Data was quantified from three independent experiments.

A *Δpep4* mutant was included in promoter shut-off experiments to obtain more insight into the extent to which vacuolar degradation is involved in α-synuclein aggregate clearance. Since the mutant had BY4741 as genetic background, an additional control consisting in

the BY4741 parental strain was included in the analysis. The *PEP4* gene of *S. cerevisiae* encodes for the vacuolar protease proteinase A, which initiates the maturation and activation of several vacuolar hydrolases, such as carboxypeptidase Y, proteinase B and aminopeptidase I (Parr *et al*., 2007; Woolford *et al*., 1986). *Δpep4* cells were able to clear α-synuclein aggregates less efficiently than control cells (Figure 21), presenting an intermediate clearance response. This supported the fact that vacuolar proteases are involved in α-synuclein aggregate clearance. Since *Δpep4* cells were able to clear most of the aggregates by the fourth hour of promoter shut-off, it was concluded that there are more proteases involved in the process than the ones controlled by proteinase A.

Taken together, the data obtained through the genetic approach corroborated the results obtained with chemical treatments and confirmed the importance of autophagic and vacuolar pathways in α-synuclein aggregate clearance in comparison to a minor function of proteasomal degradation.

3.2.5 Lack of Ypt7 Rab GTPase affects α-synuclein localization

The importance of vacuolar pathways in α-synuclein aggregate clearance raised the assumption that α-synuclein is targeted to the vacuole for degradation. To follow α-synuclein localization, fluorescence microscopy was performed with a *Δypt7* mutant. Ypt7 is a GTP-binding protein belonging to the Rab GTPase family which consists of small proteins involved in multiple stages of membrane traffiking (Grosshans *et al*., 2006; Wichmann *et al*., 1992). Ypt7 is required for the homotypic fusion event in vacuole inheritance, for endosome-endosome fusion and for endosome-to-vacuole fusion (Schimmoller and Riezman, 1993). *Δypt7* mutants are characterized by highly fragmented vacuoles and differential defects of vacuolar protein transport and maturation (Wichmann *et al*., 1992).

Overexpression of α-synuclein in *Δypt7* resulted in a re-localization phenotype, where α-synuclein accumulated in the cytosol in a ring-like granular pattern (Figure 22A right)

instead of forming the typical aggregates visible in the wild type background (Figure 22A left). The percentage of cells displaying this re-localization phenotype increased with time (Figure 22B). No aggregates developed throughout an 8h time-course. The ring-like arrangement developed gradually and was already very prominent by the first hour of induction (Figure 22C). The inability of α-synuclein to form aggregates in the *Δypt7* mutant suggested that Ypt7 promotes α-synuclein aggregate maintainance.

Ypt7-deficient cells have numerous small vacuoles (Wichmann *et al*., 1992). To determine whether α-synuclein co-localizes with them, stainings with the lypophilic dye FM4-64 were performed. FM4-64 binds lipid membranes and is internalized via endocytosis, thereby staining vacuolar as well as vesicular mebranes (Vida and Emr, 1995).

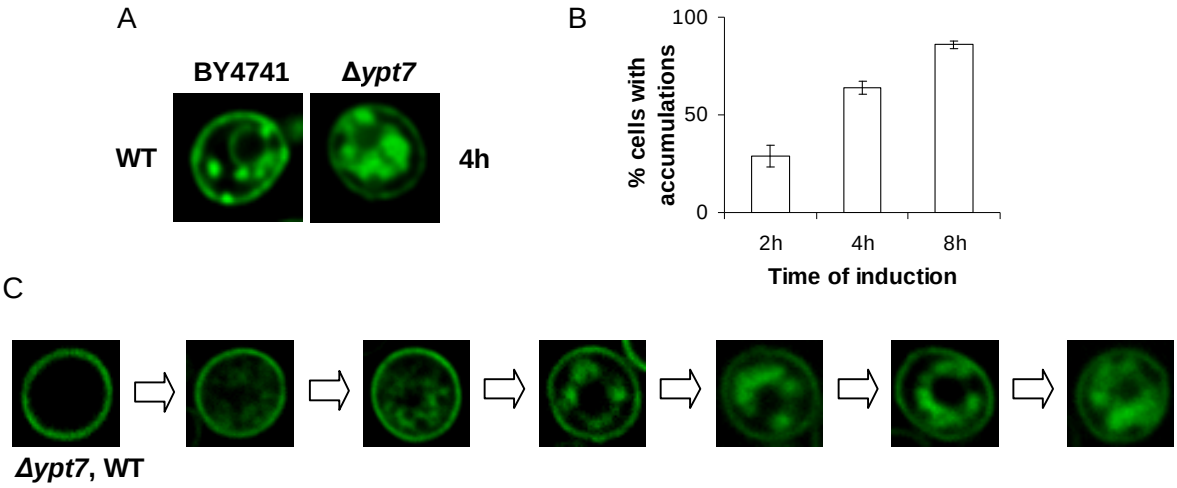

Figure 22. Lack of Ypt7 affects the localization of α-synuclein. (A) Live-cell fluorescence microscopy. *Δypt7* mutant and the parent strain BY4741 transformed with a high-copy vector carrying WT α-synuclein-KLID-GFP (WT) were induced in galactose for 4h. (B) Quantification of *Δypt7* cells with α-synuclein accumulations at 2, 4 and 8h of induction. (C) Live-cell fluorescence microscopy depicting WT α-synuclein accumulation in the *Δypt7* mutant in the first 60 min of induction.

In the BY4741 wild type control as well as in the *Δypt7* mutant the red fluorescence signal of FM4-64 overlapped with the green fluorescence signal of WT α-synuclein-GFP as a sign of collocalization. In BY4741, α-synuclein co-localized with the vacuolar membrane and with endocytic vesicles (Figure 23A), while in *Δypt7*, it co-localized with the numerous vacuoles, characteristic of the mutant (Figure 23B). In wild type cells α-synuclein binding

to the vacuolar membrane was observed only in the first two hours of induction, whereas in *Δypt7* cells the localization persisted over time. α-synuclein co-localization with *Δypt7* vacuoles was visible for all α-synuclein versions.

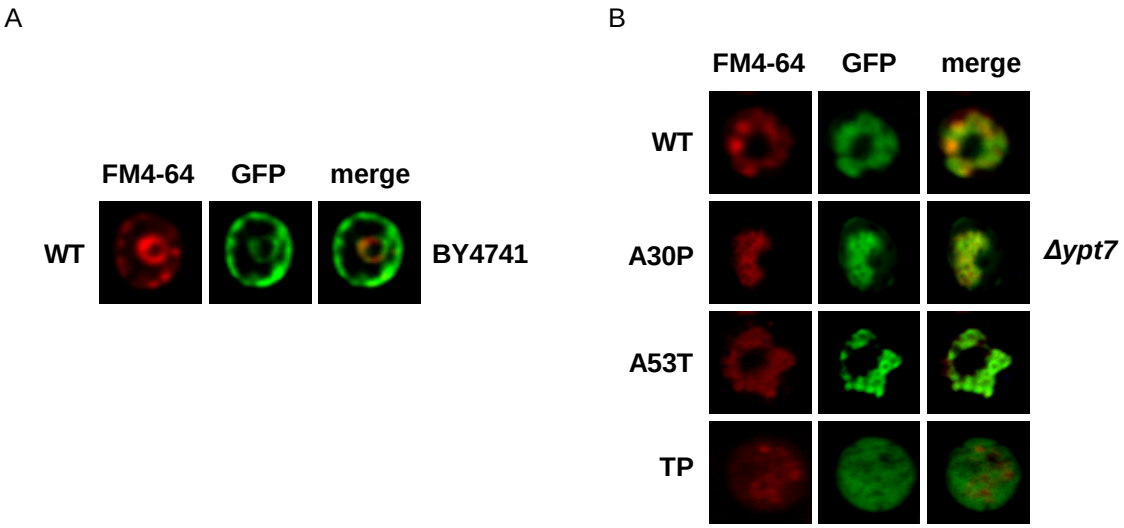

Figure 23. α-synuclein co-localizes with endocytic vesicles and vacuoles. FM4-64 stainings in (A) BY4741 cells expressing WT α-synuclein and (B) *Δypt7* cells expressing GFP-tagged WT, A30P, A53T and TP α-synuclein. After two hours of α-synuclein induction, cells were incubated with 1 nM FM4-64 for 20 min, washed and visualized by fluorescence microscopy. Red, green and merged fluorescence images are shown.

To assess whether lack of Ypt7 affects α-synuclein toxicity to yeast growth, the growth of *Δypt7* cells was compared to the growth of BY4741 cells upon α-synuclein overexpression (Figure 24 A and B).

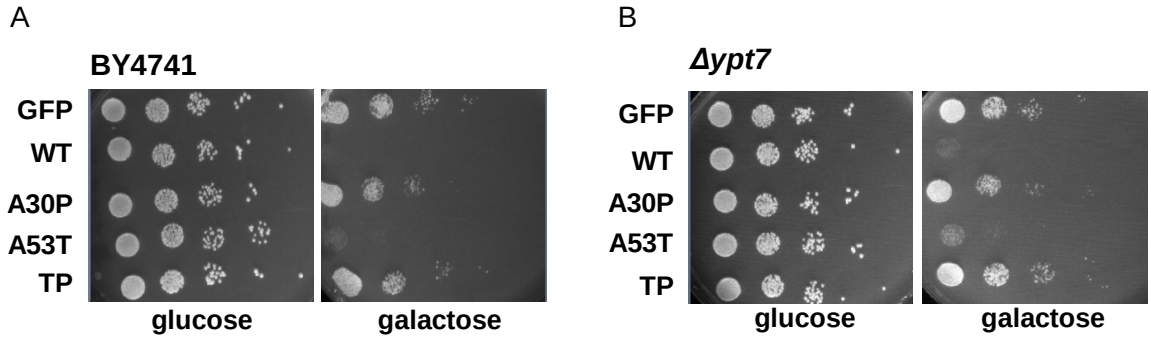

Figure 24. Lack of Ypt7 does not affect α-synuclein toxicity. Spotting analysis of (A) parent strain BY4741 and (B) *Δypt7* mutant transformed with a high-copy vector carrying GFP-tagged WT, A30P, A53T or TP α-synuclein controlled by the *GAL1* promoter. Cells expressing GFP served as control. The plates were incubated at 30°C for 2 days then photographed.

The toxicity of α-synuclein on cell growth was the same in the *Δypt7* mutant as in the parent strain. This implied that lack of Ypt7 does not render A30P or TP α-synuclein toxic and neither does it alter the toxicity of the WT and A53T versions.

Taken together, these results show that lack of Ypt7 leads to an accumulation of α-synuclein in the cytosol, which does not affect its toxic effect on yeast growth. Futhermore, α-synuclein co-localization with the vacuolar membrane and with endocytic vesicles in wild type cells as well as with fragmented vacuoles in *Δypt7* cells hint at an interaction between α-synuclein and the endocytic pathway. Thus, α-synuclein could presumably be targeted to the vacuole for degradation.

3.2.6 The autophagy-inducing drug rapamycin promotes α-synuclein aggregate clearance

Yeast autophagy is controlled by TOR kinases (Noda *et al*., 2002). A small molecule which inhibits TOR is rapamycin, a macrolide antibiotic with anti-fungal and immunosuppressive properties (Wullschleger *et al*., 2006). Rapamycin has been used in many organisms to upregulate autophagy via TOR inhibition, including yeast (Kamada *et al*., 2004).

In this study, rapamycin was applied to yeast expressing α-synuclein with the aim of obtaining a deeper insight into the contribution of autophagy to α-synuclein aggregate clearance. First, W303 cells expressing GFP-tagged α-synuclein from two genomic loci (HiTox strain, Outeiro and Lindquist, 2003) were induced to express α-synuclein for 3h then incubated with rapamycin. 6h of α-synuclein induction with 3h of rapamycin treatment resulted in a decreased α-synuclein aggregation percentage, with no major differences among several drug concentrations tested (Figure 25A and C).

When cells were pre-incubated with rapamycin for one hour and washed before α-synuclein induction, the effects were dramatic. In the first hours of α-synuclein induction, cells could not develop aggregates and only plasma membrane localization of α-synuclein

was observed (Figure 25B). 6h of induction resulted in low aggregation percentages for all rapamycin concentrations tested. Moreover, the number of aggregates per cell was drastically reduced (Figure 25B and C). These data suggested that rapamycin pre-treatment was more effective than treatment after α-synuclein induction.

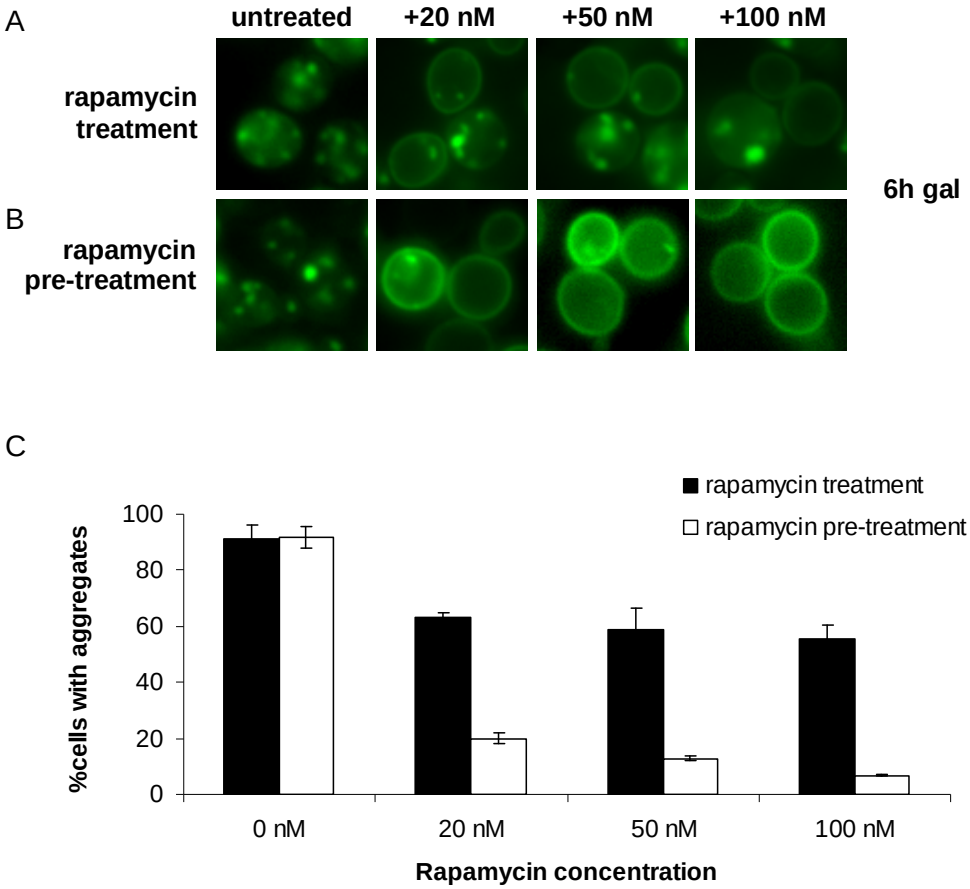

Figure 25. Rapamycin decreases α-synuclein aggregation. (A) Rapamycin treatment. W303 cells were induced in galactose to express GFP-tagged α-synuclein from two genomic loci (HiTox, Outeiro and Lindquist, 2003). At 3h of induction, when the aggregation percentage was 69% ± 8%, the galactose medium was supplemented with either 20, 50 or 100 nM rapamycin. For control, cells were left untreated. Live-cell fluorescence microscopy was performed after 6h of galactose induction and 3h of rapamycin treatment respectively. (B) Rapamycin pre-treatment. The three rapamycin concentrations were also applied to cells 1h before α-synuclein induction. After 1h of pre-treatment, cells were washed and shifted to galactose. 6h later, live-cell fluorescence microscopy was performed. No pre-treatment was applied to control cells. (C) Quantification of α-synuclein aggregation in cells treated and pre-treated with rapamycin. The column bars represent the mean values of three independent experiments.

The fact that α-synuclein aggregation percentages were reduced in both scenarios of rapamycin treatment suggested that TOR signaling is involved in α-synuclein aggregate clearance. Since TOR controls autophagy induction, the data further imply that autophagic

pathways are involved in α-synuclein aggregate clearance. Nevertheless, it should be taken into account that TOR inhibition by rapamycin affects not only autophagy but several other metabolic pathways (De Virgilio and Loewith, 2006).

As α-synuclein concentration proved to be an important factor in defining cytotoxicity and aggregate formation (Figure 13), the next step was to investigate whether rapamycin-induced aggregate clearance depends on α-synuclein dosage. Rapamycin effects on cells challenged with different α-synuclein concentrations were assessed in three scenarios of treatment. The drug was applied to cells expressing α-synuclein from two tandemic copies integrated in the genome or from a high-copy vector, before, at the same time, and after induction. Aggregation levels were monitored throughout time.

When α-synuclein was expressed from two genomic copies, rapamycin pre-treatment and treatment at the same time with α-synuclein induction prevented α-synuclein aggregate formation. Treatment started three hours after α-synuclein induction was less efficient than pre-treatment. However, it still reduced aggregation percentages with more than 50% compared to the untreated sample at the same time point. Aggregate size and number of aggregates per cell were smaller in rapamycin-exposed cells than in control cells (Figure 26A).

When α-synuclein was expressed from high-copy plasmids, rapamycin pre-treatment prevented aggregate formation in the first few hours of induction (Figure 26B). Cells were able to develop aggregates with time, reaching 49% aggregation at 8h of induction. This represented a substantial difference in comparison with untreated cells which displayed 81% aggregation at the same time point. Rapamycin treatment simultaneous with α-synuclein induction decreased aggregation with only 10% (Figure 26B) compared to 100% in the same treatment scenatio with low-copy α-synuclein expression (Figure 26A). Rapamycin treatment after α-synuclein induction from a high-copy vector resulted in 20% clearance and was less efficient than for low-copy expressed α-synuclein.

The decreased rapamycin clearance efficiency with increased α-synuclein concentration suggested that rapamycin clears α-synuclein aggregates in a dosage-dependent manner.

A

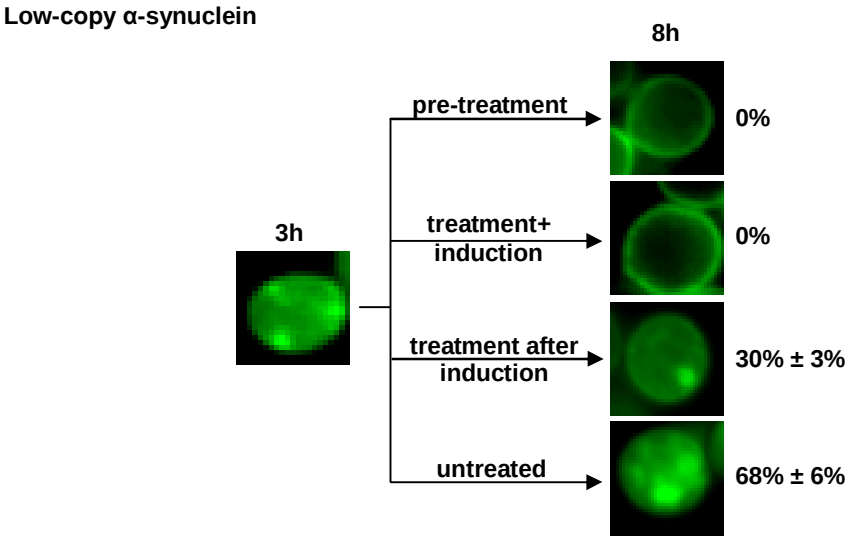

B

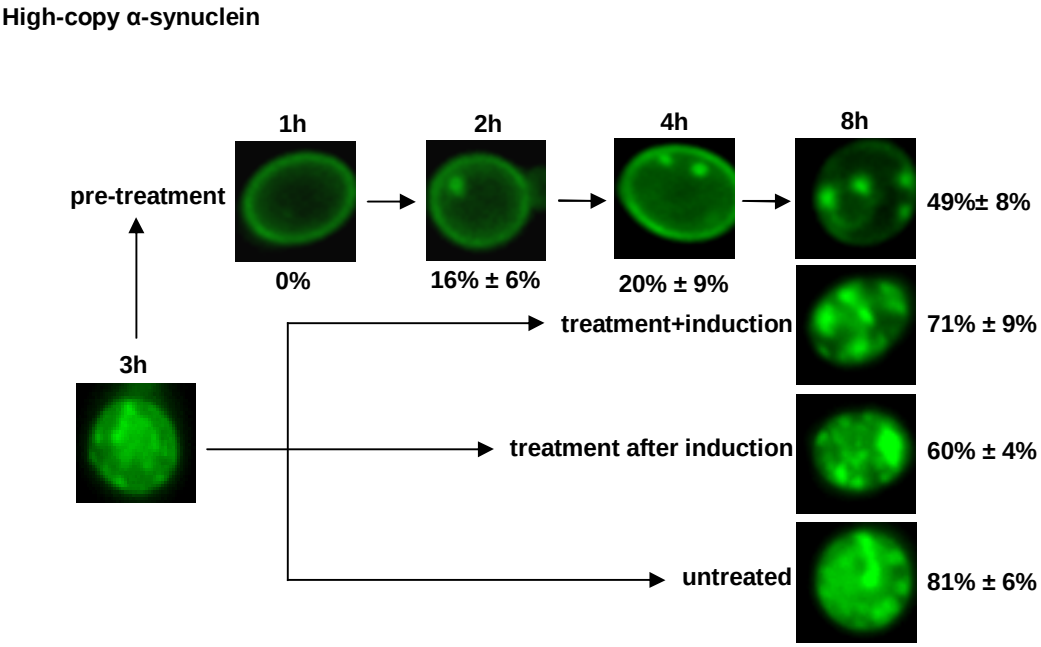

Figure 26. Rapamycin efficiency decreases with increased α-synuclein concentration. Live-cell fluorescence microscopy. W303 cells were induced to express WT α-synuclein (A) from two genomically-integrated copies (α-synuclein-AAAG-myeGFP) and (B) from a high-copy plasmid (α-synuclein-KLID-GFP). For rapamycin pre-treatment, cells were incubated in raffinose medium supplemented with 100 nM rapamycin for 1h and washed prior to transfer to galactose. For treatment+induction, cells pre-grown in raffinose were shifted to galactose supplemented with 100 nM rapamycin. For treatment after induction, at the 3h time point of α-synuclein induction rapamycin was added to the galactose medium at a final concentration of 100 nM. Untreated cells served as control. At 3h of induction the aggregation percentage of WT α-synuclein-AAAG-myeGFP expressed from two genomic copies was 29% ± 8%. Time points after α-synuclein induction and aggregation percentages are indicated.

To determine whether rapamycin discriminates between the aggregates of different α-synuclein variants, the drug was applied to cells overexpressing WT, A30P and A53T α-synuclein in different treatment scenarios (Figure 27).

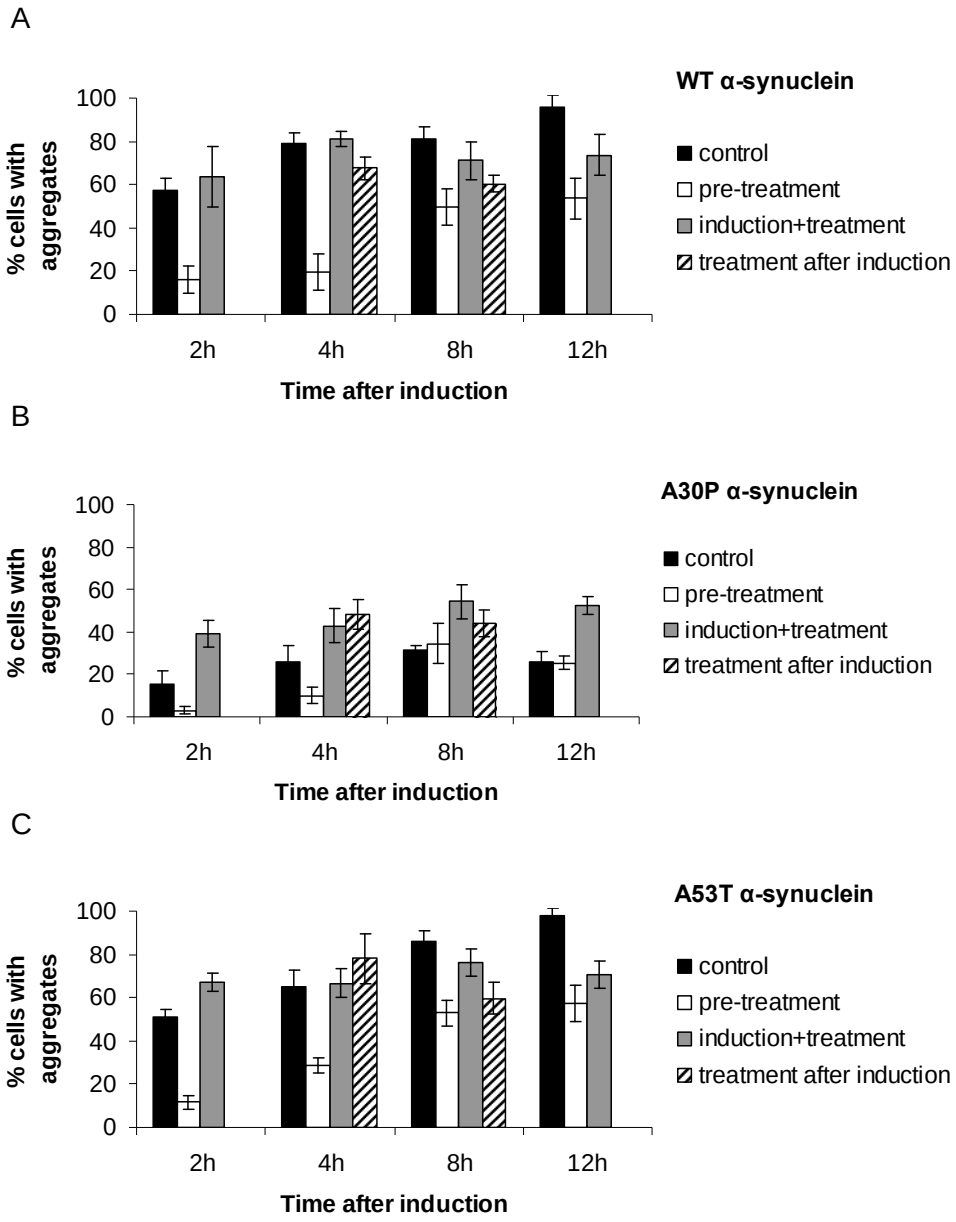

Figure 27. Rapamycin pre-treatment is impartial to α-synuclein species. Aggregation quantification. W303 cells expressed GFP-tagged (A) WT, (B) A30P and (C) A53T α-synuclein from a high-copy plasmid. For rapamycin pre-treatment, cells were incubated in raffinose supplemented with 100nM rapamycin for 1h and washed prior to transfer to galactose. For treatment+induction, cells pre-grown in raffinose were shifted to galactose supplemented with 100 nM rapamycin. For treatment after induction, 100 nM rapamycin were added to the medium after three hours of α-synuclein induction. Untreated cells served as control. α-synuclein aggregation percentages at different time points of α-synuclein induction are presented as column bars.

For all three α-synuclein variants, rapamycin pre-treatment was the most efficient treatment scenario, delaying formation of aggregates and considerably reducing their percentages later on. Rapamycin treatment after α-synuclein induction and treatment at the same time with induction reduced WT and A53T α-synuclein aggregation by 10-20% (Figure 27A and C) and seemed to increase the aggregation of A30P α-synuclein (Figure 27B), proving to be less effective than pre-treatment.

Since all α-synucleins responded similarly to rapamycin pre-treatment and WT and A53T α-synucleins showed comparable responses to treatments, it was concluded that rapamycin-induced α-synuclein aggregate clearance in yeast is not variant-specific.

3.2.7 WT and A53T α-synuclein delay induction of autophagy

The final aim of this study was to investigate the interplay between α-synuclein and autophagy in yeast. Promoter shut-off analysis and rapamycin studies demonstrated the involvement of autophagy in α-synuclein aggregate clearance in yeast. Conversely, to assess the extent to which α-synuclein influences autophagy, a macroautophagy-monitoring assay (Cheong *et al*., 2005) was employed. The assay is based on the fact that once autophagy is induced, the ubiquitin-like protein Atg8 coupled N-terminally to GFP is delivered to the vacuole via the Cvt pathway. Autophagy is inducible in yeast by nitrogen starvation which can be achieved by incubation in a nitrogen-deficient medium such as SD(-N) (Takeshige *et al*., 1992). Upon autophagy induction, GFP-Atg8 is delivered to the vacuole. Atg8 is degraded inside the vacuole and GFP is released in the cytoplasm. This can be visualized on a western membrane as the appearance of an additional protein band corresponding to GFP. The signal of processed GFP is quantified as percentage from the sum of processed and unprocessed GFP signals. This defines the percentage of autophagy processing in a sample (Cheong *et al*., 2005).

W303 wild type yeast was co-transformed with vectors harboring untagged α-synuclein and GFP-Atg8. The expression of GFP-Atg8 did not affect the typical yeast growth

reduction induced by α-synuclein (Figure 28A). In turn, α-synuclein overexpression did not interfere with GFP processing. Relocalization of the GFP signal visualized before and after transferring cells to SD(-N) mdium confirmed that autophagy was successfully induced (Figure 28B).

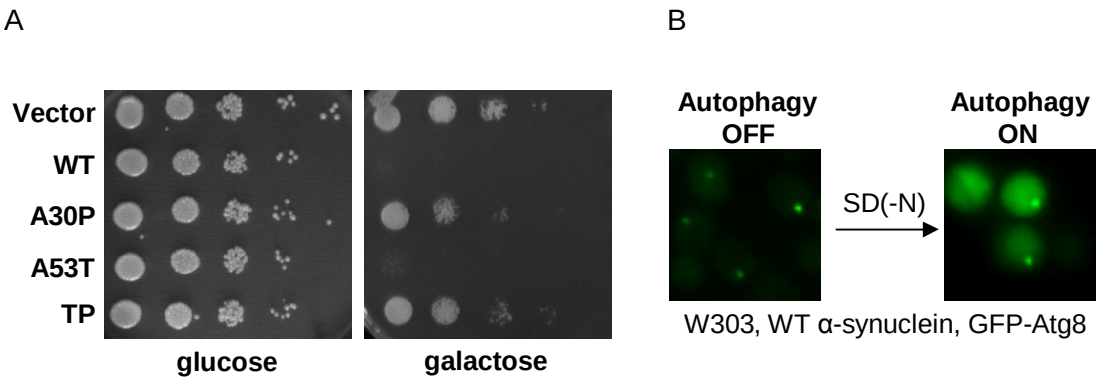

Figure 28. GFP-Atg8 does not interfere with α-synuclein toxicity and α-synuclein does not affect GFP-Atg8 processing. (A) Spotting analysis of wild type W303 yeast cells co-transformed with high-copy plasmids carrying untagged α-synuclein or mutants under the control of *GAL1* promoter and GFP-Atg8 under the control of the copper-inducible promoter *CUP1*. (B) Live-cell fluorescence microscopy of W303 cells induced for 2h in galactose supplemented with 50 µM $CuSO_4$ to express untagged WT α-synuclein and GFP-Atg8 (left). Cells were shifted to nitrogen starvation medium SD(-N) and observed by fluorescence microscopy four hours later (right).

First, the autophagy ratios of cells growing under normal conditions of α-synuclein induction were analyzed. The western membrane revealed three GFP-related protein bands. The top one correspsonded to GFP-Atg8 (~40 kDa) and the bottom one to GFP (~27 kDa). The middle one presumably corresponded to GFP-Atg8-PE, where Atg8-PE is the lipidated form of Atg8. Atg8-PE usually migrates faster than Atg8 (Huang *et al.*, 2000; Kirisako *et al.*, 2000). For calculating the GFP processing percent, the GFP-Atg8 and the GFP bands were considered. The western membrane was additionally probed with an anti-α-synuclein antibody to ensure the expression of α-synuclein.

The data showed that autophagy percents varied among cells expressing different α-synuclein variants (Figure 29A). In the first four hours of α-synuclein induction, differences between autophagy ratios of cells expressing WT, A53T and TP α-synuclein and control were minor. At 2h of induction, the autophagy ratio of cells expressing A30P was

substantially higher than that of control, suggesting that A30P can up-regulate autophagy. By the 8th hour of induction, this ratio became comparable to that of control, meaning that the effect was only transient. At 4h of induction the autophagy ratio of cells expressing A53T was smaller than that of control cells. At 8h of induction this ratio became half of the control autophagy ratio, suggesting a progressive inhibitory effect of A53T on autophagy (Figure 29A).

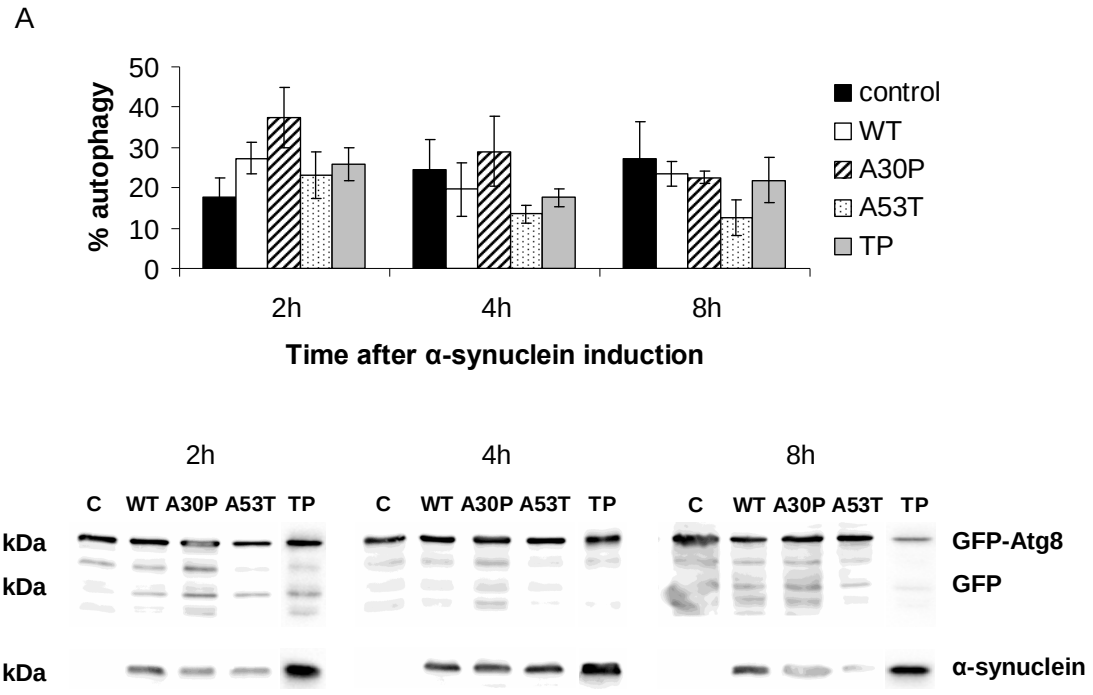

Figure 29. α-synuclein perturbs autophagy. (A) Quantification of autophagy in cells expressing untagged α-synuclein or variants at the indicated time points during eight hours of induction. Prior to α-synuclein induction cells were incubated for 2h in raffinose medium supplemented with 50 µM $CuSO_4$ to express GFP-Atg8 then washed. The column bars represent the average of four independent experiments. Cells which expressed GFP-Atg8 but not α-synuclein served as control. (B) Corresponding western blots at 2, 4 and 8h of α-synuclein induction. Membranes were probed with anti-GFP and anti α-synuclein antibodies.

Autophagy-monitoring assays were employed not only to analyze the influence of α-synuclein on autophagy but also to determine whether α-synuclein interferes with the induction of this process. Cells expressing α-synuclein for 4h were shifted to autophagy-inducing medium, SD(-N). To maintain α-synuclein expression during nitrogen starvation, the medium was prepared with galactose as carbon source. Quantifications of autophagy processing showed that A30P and TP α-synucleins did not influence autophagy

throughout time, as the autophagy ratios in cells expressing these variants were comparable to those of control (Figure 30A). In contrast, the autophagy ratios of cells expressing WT and A53T α-synuclein were considerably lower than those of control. These differences were less pronounced at 4h that at 2h of starvation, suggesting that WT and A53T α-synucleins do not inhibit but delay autophagy induction.

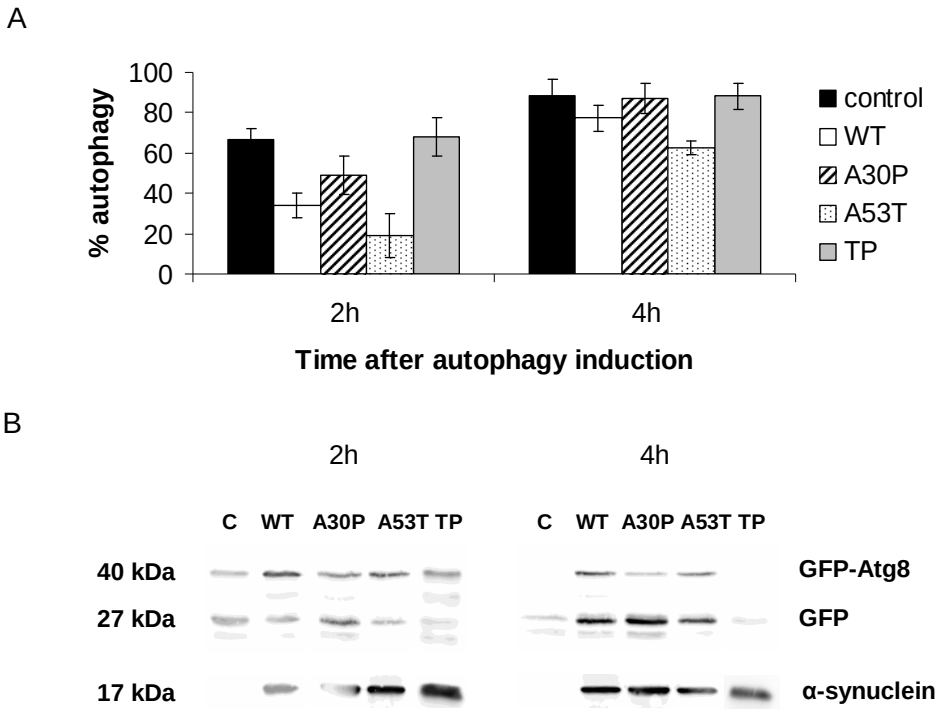

Figure 30. WT and A53T α-synucleins delay autophagy induction. (A) Quantification of autophagy under starvation conditions. Cells were induced for 4h in galactose to produce α-synuclein then shifted to nitrogen starvation medium SD(-N) medium further supplemented with galactose. Prior to α-synuclein induction cells were incubated for 2h in raffinose medium supplemented with 50 µM $CuSO_4$ to express GFP-Atg8 then washed. Probes were taken at 2 and 4h after the shift. W303 cells which expressed GFP-Atg8 but not α-synuclein served as control. The column bars represent the average of four independent experiments. (B) Corresponding western blots at 2 and 4h of starvation. Membranes were probed with anti-GFP and anti α-synuclein antibodies.

Cell culture models have proposed that besides autophagy, the 26S proteasome is involved in α-synuclein clearance (Webb *et al.*, 2003; Rott *et al.*, 2008). To determine whether proteasome inhibition would enhance the previously observed inhibitory effects of α-synuclein on autophagy, autophagy-monitoring assays were performed with the temperature-sensitive proteasome mutant *cim3-1*. Autophagy ratios were monitored in

cim3-1 cells growing at both permissive temperature (25°C) and at a sub-lethal inducing temperature (37°C). A preliminary spotting assay showed that α-synuclein cytotoxicity observed at 30°C (Figure 7) was reproducible at 25°C and was not disturbed by co-expression of GFP-Atg8 (Figure 31A).

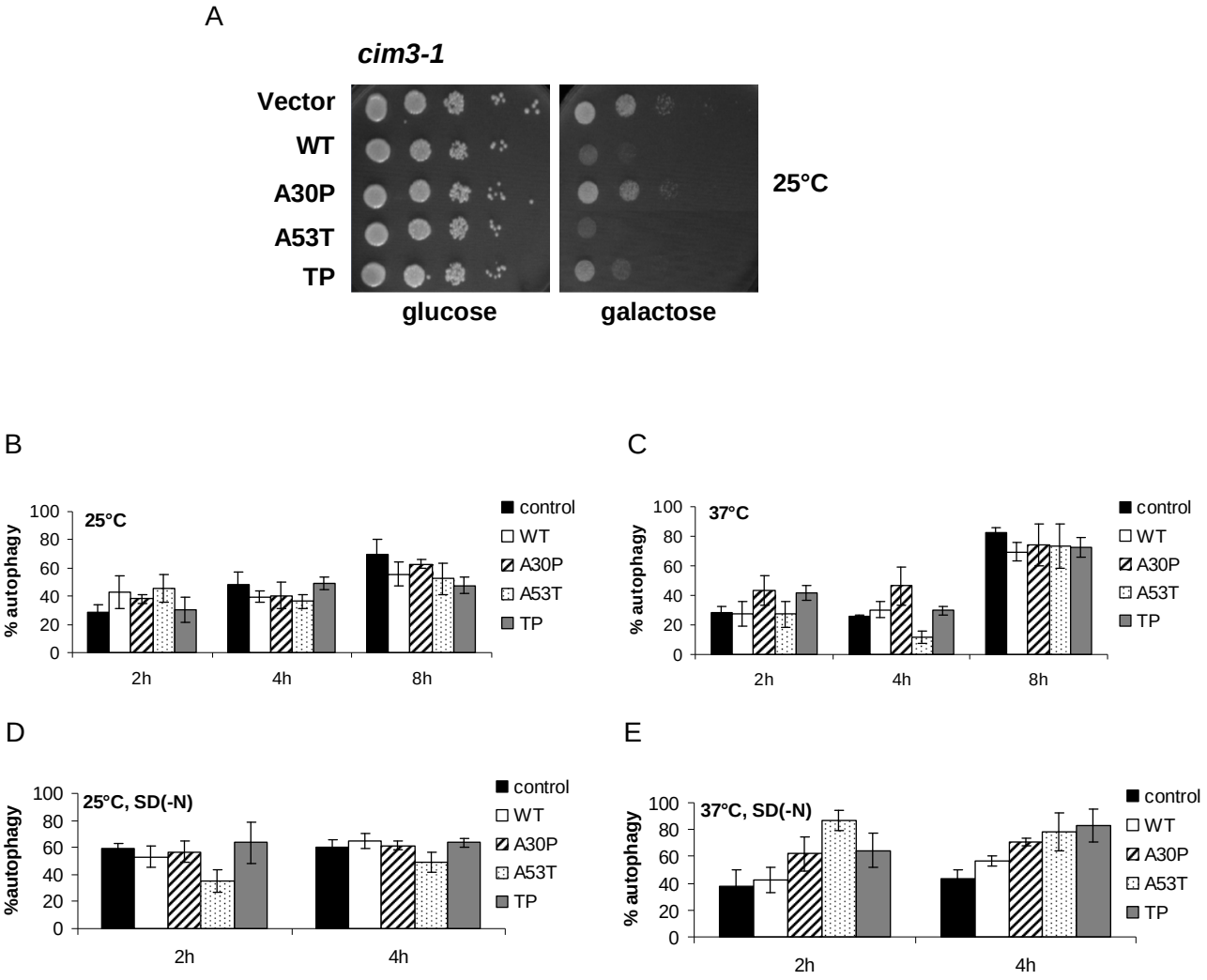

Figure 31. α-synuclein interference with autophagy in the *cim3-1* mutant. (A) Spotting analysis of temperature-sensitive *cim3-1* yeast. Cells were co-transformed with high-copy plasmids carrying untagged WT α-synuclein or versions under the control of *GAL1* promoter and GFP-Atg8 under the control of copper-inducible promoter *CUP1*. Cells which expressed GFP-Atg8 but not α-synuclein served as control. (B, C) Quantification of autophagy in *cim3-1* cells growing at (B) repressive temperature (25°C) and (C) at inducing temperature (37°C). Before α-synuclein induction, cells were incubated for 2h in raffinose medium supplemented with 50 µM $CuSO_4$ to express GFP-Atg8 then washed. (D, E). Quantification of autophagy during nitrogen starvation. Cells were induced for 4h in SC medium with galactose then shifted to SD(-N) medium with galactose. Prior to α-synuclein induction, cells were incubated for 2h in raffinose medium supplemented with 50 µM $CuSO_4$ to express GFP-Atg8 then washed. Probes were taken at 2 and 4h after the shift. Cells were grown (D) at repressive temperature (25°C) and (E) at induction temperature (37°C).

Autophagy assays in the *cim3-1* background allowed for a comparison of autophagy processing during α-synuclein induction between wild type and proteasome-deficient cells. Autophagy ratios influenced by α-synuclein were generally comparable for wild type cells and for *cim3-1* cells at non-inducing temperature during galactose induction (Figures 29A and 31B), with minor differences for A30P and TP α-synuclein. Autophagy rations were also comparable during nitrogen starvation (Figures 30A and 31D). The *cim3-1* mutation was induced at 37°C. At this temperature, the autophagy ratios of mutant cells growing in galactose (Figure 31C) were again comparable to those of the parent strain (Figure 29A), except that at 8h of induction, the inhibitory effect of A53T α-synuclein was milder in the mutant than in wild type cells. However, under nitrogen starvation conditions, in contrast to the parent strain (Figure 30A), autophagy ratios of *cim3-1* cells expressing α-synuclein were at all time points higher than those of α-synuclein-free cells (Figure 31E). This suggested that α-synuclein enhanced the induction of autophagy in the *cim3-1* mutant. Interestingly, TP α-synuclein was also able to enhance autophagy induction, although this version was not cytotoxic in the spotting assays (Figure 31A) and did not affect autophagy ratios in wild type cells (Figure 30A).

Taken together, these data suggested that under conditions of proteasomal inhibition α-synuclein can enhance autophagy up-regulation.

"The important thing in science is not so much to obtain new facts as to discover new ways of thinking about them."

William Lawrence Bragg

4. DISCUSSION

The main culprit of Parkinson's disease is α-synuclein, a small protein which misfolds and accumulates, leading to neurodegeneration (Spillantini *et al*., 1998b). The pathogenicity of the disease has not been fully elucidated, yet many attempts are being made towards understanding the mechanisms of α-synuclein toxicity. α-synuclein has been studied in cell culture as well as in diverse model organisms including *Drosophila melanogaster*, *Caenorhabditis elegans*, *Mus musculus* and *Saccharomyces cerevisiae*. Although the yeast *S. cerevisiae* is a unicellular organism, its popularity among neurodegeneration model systems has increased considerably over the past decade. Since the first characterization of the yeast PD model by Outeiro and Lindquist in 2003, yeast has been used not only for understanding the behavior of α-synuclein in PD but also for identifying novel therapeutic strategies.

4.1 Toxicity and localization of α-synuclein in yeast

A central question addressed in the present study concerns the long-debated aspect of α-synuclein toxicity in the yeast *S. cerevisiae*. It is important to note though, that the commonly used term *toxicity* is a rather general one. While α-synuclein toxicity in itself may elicit numerous and perhaps cumulative effects such as interference with the cell cycle, failure of quality control mechanisms, impairment of cellular degradation and oxidative stress, most reports often define α-synuclein toxicity in yeast solely by its ability

to impair growth. For consistency reasons, this study also referes to the ability of α-synuclein to inhibit yeast growth as toxicity or cytotoxicity.

α-synuclein toxicity and aggregation are the first and foremost requirements for modelling Parkinson's disease in yeast, corresponding to loss of dopaminergic neurons and respectively to Lewy body formation in PD brains. The first goal of this work was to determine under which conditions α-synuclein pathobiology can be studied in yeast. The challenge consisted in preserving α-synuclein's natural properties in fluorescently tagged versions of the protein, which are indispensable for microscopic studies. Since reliable fluorescently tagged α-synuclein constructs are needed to investigate aggregate dynamics in living cells and since the literature did not offer a model for such constructs, it was important to obtain a comprehensive insight into the requirements for functional α-synuclein-GFP fusions. For this purpose, a variety of constructs were analyzed, including high-copy/low-copy expression systems, GFP fusions to the N- and C- termini of α-synuclein, different fluorescent tags and different linkers separating α-synuclein and the tag.

Growth analysis revealed that tagged α-synucleins paralleled their untagged counterparts when the fluorescent tag was C-terminally fused to α-synuclein via a linker (Figures 7 and 9). Overexpressed WT and A53T α-synuclein were toxic to growth and aggregated, as reported by previous studies (Dixon *et al*., 2005; Outeiro and Lindquist, 2003). The A30P variant caused only a moderate growth reduction and formed aggregates transiently, while the designer mutant TP α-synuclein had no effect on yeast growth and did not develop aggregates. These findings suggested a link between α-synuclein cytotoxicity and aggregation.

While WT, A30P and A53T α-synuclein had previously been investigated in yeast, the phenotypic analysis of TP α-synuclein was performed here for the first time in this model organism (Figures 7, 9 and 10). The fact that TP did not aggregate in yeast (Figure 10) corresponds to previous *in vitro* results (Karpinar *et al*., 2009). However, in yeast TP was

not toxic to cell growth (Figure 7) as it was in models of worms, flies and mammalian neurons (Karpinar *et al*., 2009).

The relevance of tag position and of linker in α-synuclein fusion constructs was emphasized when cells expressing α-synuclein variants N-terminally coupled to GFP via linker and C-terminally fused to GFP without linker grew uninhibited (Figure 12). The non-toxic phenotype of these constructs correlated with their inability to aggregate. Several linkers tested (KLID, AAAG, SAAAG) showed that linker composition does not affect α-synuclein toxicity or aggregation, therefore, the presence and not the nature of a linker is important for α-synuclein-GFP fussions (Figure 11). Moreover, the nature of fluorescent tag does not interfere with α-synuclein cytotoxicity and differences among tags rely only on aggregate morphology. For example, tags like GFP or mCherry give rise to well-defined aggregates, whereas tags like myeGFP produce diffuse and unclear foci (Figure 11).

The importance of tag position can be attributed to structural and physiological differences between the α-synuclein termini. The N-terminus presumably needs to remain tag-free since the N-terminal region induces α-synuclein oligomerization and accumulation (Karube *et al*., 2008; Soper *et al*., 2008). Alternatively, the C-terminus is highly acidic and tends to inhibit aggregation (Cookson, 2005; Murray *et al*., 2003). Capping the C-terminus with a tag might therefore prevent this tendency.

Live-cell fluorescence microscopy revealed a defined pattern for α-synuclein aggregation, which, as previously reported (Soper *et al*., 2008), starts with plasma membrane localization. This is likely due to the fact that α-synuclein is an amphyphatic protein which associates with lipid membranes (Davidson *et al*., 1998; Lucking and Brice, 2000; Narayanan and Scarlata, 2001). The association of α-synuclein with the yeast plasma membrane (Figures 10 and 13) correlates with its behavior in neuronal cells. There, the protein localizes at presynaptic terminals (Hsu *et al*., 1998) and it interacts with dopamine transporters located in the neuronal membrane to regulate the amount of dopamine entering the cell (Wersinger and Sidhu, 2003).

In the first two hours of α-synuclein-GFP induction, yeast cells exhibited fluorescence not only at the plasma membrane but also at the vacuolar membrane, as demonstrated by FM4-64 stainings (Figure 23). In addition, α-synuclein co-localized with endocytic vesicles and with fragmented vacuoles in a *Δypt7* mutant, suggesting that the protein could be targeted to the vacuole, presumably for degradation. These data are consistent with recent findings that α-synuclein co-localizes with vesicular clusters involved in the secretory pathway (Soper *et al*., 2011). α-synuclein transport to the vacuole has been proven so far only for the A30P version (Flower *et al*., 2007).

4.2 A30P α-synuclein can form aggregates in yeast

Expression of untagged A30P α-synuclein as well as of A30P α-synuclein-KLID-GFP from a high-copy plasmid partially affected cell growth and resulted in aggregate formation (Figures 7, 9 and 10). Although A30P aggregated, the aggregation percentages of cells expressing this mutant were significantly lower than the aggregation percentages of cells expressing WT or A53T α-synuclein. Given that A30P aggregation was only transient, these data suggested that yeast can cope better with A30P aggregates.

The gene dosage analysis revealed that, in contrast to WT and A53T α-synuclein, genomically-integrated A30P was not toxic and did not form aggregates (Figure 13). As the mutant was partially toxic and aggregated only when expressed from a 2µ plasmid, the prerequisite for the A30P α-synuclein phenotype is strong overexpression.

The lack of A30P toxicity and aggregation upon low-copy expression as well as the moderate toxicity and transient aggregation achieved by overexpression may be due to an ability of yeast cells to degrade A30P faster than other versions. Consistently, autophagy monitoring assays revealed that in the first hours of induction A30P α-synuclein up-regulates autophagy (Figure 29). The effect was no longer visible at later time points, meaning that autophagy induction is only transitory. Perhaps the transitory induction of

autophagy is sufficient to clear toxic A30P α-synuclein species, thus preventing their accumulation and relieving the cell from growth inhibition.

Decreased binding of A30P α-synuclein to the plasma membrane, necessary for toxicity (Volles and Lansbury, 2007), might also explain the decreased toxicity of this mutant. A30P has long been reported not to associate with membranes as strongly as WT or A53T (Lashuel *et al*., 2002) due to a decreased affinity for lipid surfaces (Bussell and Eliezer, 2004).

Besides not influencing yeast growth, A30P had also been reported not to aggregate in yeast (Dixon *et al*., 2005; Outeiro and Lindquist, 2003), which contradicted its behavior in mammalian cells and *in vitro* (Cookson, 2005; Giasson *et al*., 1999; Spillantini *et al*., 1997). In this study the aggregation percentages of A30P were lower than those of WT and A53T α-synuclein and A30P aggregation was only transient, yet the ability of A30P α-synuclein to form aggregates considerably extends the yeast PD model.

4.3 α-synuclein aggregation is not a prerequisite for cytotoxicity

Strains expressing α-synuclein from genomically-integrated copies offered a deeper insight into the relationship between growth toxicity and aggregation. Integration of one, two and three copies of α-synuclein alleles in the yeast genome aimed at determining the gene dosage required for the protein to be toxic and to aggregate. Three tandemic copies of WT and two of A53T α-synuclein were defined as thresholds for toxicity (Figure 13), which corresponds to the finding that α-synuclein allele multiplication such as duplication and triplication is linked to a familial form of PD (Hardy *et al*., 2006; Singleton *et al*., 2003). The fact that the threshold for A53T toxicity was lower than for WT correlates with a higher propensity of A53T to fibrilize, reported both *in vitro* and in transgenic mouse models (Conway *et al*., 1998; Giasson *et al*., 1999). Consistently, the number of Lewy bodies in PD dopaminergic neurons is higher for A53T than for WT α-synuclein (Sampathu *et al*., 2003).

The gene dosage analysis revealed that α-synuclein was able to develop aggregates without impairing cell growth (Figure 13), which implies that a certain level of α-synuclein aggregation is needed for growth inhibition. While three copies of WT or two copies of A53T α-synuclein cause abundant aggregation and inhibit growth, one copy of WT or one copy of A53T results only in low aggregation which allows yeast to grow normally. In comparison, two copies of WT α-synuclein and overexpressed A30P α-synuclein develop moderate aggregation and do not inhibit growth (Figure 32).

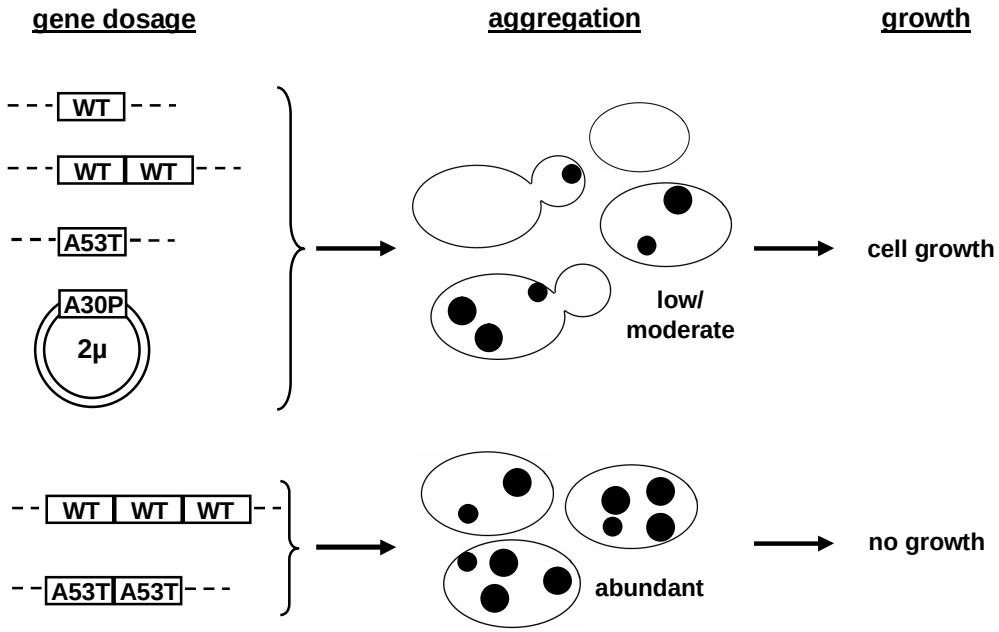

Figure 32. α-synuclein gene dosage influences its aggregation and ability to impair yeast growth. WT α-synuclein expressed from one and two genomically-integrated tandemic copies, A53T α-synuclein expressed from one genomic copy and A30P α-synuclein expressed from a high-copy vector result in low to moderate aggregation and do not impair yeast growth. Three WT and two A53T α-synuclein tandemic copies lead to abundant aggregation and impair growth. The *GAL1-SNCA-GFP* sequence is represented by squares and the α-synuclein variant is indicated in each square. The dotted lines on the left side represent genomic DNA.

Another indication that a limited amount of aggregates may not be toxic for yeast was given by growth recovery experiments (Figure 15). Once the *GAL1* promoter was shut off after 8h of α-synuclein expression, yeast cells recovered from α-synuclein-induced toxicity. Although cells could not immediately undergo cell division, later on, presumably after α-synuclein aggregates got cleared, they presented a normal colony formation kinetic

(Figure 16). Further promoter shut-off experiments proved that yeast cells can indeed clear α-synuclein aggregates as soon as the α-synuclein supply is interrupted. The observation that to a certain extent α-synuclein aggregates are not toxic is additionally supported by the fact that a number of PD neurons survive despite containing Lewy bodies (Forno *et al*., 1996). It remains unknown whether aggregates have a cytoprotective role, as they are assumed in late stages of the disease.

Furthermore, evidence emerged that oligomeric species rather than aggregates of α-synuclein are responsible for toxicity (Karpinar *et al*., 2009; Outeiro *et al*., 2008). In several PD models the rate of fibrilization and aggregation do not correlate with toxicity (Chen and Feany, 2005; Karpinar *et al*., 2009; Outeiro and Lindquist, 2003; Volles and Lansbury, 2002 and 2007). For example, the TP α-synuclein mutant is unable to aggregate, yet it causes neurotoxicity in several organisms (Karpinar *et al*., 2009). The fact that TP is not toxic to yeast growth (Figure 7) suggests that yeast might be more resistent to oligomeric states of α-synuclein than higher eukaryotes.

4.4 Minor proteasomal contribution to α-synuclein aggregate clearance

The present work questions the involvement of the ubiquitin-proteasomal system in α-synuclein aggregate clearance in yeast. The fact that proteasome-impaired cells were able to clear α-synuclein aggregates upon promoter shut-off suggested an insignificant contribution of the 26S proteasome to aggregate clearance, which is consistent with earlier findings (Biasini *et al*., 2004). In particular, MG132 treatments did not enhance α-synuclein accumulation to the extent that the protein could no longer be cleared (Figure 19). Similarly, in neuroblastoma and oligodendroglial cells, inhibition of the proteasome by MG132 did not induce α-synuclein aggregation (Dyllick-Brenzinger *et al*., 2010; Riedel *et al*., 2010) and in yeast, A30P α-synuclein was still degraded despite proteasomal inhibition with the same drug (Flower *et al*., 2007). Supporting these findings,

polyubiquitination of α-synuclein has never been reported in yeast or in higher organisms (Stefanis *et al*., 2001).

Mammalian PD models propose that most α-synuclein in the cell is degraded not by the proteasome but by lysosomal enzymes (Paxinou *et al*., 2001). A reason for diminished involvement of the proteasome in α-synuclein aggregate clearance could be that α-synuclein itself alters the composition of the proteasome and impairs proteasomal degradation (Chen *et al*., 2005). While α-synuclein may be degraded by the proteasome (Bennett *et al*., 1999; Tofaris *et al*., 2001), an accumulation of the protein could inhibit the system (Lindersson *et al*., 2004). In turn, proteasomal inhibition would favor further α-synuclein aggregation (Bedford *et al*., 2008; McNaught and Jenner, 2001).

4.5 Involvement of vacuolar and autophagic pathways in α-synuclein aggregate clearance

The main degradation site in yeast is the vacuole. This is the final destination of many vesicles, including autophagosomes delivered via autophagy (Noda *et al*., 1995). The present study offers several lines of evidence that, in yeast, autophagy and the vacuole are major players in α-synuclein aggregate clearance. Treatments with the vacuolar protease inhibitor PMSF resulted in impaired α-synuclein aggregate clearance and increased α-synuclein aggregation (Figures 19 and 20), highlighting the importance of the vacuole in α-synuclein degradation. Supporting this finding, a *Δpep4* mutant characterized by vacuolar defects presented decreased efficiency in clearing α-synuclein aggregates compared to the wild type cells (Figure 21). Both chemical and genetic approaches indicated the contribution of vacuolar pathways in α-synuclein aggregate clearance. Since aggregate clearance was not severely inhibited in *Δpep4* cells, there could be more proteases involved in the process than the ones controlled by *PEP4*. For example, cell-culture models propose that α-synuclein can be degraded by the serine protease

neurosin, which is released from the mitochondria into the cytosol upon cellular stress (Iwata *et al*., 2003).

A *Δatg1* mutant defective in autophagy was unable to clear α-synuclein aggregates in the first 2h after promoter shut-off (Figure 21B), validating cell culture findings that autophagy inhibition slows down aggregate clearance (Fortun *et al*., 2003). The fact that *Δatg1* could still clear aggregates, although with reduced efficiency, suggests that autophagy is involved in the process but not essential.

Presumably, while bulky α-synuclein aggregates are preferentially degraded by autophagy, the extent to which they are degraded by the 26S proteasome is rather small. A higher contribution of autophagy than of the proteasome to α-synuclein degradation might also reflect the situation in mammalian systems, where autophagy inhibition promotes the accumulation of monoubiquitinated forms of α-synuclein (Rott *et al*., 2008; Yu *et al*., 2009). Cell culture models provide additional evidence that macroautophagy and chaperone-mediated autophagy but not the proteasome are involved in α-synuclein degradation (Vogiatzi *et al*., 2008).

The fact that a *cim3-1Δatg1* yeast double mutant impaired in both proteasomal and autophagic degradation was still able to clear α-synuclein aggregates (Figure 21) suggests additional yet unexplored mechanisms for aggregate clearance. In neuronal cells, one additional route for α-synuclein degradation is the endosomal-lysosomal pathway (Tofaris *et al*., 2011).

4.6 Rapamycin-induced aggregate clearance

An additional proof confirming the importance of autophagy in α-synuclein degradation came from experiments involving autophagy upregulation with the drug rapamycin. Rapamycin was reported to protect against huntingtin-induced neurodegeneration in flies and mice (Berger *et al*., 2006; Ravikumar *et al*., 2002) and to reduce α-synuclein

aggregation levels in cell culture (Webb *et al*., 2003) and in yeast (Zabrocki *et al*., 2005) models of PD.

This work analyzed the conditions in which rapamycin influences α-synuclein aggregate clearance in yeast. Three different scenarios of rapamycin treatment were investigated, before, at the same time and after α-synuclein induction. The data argued in favor of rapamycin pre-treatment, i.e. before α-synuclein induction, for optimal effects. The analysis also showed that rapamycin-induced clearance is a function of α-synuclein concentration, as the drug affected high-copy expressed α-synuclein less than it affected low levels of the protein (Figure 26). Additionally, rapamycin-induced clearance does not discriminate among α-synuclein variants, which could suggest that α-synuclein aggregate clearance in yeast is a universal phenomenon (Figure 27).

Although rapamycin treatment resulted in a reduction of aggregates, autophagy might not be the only pathway responsible for this effect. While rapamycin was reported to induce autophagy by inhibiting the TOR signaling pathway (Klionsky and Emr, 2000), TOR controls several other cellular processes, including ribosome biogenesis, transcription and translation (De Virgilio and Loewith, 2006; Sarbassov *et al*., 2005; Wullschleger *et al*., 2006). Rapamycin-induced α-synuclein aggregate clearance could also occur through inhibition of protein synthesis which would reduce the monomeric concentration of α-synuclein. Less monomeric α-synuclein would result in less oligomerization and consequently, in less aggregates.

4.7 α-synuclein perturbs autophagy

Autophagy must be essential in neuronal tissue since its impairment promotes neurodegeneration (Hara *et al*., 2006; Komatsu *et al*., 2006; Kuma *et al*., 2004). It is not exclusive though, that α-synuclein accumulation itself might impair autophagy. To investigate this possibility in yeast, this study employed macroautophagy-monitoring assays (Cheong *et al.*, 2005). The transitory up-regulation of autophagy by A30P α-

synuclein in the first two hours of induction (Figure 29A) can be linked to the low A30P aggregation levels and the mildly toxic yeast growth phenotype. Autophagy up-regulation could be part of a detoxification mechanism. The enhanced autophagic degradation would remove the toxic α-synuclein which can be harmful to the cell and trigger apoptosis (Bandyopadhyay and Cuervo, 2007; Stefanis *et al*., 2001). Apart from A30P, autophagy rates of cells expressing α-synucleins were comparable to those of control, suggesting that α-synuclein overexpression does not activate autophagy. However, eight hours of A53T α-synuclein induction inhibited autophagy and when autophagy was induced by means of nitrogen starvation, both WT and A53T α-synuclein delayed its activation (Figure 30A). The more pronounced effect of A53T than of WT α-synuclein on autophagy inhibition correlates with the greater propensity of A53T to aggregate and with its lower toxicity threshold (Figure 13).

The inhibitory/delaying effects on autophagy of WT and A53T α-synucleins correlated with their ability to impair yeast growth. Generally, inhibition of autophagy means inhibition of a major cellular degradation route otherwise used by the cell to clear proteins which are no longer needed, including the aggregated α-synuclein. Thus, autophagy inhibition would increase the concentration of α-synuclein and at the same time its probability to aggregate and burden the cell. This would be detrimental to cellular homeostasis, preventing the degradation not only of α-synuclein but of other dysfunctional proteins or organelles and would further trigger apoptotic signals, as already observed in many PD models (Ravikumar and Rubinsztein, 2006; Stefanis *et al*., 2001). Correspondingly, in yeast, the end effect would be growth inhibition, as observed in spotting assays (Figure 7).

Autophagy-monitoring experiments in W303 yeast revealed that α-synuclein has an inhibitory effect on autophagy. Previous studies reported that α-synuclein inhibits autophagic pathways in neuronal cells and mice (Winslow *et al*., 2010; Xilouri *et al*., 2009). This means that the mechanism of autophagy inhibition by α-synuclein is conserved from yeast to higher organisms. With its extensive genetic tools, yeast can thus be conveniently employed to study autophagy inhibition by α-synuclein in more detail.

Interestingly, under conditions of proteasomal impairment, the induction of autophagy through nitrogen starvation was enhanced by α-synuclein overexpression (Figure 31E). Although this effect was not detected under non-starvation conditions, it might suggest a link between proteasome inhibition and autophagy up-regulation by α-synuclein. If proteasomal inhibition in PD causes α-synuclein to enhance autophagy induction, the effect might correlate with the increased amount of autophagic structures in PD neurons (Anglade *et al*., 1997).

Overall, this study had found that α-synuclein can inhibit autophagy and that autophagy and vacuolar pathways but not so much the proteasome are involved in α-synuclein aggregate clearance. It is possible that monomeric forms of α-synuclein are degraded by the proteasome while more complex oligomeric species are cleared by vacuolar pathways such as autophagy. Presumably, once accumulation and aggregation of α-synuclein impairs the proteasome (Chen *et al.*, 2005), α-synuclein can no longer be degraded by this system and clearance of α-synuclein aggregated relies on the vacuole via autophagic pathways. Eventually, an increase in α-synuclein aggregation levels would also impair autophagy. As suggested by proter shut-off analysis (Figure 21), there may be additional pathways clearing α-synuclein aggregates (Figure 33).

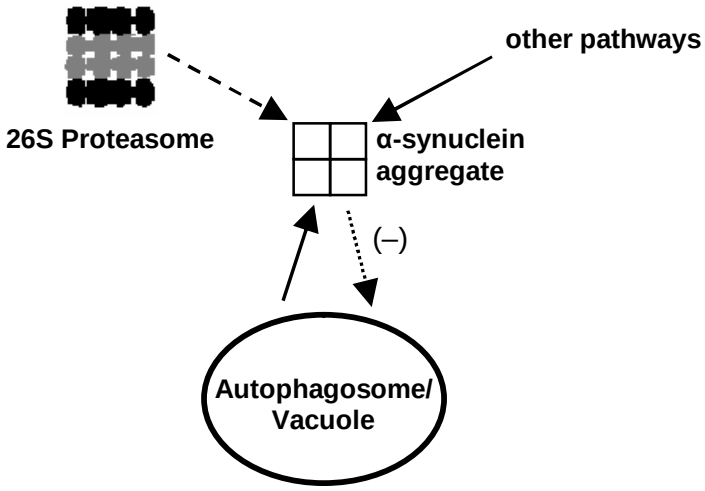

Figure 33. Model of α-synuclein clearance. The 26 proteasome has a minor contribution to α-synuclein aggregate clearance (interrupted arrow) while autophagy/vacuolar pathways clear α-synuclein aggregates (straight arrow). Accumulation of α-synuclein affects and delays autophagy (dotted arrow). Inhibitory effects are indicated by the minus sign. Additional unexplored pathways can be invlolved in α-synuclein aggregate clearance.

"We know very little, and yet it is astonishing that we know so much, and still more astonishing that so little knowledge can give us so much power."

Bertrand Russell

5. OUTLOOK AND FINAL REMARKS

This study employed yeast to model pathological features of Parkinson's disease with the aim of gaining a deeper insight into the cellular pathways responsible for α-synuclein degradation. Yeast offers unsurpassed advantages to study mechanisms of disease and the functionality of the yeast PD model is one of the proofs.

To date, the toxic mechanisms of PD have not yet been fully elucidated and there is no effective treatment for the disease. The findings of this work can be used as a new starting point for developing therapeutic strategies for PD and related synucleopathies. Details like aggregation-prone constructs and gene dosage will have a major impact in designing future experiments, particularly genetic screens. Additionally, autophagy, shown to be involved in α-synuclein aggregate clearance and at the same time to be inhibited by α-synuclein accumulation, may serve as a target for therapeutic intervention. A curative solution could be either preventing autophagy inhibition or up-regulating the process. This could be extensively investigated in yeast by up-regulating the transcription of autophagy-specific genes and by screening for chemicals that enhance the process.

Taken together, the molecular biology, biochemistry and cell biology experiments in this study shed new light into the yeast model for Parkinson's disease and have noteworthy implications for future research in the field. The results contribute to the understanding of α-synuclein toxicity mechanisms and can be further extended to higher model systems. Most importantly, yeast can be employed as a model for toxicity rescue and aggregate clearance, offering new inspiration in the quest for finding appropriate PD treatments.

"If I have seen further than others, it is by standing upon the shoulders of giants."

Isaac Newton

6. REFERENCES

Abeliovich, A., Schmitz, Y., Farinas, I., Choi-Lundberg, D., Ho, W.H., Castillo, P.E., Shinsky, N., Verdugo, J.M., Armanini, M., Ryan, A.*, et al.* (2000). Mice lacking alpha-synuclein display functional deficits in the nigrostriatal dopamine system. Neuron *25*, 239-252.

Abramoff, M., Magelhaes, P., and Ram, S. (2004). Image processing with ImageJ. Biophotonics Int *11*, 36-42.

Alim, M.A., Hossain, M.S., Arima, K., Takeda, K., Izumiyama, Y., Nakamura, M., Kaji, H., Shinoda, T., Hisanaga, S., and Ueda, K. (2002). Tubulin seeds alpha-synuclein fibril formation. J Biol Chem *277*, 2112-2117.

Alim, M.A., Ma, Q.L., Takeda, K., Aizawa, T., Matsubara, M., Nakamura, M., Asada, A., Saito, T., Kaji, H., Yoshii, M.*, et al.* (2004). Demonstration of a role for alpha-synuclein as a functional microtubule-associated protein. J Alzheimers Dis *6*, 435-442; discussion 443-439.

Ancolio, K., Alves da Costa, C., Ueda, K., and Checler, F. (2000). Alpha-synuclein and the Parkinson's disease-related mutant Ala53Thr-alpha-synuclein do not undergo proteasomal degradation in HEK293 and neuronal cells. Neurosci Lett *285*, 79-82.

Anglade, P., Vyas, S., Hirsch, E.C., and Agid, Y. (1997). Apoptosis in dopaminergic neurons of the human substantia nigra during normal aging. Histol Histopathol *12*, 603-610.

Auluck, P.K., Caraveo, G., and Lindquist, S. (2010). alpha-Synuclein: membrane interactions and toxicity in Parkinson's disease. Annu Rev Cell Dev Biol *26*, 211-233.

Bandyopadhyay, U., and Cuervo, A.M. (2007). Chaperone-mediated autophagy in aging and neurodegeneration: lessons from alpha-synuclein. Exp Gerontol *42*, 120-128.

Bedford, L., Hay, D., Devoy, A., Paine, S., Powe, D.G., Seth, R., Gray, T., Topham, I., Fone, K., Rezvani, N.*, et al.* (2008). Depletion of 26S proteasomes in mouse brain neurons causes neurodegeneration and Lewy-like inclusions resembling human pale bodies. J Neurosci *28*, 8189-8198.

Bennett, M.C., Bishop, J.F., Leng, Y., Chock, P.B., Chase, T.N., and Mouradian, M.M. (1999). Degradation of alpha-synuclein by proteasome. J Biol Chem *274*, 33855-33858.

Berger, Z., Ravikumar, B., Menzies, F.M., Oroz, L.G., Underwood, B.R., Pangalos, M.N., Schmitt, I., Wullner, U., Evert, B.O., O'Kane, C.J.*, et al.* (2006). Rapamycin alleviates toxicity of different aggregate-prone proteins. Hum Mol Genet *15*, 433-442.

Betarbet, R., Sherer, T.B., and Greenamyre, J.T. (2005). Ubiquitin-proteasome system and Parkinson's diseases. Exp Neurol *191 Suppl 1*, S17-27.

Biasini, E., Fioriti, L., Ceglia, I., Invernizzi, R., Bertoli, A., Chiesa, R., and Forloni, G. (2004). Proteasome inhibition and aggregation in Parkinson's disease: a comparative study in untransfected and transfected cells. J Neurochem *88*, 545-553.

Biskup, S., Gerlach, M., Kupsch, A., Reichmann, H., Riederer, P., Vieregge, P., Wullner, U., and Gasser, T. (2008). Genes associated with Parkinson syndrome. J Neurol *255 Suppl 5*, 8-17.

Bonini, N.M., and Giasson, B.I. (2005). Snaring the function of alpha-synuclein. Cell *123*, 359-361.

Bradford, M.M. (1976). A rapid and sensitive method for the quantitation of microgram quantities of protein utilizing the principle of protein-dye binding. Anal Biochem *72*, 248-254.

Bryant, N.J., and Stevens, T.H. (1998). Vacuole biogenesis in Saccharomyces cerevisiae: protein transport pathways to the yeast vacuole. Microbiol Mol Biol Rev *62*, 230-247.

Bussell, R., Jr., and Eliezer, D. (2004). Effects of Parkinson's disease-linked mutations on the structure of lipid-associated alpha-synuclein. Biochemistry *43*, 4810-4818.

Chandra, S., Chen, X., Rizo, J., Jahn, R., and Sudhof, T.C. (2003). A broken alpha -helix in folded alpha -Synuclein. J Biol Chem *278*, 15313-15318.

Chandra, S., Gallardo, G., Fernandez-Chacon, R., Schluter, O.M., and Sudhof, T.C. (2005). Alpha-synuclein cooperates with CSPalpha in preventing neurodegeneration. Cell *123*, 383-396.

Chen, L., and Feany, M.B. (2005). Alpha-synuclein phosphorylation controls neurotoxicity and inclusion formation in a Drosophila model of Parkinson disease. Nat Neurosci *8*, 657-663.

Chen, Q., Thorpe, J., and Keller, J.N. (2005). Alpha-synuclein alters proteasome function, protein synthesis, and stationary phase viability. J Biol Chem *280*, 30009-30017.

Cheong, H., Yorimitsu, T., Reggiori, F., Legakis, J.E., Wang, C.W., and Klionsky, D.J. (2005). Atg17 regulates the magnitude of the autophagic response. Mol Biol Cell *16*, 3438-3453.

Chiueh, C.C., Andoh, T., Lai, A.R., Lai, E., and Krishna, G. (2000). Neuroprotective strategies in Parkinson's disease: protection against progressive nigral damage induced by free radicals. Neurotox Res *2*, 293-310.

Ciechanover, A. (2006). The ubiquitin proteolytic system: from a vague idea, through basic mechanisms, and onto human diseases and drug targeting. Neurology *66*, S7-19.

Clayton, D.F., and George, J.M. (1998). The synucleins: a family of proteins involved in synaptic function, plasticity, neurodegeneration and disease. Trends Neurosci *21*, 249-254.

Cole, N.B., Murphy, D.D., Grider, T., Rueter, S., Brasaemle, D., and Nussbaum, R.L. (2002). Lipid droplet binding and oligomerization properties of the Parkinson's disease protein alpha-synuclein. J Biol Chem *277*, 6344-6352.

Collins, G.A., Gomez, T.A., Deshaies, R.J., and Tansey, W.P. (2010). Combined chemical and genetic approach to inhibit proteolysis by the proteasome. Yeast *27*, 965-974.

Conway, K.A., Harper, J.D., and Lansbury, P.T. (1998). Accelerated in vitro fibril formation by a mutant alpha-synuclein linked to early-onset Parkinson disease. Nat Med *4*, 1318-1320.

Cookson, M.R. (2005). The biochemistry of Parkinson's disease. Annu Rev Biochem *74*, 29-52.

Cooper, A.A., Gitler, A.D., Cashikar, A., Haynes, C.M., Hill, K.J., Bhullar, B., Liu, K., Xu, K., Strathearn, K.E., Liu, F.*, et al.* (2006). Alpha-synuclein blocks ER-Golgi traffic and Rab1 rescues neuron loss in Parkinson's models. Science *313*, 324-328.

Cuervo, A.M. (2004). Autophagy: in sickness and in health. Trends Cell Biol *14*, 70-77.

Cuervo, A.M. (2008). Autophagy and aging: keeping that old broom working. Trends Genet *24*, 604-612.

Cuervo, A.M., and Dice, J.F. (1998). Lysosomes, a meeting point of proteins, chaperones, and proteases. J Mol Med (Berl) *76*, 6-12.

Cuervo, A.M., Stefanis, L., Fredenburg, R., Lansbury, P.T., and Sulzer, D. (2004). Impaired degradation of mutant alpha-synuclein by chaperone-mediated autophagy. Science *305*, 1292-1295.

Davidson, W.S., Jonas, A., Clayton, D.F., and George, J.M. (1998). Stabilization of alpha-synuclein secondary structure upon binding to synthetic membranes. J Biol Chem *273*, 9443-9449.

De Virgilio, C., and Loewith, R. (2006). The TOR signalling network from yeast to man. Int J Biochem Cell Biol *38*, 1476-1481.

DeMartino, G.N., and Slaughter, C.A. (1999). The proteasome, a novel protease regulated by multiple mechanisms. J Biol Chem *274*, 22123-22126.

Dixon, C., Mathias, N., Zweig, R.M., Davis, D.A., and Gross, D.S. (2005). Alpha-synuclein targets the plasma membrane via the secretory pathway and induces toxicity in yeast. Genetics *170*, 47-59.

Dubiel, W., Ferrell, K., Pratt, G., and Rechsteiner, M. (1992). Subunit 4 of the 26 S protease is a member of a novel eukaryotic ATPase family. J Biol Chem *267*, 22699-22702.

Duda, J.E., Giasson, B.I., Chen, Q., Gur, T.L., Hurtig, H.I., Stern, M.B., Gollomp, S.M., Ischiropoulos, H., Lee, V.M., and Trojanowski, J.Q. (2000). Widespread nitration of pathological inclusions in neurodegenerative synucleinopathies. Am J Pathol *157*, 1439-1445.

Dyllick-Brenzinger, M., D'Souza, C.A., Dahlmann, B., Kloetzel, P.M., and Tandon, A. (2010). Reciprocal effects of alpha-synuclein overexpression and proteasome inhibition in neuronal cells and tissue. Neurotox Res *17*, 215-227.

Ellis, C.E., Schwartzberg, P.L., Grider, T.L., Fink, D.W., and Nussbaum, R.L. (2001). alpha-synuclein is phosphorylated by members of the Src family of protein-tyrosine kinases. J Biol Chem *276*, 3879-3884.

Fearnley, J.M., and Lees, A.J. (1991). Ageing and Parkinson's disease: substantia nigra regional selectivity. Brain *114 (Pt 5)*, 2283-2301.

Fiske, M., Valtierra, S., Solvang, K., Zorniak, M., White, M., Herrera, S., Konnikova, A., Brezinsky, R., and Debburman, S. (2011). Contribution of Alanine-76 and Serine Phosphorylation in alpha-Synuclein Membrane Association and Aggregation in Yeasts. Parkinsons Dis *2011*, 392180.

Flower, T.R., Clark-Dixon, C., Metoyer, C., Yang, H., Shi, R., Zhang, Z., and Witt, S.N. (2007). YGR198w (YPP1) targets A30P alpha-synuclein to the vacuole for degradation. J Cell Biol *177*, 1091-1104.

Forno, L.S., DeLanney, L.E., Irwin, I., and Langston, J.W. (1996). Electron microscopy of Lewy bodies in the amygdala-parahippocampal region. Comparison with inclusion bodies in the MPTP-treated squirrel monkey. Adv Neurol *69*, 217-228.

Fortun, J., Dunn, W.A., Jr., Joy, S., Li, J., and Notterpek, L. (2003). Emerging role for autophagy in the removal of aggresomes in Schwann cells. J Neurosci *23*, 10672-10680.

Fujiwara, H., Hasegawa, M., Dohmae, N., Kawashima, A., Masliah, E., Goldberg, M.S., Shen, J., Takio, K., and Iwatsubo, T. (2002). alpha-Synuclein is phosphorylated in synucleinopathy lesions. Nat Cell Biol *4*, 160-164.

Galvin, J.E., Lee, V.M. and Trojanowski, J.Q. (2001). Synucleinopathies: clinical and pathological implications. Arch Neurol *58*, 186-190.

Ghislain, M., Udvardy, A., and Mann, C. (1993). S. cerevisiae 26S protease mutants arrest cell division in G2/metaphase. Nature *366*, 358-362.

Giasson, B.I., Duda, J.E., Murray, I.V., Chen, Q., Souza, J.M., Hurtig, H.I., Ischiropoulos, H., Trojanowski, J.Q., and Lee, V.M. (2000). Oxidative damage linked to neurodegeneration by selective alpha-synuclein nitration in synucleinopathy lesions. Science *290*, 985-989.

Giasson, B.I., Duda, J.E., Quinn, S.M., Zhang, B., Trojanowski, J.Q., and Lee, V.M. (2002). Neuronal alpha-synucleinopathy with severe movement disorder in mice expressing A53T human alpha-synuclein. Neuron *34*, 521-533.

Giasson, B.I., and Lee, V.M. (2001). Parkin and the molecular pathways of Parkinson's disease. Neuron *31*, 885-888.

Giasson, B.I., Uryu, K., Trojanowski, J.Q., and Lee, V.M. (1999). Mutant and wild type human alpha-synucleins assemble into elongated filaments with distinct morphologies in vitro. J Biol Chem *274*, 7619-7622.

Gietz, D., St Jean, A., Woods, R.A., and Schiestl, R.H. (1992). Improved method for high efficiency transformation of intact yeast cells. Nucleic Acids Res *20*, 1425.

Gimeno, C.J., Ljungdahl, P.O., Styles, C.A., and Fink, G.R. (1992). Unipolar cell divisions in the yeast S. cerevisiae lead to filamentous growth: regulation by starvation and RAS. Cell *68*, 1077-1090.

Giupponi, G., Pycha, R., Erfurth, A., Hausmann, A., and Conca, A. (2008). [Depressive symptoms and the Idiopathic Parkinson's Syndrome (IPS): a review]. Neuropsychiatr *22*, 71-82.

Glickman, M.H., and Ciechanover, A. (2002). The ubiquitin-proteasome proteolytic pathway: destruction for the sake of construction. Physiol Rev *82*, 373-428.

Goffeau, A., Barrell, B.G., Bussey, H., Davis, R.W., Dujon, B., Feldmann, H., Galibert, F., Hoheisel, J.D., Jacq, C., Johnston, M.*, et al.* (1996). Life with 6000 genes. Science *274*, 546, 563-547.

Goldberg, M.S., and Lansbury, P.T., Jr. (2000). Is there a cause-and-effect relationship between alpha-synuclein fibrillization and Parkinson's disease? Nat Cell Biol *2*, E115-119.

Golovko, M.Y., Barcelo-Coblijn, G., Castagnet, P.I., Austin, S., Combs, C.K., and Murphy, E.J. (2009). The role of alpha-synuclein in brain lipid metabolism: a downstream impact on brain inflammatory response. Mol Cell Biochem *326*, 55-66.

Graham, T.R., Scott, P.A., and Emr, S.D. (1993). Brefeldin A reversibly blocks early but not late protein transport steps in the yeast secretory pathway. EMBO J *12*, 869-877.

Greenamyre, J.T., Betarbet, R., and Sherer, T.B. (2003). The rotenone model of Parkinson's disease: genes, environment and mitochondria. Parkinsonism Relat Disord *9 Suppl 2*, S59-64.

Greenbaum, E.A., Graves, C.L., Mishizen-Eberz, A.J., Lupoli, M.A., Lynch, D.R., Englander, S.W., Axelsen, P.H., and Giasson, B.I. (2005). The E46K mutation in alpha-synuclein increases amyloid fibril formation. J Biol Chem *280*, 7800-7807.

Grosshans, B.L., Ortiz, D., and Novick, P. (2006). Rabs and their effectors: achieving specificity in membrane traffic. Proc Natl Acad Sci U S A *103*, 11821-11827.

Guthrie, C., and Fink, G.R. (1991). Guide to yeast genetics and molecular biology. Methods Enzymol *194*, 1-863.

Haas, A.L., and Siepmann, T.J. (1997). Pathways of ubiquitin conjugation. FASEB J *11*, 1257-1268.

Hara, T., Nakamura, K., Matsui, M., Yamamoto, A., Nakahara, Y., Suzuki-Migishima, R., Yokoyama, M., Mishima, K., Saito, I., Okano, H.*, et al.* (2006). Suppression of basal autophagy in neural cells causes neurodegenerative disease in mice. Nature *441*, 885-889.

Hardy, J., Cai, H., Cookson, M.R., Gwinn-Hardy, K., and Singleton, A. (2006). Genetics of Parkinson's disease and parkinsonism. Ann Neurol *60*, 389-398.

Hoffman, C.S., and Winston, F. (1987). A ten-minute DNA preparation from yeast efficiently releases autonomous plasmids for transformation of Escherichia coli. Gene *57*, 267-272.

Hsu, L.J., Mallory, M., Xia, Y., Veinbergs, I., Hashimoto, M., Yoshimoto, M., Thal, L.J., Saitoh, T., and Masliah, E. (1998). Expression pattern of synucleins (non-Abeta component of Alzheimer's disease amyloid precursor protein/alpha-synuclein) during murine brain development. J Neurochem *71*, 338-344.

Huang, W.P., Scott, S.V., Kim, J., and Klionsky, D.J. (2000). The itinerary of a vesicle component, Aut7p/Cvt5p, terminates in the yeast vacuole via the autophagy/Cvt pathways. J Biol Chem 275, 5845-5851.

Ichimura, Y., Kirisako, T., Takao, T., Satomi, Y., Shimonishi, Y., Ishihara, N., Mizushima, N., Tanida, I., Kominami, E., Ohsumi, M.*, et al.* (2000). A ubiquitin-like system mediates protein lipidation. Nature *408*, 488-492.

Iwata, A., Maruyama, M., Akagi, T., Hashikawa, T., Kanazawa, I., Tsuji, S., and Nukina, N. (2003). Alpha-synuclein degradation by serine protease neurosin: implication for pathogenesis of synucleinopathies. Hum Mol Genet *12*, 2625-2635.

Jenner, P. (1998). Oxidative mechanisms in nigral cell death in Parkinson's disease. Mov Disord *13 Suppl 1*, 24-34.

Jensen, P.H., Nielsen, M.S., Jakes, R., Dotti, C.G., and Goedert, M. (1998). Binding of alpha-synuclein to brain vesicles is abolished by familial Parkinson's disease mutation. J Biol Chem *273*, 26292-26294.

Jones, E.W. (1991). Three proteolytic systems in the yeast *Saccharomyces cerevisiae*. J Biol Chem *266*, 7963-7966.

Kahle, P.J., Neumann, M., Ozmen, L., and Haass, C. (2000). Physiology and pathophysiology of alpha-synuclein. Cell culture and transgenic animal models based on a Parkinson's disease-associated protein. Ann N Y Acad Sci *920*, 33-41.

Kamada, Y., Funakoshi, T., Shintani, T., Nagano, K., Ohsumi, M., and Ohsumi, Y. (2000). Tor-mediated induction of autophagy via an Apg1 protein kinase complex. J Cell Biol *150*, 1507-1513.

Kamada, Y., Sekito, T., and Ohsumi, Y. (2004). Autophagy in yeast: a TOR-mediated response to nutrient starvation. Curr Top Microbiol Immunol *279*, 73-84.

Karpinar, D.P., Balija, M.B., Kugler, S., Opazo, F., Rezaei-Ghaleh, N., Wender, N., Kim, H.Y., Taschenberger, G., Falkenburger, B.H., Heise, H.*, et al.* (2009). Pre-fibrillar alpha-synuclein variants with impaired beta-structure increase neurotoxicity in Parkinson's disease models. EMBO J *28*, 3256-3268.

Karube, H., Sakamoto, M., Arawaka, S., Hara, S., Sato, H., Ren, C.H., Goto, S., Koyama, S., Wada, M., Kawanami, T.*, et al.* (2008). N-terminal region of alpha-synuclein is essential for the fatty acid-induced oligomerization of the molecules. FEBS Lett *582*, 3693-3700.

Kawamoto, Y., Kobayashi, Y., Suzuki, Y., Inoue, H., Tomimoto, H., Akiguchi, I., Budka, H., Martins, L.M., Downward, J., and Takahashi, R. (2008). Accumulation of HtrA2/Omi in neuronal and glial inclusions in brains with alpha-synucleinopathies. J Neuropathol Exp Neurol *67*, 984-993.

Khalfan, W.A., and Klionsky, D.J. (2002). Molecular machinery required for autophagy and the cytoplasm to vacuole targeting (Cvt) pathway in S. cerevisiae. Curr Opin Cell Biol *14*, 468-475.

Kirisako, T., Ichimura, Y., Okada, H., Kabeya, Y., Mizushima, N., Yoshimori, T., Ohsumi, M., Takao, T., Noda, T., and Ohsumi, Y. (2000). The reversible modification regulates the membrane-binding state of Apg8/Aut7 essential for autophagy and the cytoplasm to vacuole targeting pathway. J Cell Biol *151*, 263-276.

Klionsky, D.J. (2005). Autophagy. Curr Biol *15*, R282-283.

Klionsky, D.J., and Emr, S.D. (2000). Autophagy as a regulated pathway of cellular degradation. Science *290*, 1717-1721.

Klionsky, D.J., Cregg, J.M., Dunn, W.A., Jr., Emr, S.D., Sakai, Y., Sandoval, I.V., Sibirny, A., Subramani, S., Thumm, M., Veenhuis, M.*, et al.* (2003). A unified nomenclature for yeast autophagy-related genes. Dev Cell *5*, 539-545.

Komatsu, M., Kominami, E., and Tanaka, K. (2006). Autophagy and neurodegeneration. Autophagy *2*, 315-317.

Kontopoulos, E., Parvin, J.D., and Feany, M.B. (2006). Alpha-synuclein acts in the nucleus to inhibit histone acetylation and promote neurotoxicity. Hum Mol Genet *15*, 3012-3023.

Krüger, R., Kuhn, W., Muller, T., Woitalla, D., Graeber, M., Kosel, S., Przuntek, H., Epplen, J.T., Schols, L., and Riess, O. (1998). Ala30Pro mutation in the gene encoding alpha-synuclein in Parkinson's disease. Nat Genet *18*, 106-108.

Kuma, A., Hatano, M., Matsui, M., Yamamoto, A., Nakaya, H., Yoshimori, T., Ohsumi, Y., Tokuhisa, T., and Mizushima, N. (2004). The role of autophagy during the early neonatal starvation period. Nature *432*, 1032-1036.

Kuma, A., Mizushima, N., Ishihara, N., and Ohsumi, Y. (2002). Formation of the approximately 350-kDa Apg12-Apg5.Apg16 multimeric complex, mediated by Apg16 oligomerization, is essential for autophagy in yeast. J Biol Chem *277*, 18619-18625.

Lakso, M., Vartiainen, S., Moilanen, A.M., Sirvio, J., Thomas, J.H., Nass, R., Blakely, R.D., and Wong, G. (2003). Dopaminergic neuronal loss and motor deficits in *Caenorhabditis elegans* overexpressing human alpha-synuclein. J Neurochem *86*, 165-172.

Lamphier, M.S., and Ptashne, M. (1992). Multiple mechanisms mediate glucose repression of the yeast *GAL1* gene. Proc Natl Acad Sci U S A *89*, 5922-5926.

Lang, A.E., and Lozano, A.M. (1998). Parkinson's disease. First of two parts. N Engl J Med *339*, 1044-1053.

Lashuel, H.A., Petre, B.M., Wall, J., Simon, M., Nowak, R.J., Walz, T., and Lansbury, P.T., Jr. (2002). Alpha-synuclein, especially the Parkinson's disease-associated mutants, forms pore-like annular and tubular protofibrils. J Mol Biol *322*, 1089-1102.

Lavedan, C. (1998) The synuclein family. *Genome Res*, **8**, 871-880.

Lee, D.H., and Goldberg, A.L. (1996). Selective inhibitors of the proteasome-dependent and vacuolar pathways of protein degradation in *Saccharomyces cerevisiae*. J Biol Chem *271*, 27280-27284.

Lee, D.H., and Goldberg, A.L. (1998). Proteasome inhibitors: valuable new tools for cell biologists. Trends Cell Biol *8*, 397-403.

Lindersson, E., Beedholm, R., Hojrup, P., Moos, T., Gai, W., Hendil, K.B., and Jensen, P.H. (2004). Proteasomal inhibition by alpha-synuclein filaments and oligomers. J Biol Chem *279*, 12924-12934.

Liu, C.W., Giasson, B.I., Lewis, K.A., Lee, V.M., Demartino, G.N., and Thomas, P.J. (2005). A precipitating role for truncated alpha-synuclein and the proteasome in alpha-synuclein aggregation: implications for pathogenesis of Parkinson disease. J Biol Chem *280*, 22670-22678.

Lucking, C.B., and Brice, A. (2000). Alpha-synuclein and Parkinson's disease. Cell Mol Life Sci *57*, 1894-1908.

Maeder, C.I., Hink, M.A., Kinkhabwala, A., Mayr, R., Bastiaens, P.I., and Knop, M. (2007). Spatial regulation of Fus3 MAP kinase activity through a reaction-diffusion mechanism in yeast pheromone signalling. Nat Cell Biol *9*, 1319-1326.

Mager, W.H., and Winderickx, J. (2005). Yeast as a model for medical and medicinal research. Trends Pharmacol Sci *26*, 265-273.

Marino, G., and Lopez-Otin, C. (2008). Autophagy and aging: new lessons from progeroid mice. Autophagy *4*, 807-809.

Maroteaux, L., and Scheller, R.H. (1991). The rat brain synucleins; family of proteins transiently associated with neuronal membrane. Brain Res Mol Brain Res *11*, 335-343.

Martin, L.J., Pan, Y., Price, A.C., Sterling, W., Copeland, N.G., Jenkins, N.A., Price, D.L., and Lee, M.K. (2006). Parkinson's disease alpha-synuclein transgenic mice develop neuronal mitochondrial degeneration and cell death. J Neurosci *26*, 41-50.

Marzella, L., Ahlberg, J., and Glaumann, H. (1981). Autophagy, heterophagy, microautophagy and crinophagy as the means for intracellular degradation. Virchows Arch B Cell Pathol Incl Mol Pathol *36*, 219-234.

Matsuoka, Y., Vila, M., Lincoln, S., McCormack, A., Picciano, M., LaFrancois, J., Yu, X., Dickson, D., Langston, W.J., McGowan, E.*, et al.* (2001). Lack of nigral pathology in transgenic mice expressing human alpha-synuclein driven by the tyrosine hydroxylase promoter. Neurobiol Dis *8*, 535-539.

Matsuura, A., Tsukada, M., Wada, Y., and Ohsumi, Y. (1997). Apg1p, a novel protein kinase required for the autophagic process in *Saccharomyces cerevisiae*. Gene *192*, 245-250.

McNaught, K.S., and Jenner, P. (2001). Proteasomal function is impaired in substantia nigra in Parkinson's disease. Neurosci Lett *297*, 191-194.

Meissner, W.G., Frasier, M., Gasser, T., Goetz, C.G., Lozano, A., Piccini, P., Obeso, J.A., Rascol, O., Schapira, A., Voon, V.*, et al.* (2011). Priorities in Parkinson's disease research. Nat Rev Drug Discov *10*, 377-393.

Mishizen-Eberz, A.J., Norris, E.H., Giasson, B.I., Hodara, R., Ischiropoulos, H., Lee, V.M., Trojanowski, J.Q., and Lynch, D.R. (2005). Cleavage of alpha-synuclein by calpain: potential role in degradation of fibrillized and nitrated species of alpha-synuclein. Biochemistry *44*, 7818-7829.

Mizushima, N., Levine, B., Cuervo, A.M., and Klionsky, D.J. (2008). Autophagy fights disease through cellular self-digestion. Nature *451*, 1069-1075.

Mizushima, N., Sugita, H., Yoshimori, T., and Ohsumi, Y. (1998). A new protein conjugation system in human. The counterpart of the yeast Apg12p conjugation system essential for autophagy. J Biol Chem *273*, 33889-33892.

Mizushima, N., Yamamoto, A., Matsui, M., Yoshimori, T., and Ohsumi, Y. (2004). In vivo analysis of autophagy in response to nutrient starvation using transgenic mice expressing a fluorescent autophagosome marker. Mol Biol Cell *15*, 1101-1111.

Murray, I.V., Giasson, B.I., Quinn, S.M., Koppaka, V., Axelsen, P.H., Ischiropoulos, H., Trojanowski, J.Q., and Lee, V.M. (2003). Role of alpha-synuclein carboxy-terminus on fibril formation in vitro. Biochemistry *42*, 8530-8540.

Narayanan, V., and Scarlata, S. (2001). Membrane binding and self-association of alpha-synucleins. Biochemistry *40*, 9927-9934.

Naujokat, C., and Hoffmann, S. (2002). Role and function of the 26S proteasome in proliferation and apoptosis. Lab Invest *82*, 965-980.

Neuhoff, V., Arold, N., Taube, D., and Ehrhardt, W. (1988). Improved staining of proteins in polyacrylamide gels including isoelectric focusing gels with clear background at nanogram sensitivity using Coomassie Brilliant Blue G-250 and R-250. Electrophoresis *9*, 255-262.

Noda, T., Matsuura, A., Wada, Y., and Ohsumi, Y. (1995). Novel system for monitoring autophagy in the yeast *Saccharomyces cerevisiae*. Biochem Biophys Res Commun *210*, 126-132.

Noda, T., Suzuki, K., and Ohsumi, Y. (2002). Yeast autophagosomes: de novo formation of a membrane structure. Trends Cell Biol *12*, 231-235.

Olanow, C.W., and McNaught, K.S. (2006). Ubiquitin-proteasome system and Parkinson's disease. Mov Disord *21*, 1806-1823.

Opazo, F., Krenz, A., Heermann, S., Schulz, J.B., and Falkenburger, B.H. (2008). Accumulation and clearance of alpha-synuclein aggregates demonstrated by time-lapse imaging. J Neurochem *106*, 529-540.

Outeiro, T.F., and Lindquist, S. (2003). Yeast cells provide insight into alpha-synuclein biology and pathobiology. Science *302*, 1772-1775.

Outeiro, T.F., Putcha, P., Tetzlaff, J.E., Spoelgen, R., Koker, M., Carvalho, F., Hyman, B.T., and McLean, P.J. (2008). Formation of toxic oligomeric alpha-synuclein species in living cells. PLoS One *3*, e1867.

Pan, T., Kondo, S., Le, W., and Jankovic, J. (2008). The role of autophagy-lysosome pathway in neurodegeneration associated with Parkinson's disease. Brain *131*, 1969-1978.

Pandey, U.B., Batlevi, Y., Baehrecke, E.H., and Taylor, J.P. (2007). HDAC6 at the intersection of autophagy, the ubiquitin-proteasome system and neurodegeneration. Autophagy *3*, 643-645.

Parr, C.L., Keates, R.A., Bryksa, B.C., Ogawa, M., and Yada, R.Y. (2007). The structure and function of *Saccharomyces cerevisiae* proteinase A. Yeast *24*, 467-480.

Paxinou, E., Chen, Q., Weisse, M., Giasson, B.I., Norris, E.H., Rueter, S.M., Trojanowski, J.Q., Lee, V.M., and Ischiropoulos, H. (2001). Induction of alpha-synuclein aggregation by intracellular nitrative insult. J Neurosci *21*, 8053-8061.

Phizicky, E.M., and Fields, S. (1995). Protein-protein interactions: methods for detection and analysis. Microbiol Rev *59*, 94-123.

Polymeropoulos, M.H., Lavedan, C., Leroy, E., Ide, S.E., Dehejia, A., Dutra, A., Pike, B., Root, H., Rubenstein, J., Boyer, R.*, et al.* (1997). Mutation in the alpha-synuclein gene identified in families with Parkinson's disease. Science *276*, 2045-2047.

Puig, O., Caspary, F., Rigaut, G., Rutz, B., Bouveret, E., Bragado-Nilsson, E., Wilm, M., and Seraphin, B. (2001). The tandem affinity purification (TAP) method: a general procedure of protein complex purification. Methods *24*, 218-229.

Ravikumar, B., Duden, R., and Rubinsztein, D.C. (2002). Aggregate-prone proteins with polyglutamine and polyalanine expansions are degraded by autophagy. Hum Mol Genet *11*, 1107-1117.

Ravikumar, B., and Rubinsztein, D.C. (2006). Role of autophagy in the clearance of mutant huntingtin: a step towards therapy? Mol Aspects Med *27*, 520-527.

Recchia, A., Debetto, P., Negro, A., Guidolin, D., Skaper, S.D., and Giusti, P. (2004). Alpha-synuclein and Parkinson's disease. FASEB J *18*, 617-626.

Rideout, H.J., Lang-Rollin, I., and Stefanis, L. (2004). Involvement of macroautophagy in the dissolution of neuronal inclusions. Int J Biochem Cell Biol *36*, 2551-2562.

Riedel, M., Goldbaum, O., Schwarz, L., Schmitt, S., and Richter-Landsberg, C. (2010). 17-AAG induces cytoplasmic alpha-synuclein aggregate clearance by induction of autophagy. PLoS One *5*, e8753.

Rott, R., Szargel, R., Haskin, J., Shani, V., Shainskaya, A., Manov, I., Liani, E., Avraham, E., and Engelender, S. (2008). Monoubiquitylation of alpha-synuclein by seven in absentia homolog (SIAH) promotes its aggregation in dopaminergic cells. J Biol Chem *283*, 3316-3328.

Rubinsztein, D.C. (2007). Autophagy induction rescues toxicity mediated by proteasome inhibition. Neuron *54*, 854-856.

Sampathu, D.M., Giasson, B.I., Pawlyk, A.C., Trojanowski, J.Q., and Lee, V.M. (2003). Ubiquitination of alpha-synuclein is not required for formation of pathological inclusions in alpha-synucleinopathies. Am J Pathol *163*, 91-100.

Saiki, R.K., Gelfand, D.H., Stoffel, S., Scharf, S.J., Higuchi, R., Horn, G.T., Mullis, K.B., and Erlich, H.A. (1988). Primer-directed enzymatic amplification of DNA with a thermostable DNA polymerase. Science *239*, 487-491.

Sarbassov, D.D., Ali, S.M., and Sabatini, D.M. (2005). Growing roles for the mTOR pathway. Curr Opin Cell Biol *17*, 596-603.

Schimmoller, F., and Riezman, H. (1993). Involvement of Ypt7p, a small GTPase, in traffic from late endosome to the vacuole in yeast. J Cell Sci *106 (Pt 3)*, 823-830.

Sharma, N., Brandis, K.A., Herrera, S.K., Johnson, B.E., Vaidya, T., Shrestha, R., and Debburman, S.K. (2006). alpha-Synuclein budding yeast model: toxicity enhanced by impaired proteasome and oxidative stress. J Mol Neurosci *28*, 161-178.

Sharon, R., Goldberg, M.S., Bar-Josef, I., Betensky, R.A., Shen, J., and Selkoe, D.J. (2001). alpha-Synuclein occurs in lipid-rich high molecular weight complexes, binds fatty acids, and shows homology to the fatty acid-binding proteins. Proc Natl Acad Sci U S A *98*, 9110-9115.

Shevchenko, A., Wilm, M., Vorm, O., and Mann, M. (1996). Mass spectrometric sequencing of proteins silver-stained polyacrylamide gels. Anal Chem *68*, 850-858.

Shimura, H., Schlossmacher, M.G., Hattori, N., Frosch, M.P., Trockenbacher, A., Schneider, R., Mizuno, Y., Kosik, K.S., and Selkoe, D.J. (2001). Ubiquitination of a new form of alpha-synuclein by parkin from human brain: implications for Parkinson's disease. Science *293*, 263-269.

Sikorski, R.S., and Hieter, P. (1989). A system of shuttle vectors and yeast host strains designed for efficient manipulation of DNA in *Saccharomyces cerevisiae*. Genetics *122*, 19-27.

Singleton, A.B., Farrer, M., Johnson, J., Singleton, A., Hague, S., Kachergus, J., Hulihan, M., Peuralinna, T., Dutra, A., Nussbaum, R.*, et al.* (2003). alpha-Synuclein locus triplication causes Parkinson's disease. Science *302*, 841.

Soper, J.H., Kehm, V., Burd, C.G., Bankaitis, V.A., and Lee, V.M. (2011). Aggregation of alpha-synuclein in S. cerevisiae is associated with defects in endosomal trafficking and phospholipid biosynthesis. J Mol Neurosci *43*, 391-405.

Soper, J.H., Roy, S., Stieber, A., Lee, E., Wilson, R.B., Trojanowski, J.Q., Burd, C.G., and Lee, V.M. (2008). Alpha-synuclein-induced aggregation of cytoplasmic vesicles in *Saccharomyces cerevisiae*. Mol Biol Cell *19*, 1093-1103.

Southern, E.M. (1975). Detection of specific sequences among DNA fragments separated by gel electrophoresis. J Mol Biol *98*, 503-517.

Spillantini, M.G., Crowther, R.A., Jakes, R., Cairns, N.J., Lantos, P.L., and Goedert, M. (1998a). Filamentous alpha-synuclein inclusions link multiple system atrophy with Parkinson's disease and dementia with Lewy bodies. Neurosci Lett *251*, 205-208.

Spillantini, M.G., Crowther, R.A., Jakes, R., Hasegawa, M., and Goedert, M. (1998b). alpha-Synuclein in filamentous inclusions of Lewy bodies from Parkinson's disease and dementia with lewy bodies. Proc Natl Acad Sci U S A *95*, 6469-6473.

Spillantini, M.G., Schmidt, M.L., Lee, V.M., Trojanowski, J.Q., Jakes, R., and Goedert, M. (1997). Alpha-synuclein in Lewy bodies. Nature *388*, 839-840.

Stefanis, L., Larsen, K.E., Rideout, H.J., Sulzer, D., and Greene, L.A. (2001). Expression of A53T mutant but not wild-type alpha-synuclein in PC12 cells induces alterations of the ubiquitin-dependent degradation system, loss of dopamine release, and autophagic cell death. J Neurosci *21*, 9549-9560.

Suzuki, K., and Ohsumi, Y. (2007). Molecular machinery of autophagosome formation in yeast, *Saccharomyces cerevisiae*. FEBS Lett *581*, 2156-2161.

Takeshige, K., Baba, M., Tsuboi, S., Noda, T., and Ohsumi, Y. (1992). Autophagy in yeast demonstrated with proteinase-deficient mutants and conditions for its induction. J Cell Biol *119*, 301-311.

Tanaka, M., Kim, Y.M., Lee, G., Junn, E., Iwatsubo, T., and Mouradian, M.M. (2004). Aggresomes formed by alpha-synuclein and synphilin-1 are cytoprotective. J Biol Chem *279*, 4625-4631.

Tanaka, Y., Engelender, S., Igarashi, S., Rao, R.K., Wanner, T., Tanzi, R.E., Sawa, A., V, L.D., Dawson, T.M., and Ross, C.A. (2001). Inducible expression of mutant alpha-synuclein decreases proteasome activity and increases sensitivity to mitochondria-dependent apoptosis. Hum Mol Genet *10*, 919-926.

Tofaris, G.K., Kim, H.T., Hourez, R., Jung, J.W., Kim, K.P., and Goldberg, A.L. (2011). Ubiquitin ligase Nedd4 promotes alpha-synuclein degradation by the endosomal-lysosomal pathway. Proc Natl Acad Sci U S A *108*, 17004-17009.

Tofaris, G.K., Layfield, R., and Spillantini, M.G. (2001). alpha-synuclein metabolism and aggregation is linked to ubiquitin-independent degradation by the proteasome. FEBS Lett *509*, 22-26.

Tofaris, G.K., and Spillantini, M.G. (2007). Physiological and pathological properties of alpha-synuclein. Cell Mol Life Sci *64*, 2194-2201.

Tong, J., Wong, H., Guttman, M., Ang, L.C., Forno, L.S., Shimadzu, M., Rajput, A.H., Muenter, M.D., Kish, S.J., Hornykiewicz, O. *et al.* (2010) Brain alpha-synuclein accumulation in multiple system atrophy, Parkinson's disease and progressive supranuclear palsy: a comparative investigation. *Brain*, **133**, 172-188.

Traven, A., Jelicic, B., and Sopta, M. (2006). Yeast Gal4: a transcriptional paradigm revisited. EMBO Rep *7*, 496-499.

Vamvaca, K., Volles, M.J., and Lansbury, P.T., Jr. (2009). The first N-terminal amino acids of alpha-synuclein are essential for alpha-helical structure formation in vitro and membrane binding in yeast. J Mol Biol *389*, 413-424.

van der Putten, H., Wiederhold, K.H., Probst, A., Barbieri, S., Mistl, C., Danner, S., Kauffmann, S., Hofele, K., Spooren, W.P., Ruegg, M.A*., et al.* (2000). Neuropathology in mice expressing human alpha-synuclein. J Neurosci *20*, 6021-6029.

Vida, T.A., and Emr, S.D. (1995). A new vital stain for visualizing vacuolar membrane dynamics and endocytosis in yeast. J Cell Biol *128*, 779-792.

Vogiatzi, T., Xilouri, M., Vekrellis, K., and Stefanis, L. (2008). Wild type alpha-synuclein is degraded by chaperone-mediated autophagy and macroautophagy in neuronal cells. J Biol Chem *283*, 23542-23556.

Volles, M.J., and Lansbury, P.T., Jr. (2002). Vesicle permeabilization by protofibrillar alpha-synuclein is sensitive to Parkinson's disease-linked mutations and occurs by a pore-like mechanism. Biochemistry *41*, 4595-4602.

Volles, M.J., and Lansbury, P.T., Jr. (2007). Relationships between the sequence of alpha-synuclein and its membrane affinity, fibrillization propensity, and yeast toxicity. J Mol Biol *366*, 1510-1522.

Webb, J.L., Ravikumar, B., Atkins, J., Skepper, J.N., and Rubinsztein, D.C. (2003). Alpha-Synuclein is degraded by both autophagy and the proteasome. J Biol Chem *278*, 25009-25013.

Wersinger, C., and Sidhu, A. (2003). Attenuation of dopamine transporter activity by alpha-synuclein. Neurosci Lett *340*, 189-192.

Wichmann, H., Hengst, L., and Gallwitz, D. (1992). Endocytosis in yeast: evidence for the involvement of a small GTP-binding protein (Ypt7p). Cell *71*, 1131-1142.

Wichmann, T., and DeLong, M.R. (2003). Functional neuroanatomy of the basal ganglia in Parkinson's disease. Adv Neurol *91*, 9-18.

Winslow, A.R., Chen, C.W., Corrochano, S., Acevedo-Arozena, A., Gordon, D.E., Peden, A.A., Lichtenberg, M., Menzies, F.M., Ravikumar, B., Imarisio, S.*, et al.* (2010). alpha-Synuclein impairs macroautophagy: implications for Parkinson's disease. J Cell Biol *190*, 1023-1037.

Wojcik, C., and DeMartino, G.N. (2003). Intracellular localization of proteasomes. Int J Biochem Cell Biol *35*, 579-589.

Woolford, C.A., Daniels, L.B., Park, F.J., Jones, E.W., Van Arsdell, J.N., and Innis, M.A. (1986). The PEP4 gene encodes an aspartyl protease implicated in the posttranslational regulation of *Saccharomyces cerevisiae* vacuolar hydrolases. Mol Cell Biol *6*, 2500-2510.

Wullschleger, S., Loewith, R., and Hall, M.N. (2006). TOR signaling in growth and metabolism. Cell *124*, 471-484.

Xilouri, M., Vogiatzi, T., Vekrellis, K., Park, D., and Stefanis, L. (2009). Abberant alpha-synuclein confers toxicity to neurons in part through inhibition of chaperone-mediated autophagy. PLoS One *4*, e5515.

Yorimitsu, T., and Klionsky, D.J. (2005). Autophagy: molecular machinery for self-eating. Cell Death Differ *12 Suppl 2*, 1542-1552.

Yu, Z., Xu, X., Xiang, Z., Zhou, J., Zhang, Z., Hu, C., and He, C. (2009). Nitrated alpha-synuclein induces the loss of dopaminergic neurons in the substantia nigra of rats. PLoS One *5*, e9956.

Zabrocki, P., Pellens, K., Vanhelmont, T., Vandebroek, T., Griffioen, G., Wera, S., Van Leuven, F., and Winderickx, J. (2005). Characterization of alpha-synuclein aggregation and synergistic toxicity with protein tau in yeast. FEBS J *272*, 1386-1400.

Zhu, M., Li, J. and Fink, A.L. (2003) The association of alpha-synuclein with membranes affects bilayer structure, stability, and fibril formation. *J Biol Chem*, **278**, 40186-40197.

7. CV

DORIS PETROI

Born June 3, 1985 in Galati, Romania

EDUCATION

10/2008 – 03/2012	**Institute of Microbiology and Genetics, Göttingen, Germany** PhD in the MSc/PhD Molecular Biology program of the International Max Plank Research School Thesis: α-synuclein in *Saccharomyces cerevisiae*: model for aggregate clearance, cell survival and influence of autophagy
09/2007 – 08/2008	**Georg-August-Universität Göttingen, Germany** MSc in the MSc/PhD Molecular Biology program of the International Max Plank Research School Thesis: Analysis of *ATG7* in the context of alpha-synuclein toxicity in *Saccharomyces cerevisiae*
08/2004 – 06/2007	**Jacobs University Bremen, Germany** BSc in Biochemistry and Cell Biology Thesis: Dnmt3a and Dnmt3b expression in Bac-to-Bac system and further Dnmt3a molecular analysis
09/2000 – 06/2004	**Vasile Alecsandri High-School, Galati, Romania** Graduated with honors, top 3% of batch

TEACHING AND PROJECT EXPERIENCE

01/2011 – 02/2011	**Supervisor** of master rotation project: α-synuclein degradation in the yeast model system
04/2009 – 06/2009	**Supervisor** of bachelor project: The role of autophagy in haploid and diploid yeast
06/2006 – 08/2006	**Intern** in the Biocatalyst Research Department at BASF Ludwigshafen, Germany. Characterized alcohol dehydrogenase genes from *Clostridium perfringens*
03/2005 – 04/2006	**Research assistant** in the Biochemical Engineering Department at Jacobs University Bremen, Germany. Investigated metabolic compensation of temperature acclimation in *Saccharomyces cerevisiae*

CONFERENCE CONTRIBUTIONS

- **Organization Committee**: International PhD Student Symposium: Horizons in Molecular Biology, 2009 and 2010 editions, Göttingen, Germany
- **Poster presentation**: "Modelling Parkinson's Disease in Saccharomyces cerevisiae" at Genetics 2010: model organisms to human biology, 2010, Boston, MA, USA
- **Poster presentation**: "The yeast HtrA orthologue Ynm3 is a protease with chaperone activity that aids survival under heat stress" at the 24th International Conference on Yeast Genetics and Molecular Biology, 2009, Manchester, UK

HONORS AND AWARDS

- Stipend of the Excellence Foundation for the Promotion of the Max Plank Society for 2007/2008, Göttingen, Germany
- DAAD STIBET-I Award for Community Involvement in 2006, Bremen, Germany